Protein-protein interactions, sub-cellular localisation and mobility of the human Cdc45 protein.

Ronan Broderick

Ph.D

School of Natural Science

Centre for Chromosome Biology

National University of Ireland, Galway

October 2012

Head of School of Natural Science: Dr. Heinz Peter Nasheuer

Supervisor: Dr. Heinz Peter Nasheuer

Table of Contents:

Chapter 3: Sub-cellular localisation of Cdc45 in the cell cycle and following DNA damage.

List of figures:

Chapter 1

Chapter 2

Chapter 3

Chapter 4:

List of Tables

Chapter 3:

Chapter 4:

Declaration

I, Ronan Broderick declare that the data obtained and presented in this thesis has been acquired and analysed by myself, with the following exceptions.

Dr. Michael D. Rainey contributed to the production of chapter 3 of this thesis, specifically performing the experiments and providing the raw data for figure 1 panel B, and figure four panels D and E as well as supplementary figure 5 in this chapter.

Dr. Siva Ramadurai contributed to the production of chapter 4 of this thesis, specifically performing the fluorescence correlation spectroscopy experiments outlined in this chapter and analysing the data obtained from these experiments. Figure 2, table 1 and all the supplementary information in this chapter were provided by Dr. Ramadurai and this chapter has since been published as a paper by PLoS ONE (Broderick et al, 2012).

Summary

Eukaryotic DNA replication is a dynamic process requiring the co-operation of specific replication proteins. The replication factor Cdc45 has essential functions in the initiation and elongation steps of eukaryotic DNA replication and plays a role in the intra-S-phase checkpoint. Its interactions with a variety of replication proteins forming two central complexes, *Cdc45/Mcm2-7/GINS* (CMG) the putative replicative helicase of eukaryotes, and *replisome progression complex* (RPC) during the cell cycle and after intra-S-phase checkpoint activation remain to be fully characterized.

The C terminal part of Cdc45 is important for its interaction with Claspin. The interactions of human Cdc45 with the three replication factors Claspin, *replication protein A* (RPA) and DNA polymerase δ are maximal during S phase. Following UVC-mediated DNA damage, Cdc45-Claspin complex formation is reduced whereas the binding of Cdc45 to RPA is not affected. We also show that treatment of cells with UCN-01, Caffeine or Wortmannin does not rescue the UV-mediated destabilisation of Cdc45-Claspin interactions, suggesting that the loss of interaction between Cdc45 and Claspin occurs independently of ATR activation in the intra-S-phase checkpoint.

The sub-cellular localisation of Cdc45 in the cell cycle and following activation of the intra-S-phase checkpoint was also determined. Cdc45 showed a specific nuclear and nucleolar localisation and the Cdc45 association with nucleoli was abolished following UV damage and inhibiting nucleolar transcription. We then determined the regions of Cdc45 needed for its localisation to nuclear compartments. Spcifically, aa101-155 and aa156-169 are required for recruitment of Cdc45 to the nucleus and nucleolus, respectively.

Measuring the mobility of eGFP-Cdc45 by Fluorescence Correlation Spectroscopy (FCS) *in vivo* in asynchronous cells and in cells synchronized at the G1/S transition and during S phase showed that eGFP-Cdc45 mobility is faster in G1/S transition compared to S phase suggesting that Cdc45 is part of larger protein complex formed in S phase. Furthermore, the size of complexes containing Cdc45 was estimated in asynchronous, G1/S and S phase-synchronized cells using gel filtration chromatography; these findings complemented the *in vivo* FCS data. Analysis of the mobility of eGFP-Cdc45 and the size of complexes containing Cdc45 and

eGFP-Cdc45 after UVC-mediated DNA damage revealed no significant changes in diffusion rates and complex sizes using FCS and gel filtration chromatography analyses. These findings suggest that after UV-damage, Cdc45 is still present in a large multi-protein complex and that its mobility within living cells is consistently similar following UVC-mediated DNA damage.

Chapter 1

Introduction

1.1 The Cell Cycle

All eukaryotic cells replicate via the organized duplication and spatial separation of their genetic material in a process called cell division (H Funabiki, 1993). The series of events that takes place in a cell leading to cell division are termed collectively as the cell cycle (Smith & Martin, 1973). The cell cycle consists of four distinct phases: G1 phase (gap), S phase (synthesis), G2 phase and M phase (mitosis + cytokinesis) (Alberts et al, 2008). Alternatively depending on environmental conditions, cells may stop dividing and can enter the state in which they are quiescent, known as G_0 (Martin & Stein, 1976). Mitosis consists of four stages: prophase, metaphase, anaphase and telophase (Alberts et al, 2008). At prophase, the chromatin condenses into well defined visible chromosome structures with two sister chomatids bound together by the cohesin protein complex (Alberts et al, 2008). At late prophase microtubles that are part of the cytoskeleton disassemble and the mitotic spindle, a bipolar structure composed of microtubules and associated proteins begin to assemble outside the nucleus starting at each of the cells two centrosomes (Alberts et al, 2008).

In pro-metaphase, the nuclear envelope breaks down, allowing the spindle microtubules to enter the nuclear region and attach to specialised protein complexes termed kinetochores which form around the centromeric regions of the condensed chromosomes (Alberts et al, 2008). These attached microtubules are then termed the kinetochore microtubules (Alberts et al, 2008). In metaphase, the kinetochore-attached microtubules move the chromosomes around within the cell and align the chromosomes into one plane roughly equidistant from each of the anchoring centrosomes (Alberts et al, 2008). At anaphase, the paired kinetochores on each chromosome separate, the kinetochore microtubules shorten, causing each chromatid to be pulled slowly towards the centrosome the microtubules are anchored to (Alberts et al, 2008). In telophase, the separated chromosomes arrive at the centrosomes and the kinetochore-attached microtubules disassemble (Alberts et al, 2008). The polar microtubules (microtubules originating from the centrosomes that are not attached to the kinetochore) elongate and new nuclear membranes begin to form, enclosing each set of separated chromosomes (Alberts et al, 2008). The chromatin in these chromosomes then de-condenses and the nucleoli, which had disassembled at prophase form again (Alberts et al, 2008).

Finally, the cytoplasm of such a mitotic cell is separated to form two daughter cells in a process termed cytokinesis (Alberts et al, 2008). The process of dividing the cytoplasm, termed cleavage, begins during anaphase. Here the cytoplasmic membrane in the middle of the cell, perpendicular to the spindle axis between the two daughter nuclei is drawn inward via a contractile actin-myosin ring creating a cleavage furrow which deepens until it encounters the remnants of the mitotic spindle between the two nuclei forming the midbody (Alberts et al, 2008). This midbody continues to narrow and finally breaks at each end, creating two separate daughter cells (Alberts et al, 2008).

The G1, S, and G2 phases are also summarised as interphase (Alberts et al, 2008). In the cell cycle before mitosis can take place there must be a duplication of all components of the cell, a process that at least in part gradually occurs throughout the cell cycle resulting in the doubling of the cell size (Nurse et al, 1976). During G1 phase cells undergo a growth in mass with proteins and RNA synthesized .During S phase chromosomes are duplicated and all chromosomal DNA is replicated but also other components of chromosomes such as the histones are duplicated (Alberts et al, 2008). After the conclusion of S phase, which is completed when the genome has been fully replicated, the G2-phase begins and the cell is prepared for mitosis (Alberts et al, 2008). Alternatively, in G_0 phase, the cell in a resting or quiescent state and is neither dividing or preparing to divide (Alberts et al, 2008). However, such a cell is not dormant state but is actively involved in cellular metabolic processes such as protein synthesis (Alberts et al, 2008).

In the eukaryotic cell cycle, S phase is bordered by the two gap phases G1 and G2, and represents the part when DNA replication takes place. The progression from one phase to the next is regulated by extra-cellular environmental signals as well as internal signals which monitor and coordinate the various processes that take place in the cell during each stage of the cell cycle. The progression of a cell into S phase is a tightly regulated process and once a cell initiates DNA replication it cannot abort this process it until it is complete (Stillman, 1996). The main classes of replication regulatory molecules, cyclins, cyclin-dependent kinases (CDKs) and Dbf4-dependent kinase (DDK) play a key role in the progression of a cell into S phase (Alberts et al, 2008). Cyclins were first characterised as proteins whose

expression oscillates in synchrony with the cell cycle, accumulating progressively through interphase and disappearing abruptly at mitosis (Fung & Poon, 2005). Cyclins associate with CDKs and potentiate their kinase activity to phosphorylate substrate proteins which effect cell cycle progression (Alberts et al, 2008). Cell cycle progression is controlled by the relative levels of individual cyclin family members (Coverley et al, 2002). Progression through the G1-S-G2-M cycle follows successive oscillations in the levels of cyclins, D, E, A and B (Coverley et al, 2002). Cyclins are grouped into classes according to the phases of the cell cycle they regulate. Cyclin D couples with Cdk4 and Cdk6. Cyclin E and cyclin A are able to bind Cdk2 and promote the cell cycle progression through the G1/S transition (Leone et al, 1998). Activation of the DNA replication at the onset of S phase is mediated by CDKs and DDK, which is described in detail below.

1.2 DNA Replication

Duplication of chromosomal DNA is an essential process both for normal cell division and to maintain stability of the genome (Hoeijmakers, 2001). Replication of damaged DNA or errors in DNA replication can lead to genetic mutation, with accumulated mutations leading to diseases such as cancer (Hoeijmakers, 2001). In human cells, accurate duplication of the genome is carried out by a large multi-subunit protein complex termed the "replisome progression complex" (RPC) which consists of a variety of replication proteins, which work in concert and at different stages of the cell cycle to facilitate DNA replication (Bauerschmidt et al, 2007; Broderick & Nasheuer, 2009; Gambus et al, 2009; Machida et al, 2005; Takeda & Dutta, 2005; Zhu et al, 2007). The replicative DNA polymerases, as part of the RPC carry out DNA replication of the 3 billion or so base pairs of the human genome at a rate of 2 to 3 kb/min (Mechali, 2010). Duplication of the genome occurs with an amazing degree of fidelity, with studies in *E. coli* indicating that *in vivo* replication error rates are in the range of 1 in every 10^{-7} to 10^{-8} base pairs polymerised, with error rates in higher eukaryotes likely to be equally or even more accurate than this (Kunkel, 2004).

Eukaryotic DNA replication is a highly co-ordinated process which requires with the binding of the multi-subunit origin recognition complex (ORC) to discreet loci in the genome, the origins of replication, at the early G1-phase of the cell cycle

(Blow & Dutta, 2005; Nasheuer et al, 2006) (Figure 1). Studies in yeast have revealed conserved sequences which the yeast ORC complex recognises as the origins of replication, termed "autonomously replicating sequences" (ARS) (Alabert & Groth, 2012). In the human genome, DNA replication is carried out by the sequential "firing" of 30,000 to 50,000 origins of replication, distributed throughout the genome with an average interval of 100 kb. (Alabert & Groth, 2012). In contrast to yeast, no consensus DNA sequence for human origins of replication has been identified (Alabert & Groth, 2012). ORC binding occurs mainly in nucleosome-free regions of the genome and the question whether the absence of nucleosomes mediates ORC binding, or whether ORC binding brings about histone displacement, creating nucleosome free DNA remains open (Alabert & Groth, 2012). Recent studies provide evidence that non-histone chromatin factors such as heterochromatin protein 1 (HP1) and high mobility group AT-hook protein 1 (HMG A1) facilitate targeting of ORC to particular regions in the genome thereby specifying these regions as origins of replication (Atanasiu et al, 2006; Schwaiger et al, 2010; Thomae et al, 2008).

The binding of ORC allows the association of additional proteins such as Cdc6 (cell division cycle protein 6) and Cdt1 (Cdc10-dependent target 1) to the ORC complex mediating the loading of the Mcm2–7 complex to chromatin (summarized in Figure 1). The latter is the putative replicative helicase in eukaryotes. The association of the Mcm2-7 complex with chromatin is the last step in the formation of the preRC (pre-replicative complex) (Blow & Dutta, 2005; Nasheuer et al, 2006). Cdc6, Cdt1 and Geminin control replication early in the cell cycle, with ORC binding allowing the sequestering of Cdc6 and Cdt1 to chromatin (Figure 1) (Nasheuer et al, 2006). Cdc6 binds to Cdt1 and both together load the Mcm2 to Mcm7 complex (MCM complex) onto chromatin, which represents a requirement for the licensing of DNA replication (Nasheuer et al, 2006). The function of Cdc6 is tightly regulated, and at the onset of S phase in yeast, Cdc6 is phosphorylated targeting the protein for proteolytic degradation (Nasheuer et al, 2006). In higher eukaryotes Cdc6 is also phosphorylated, but phosphorylation induces its export from the nucleus rather than its degradation (Nasheuer et al, 2006). The function

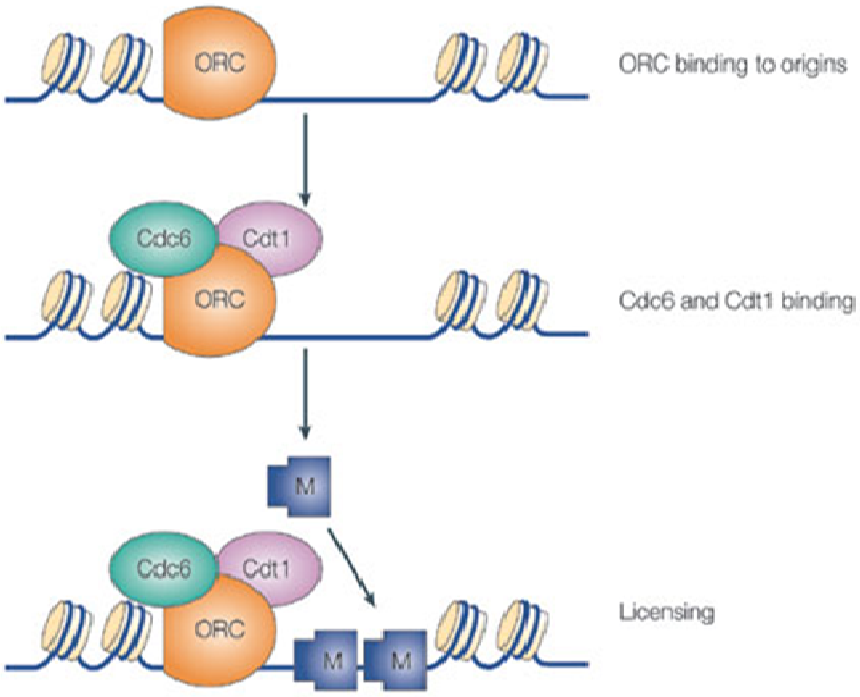

Figure 1: ORC binding to origins of replication mediates licencing
DNA replication begins with the ORC protein complex binding to the origins of replication. Subsequent binding of Cdc6 and Cdt1 proteins allow loading of the Mcm2-7 complex, the core of the replicative helicase. (Figure adapted from (Blow & Dutta, 2005))

of Cdt1 is also tightly controlled. In budding yeast Cdt1 protein levels are constant throughout the cell cycle and Cdt1 is controlled via its export from the nucleus, whereas in *S. pombe*, *Drosophila*, and humans Cdt1 protein levels are high in G1 phase and become reduced as the cell cycle progesses (Nasheuer et al, 2006). In higher eukaryotes, including humans, Cdt1 is in addition inactivated in a cell cycle-dependent manner via the binding of the protein geminin in S and G2 phase (McGarry & Kirschner, 1998). Geminin localises to the nucleus and is degraded in mitosis, therefore being absent in G1 when pre-RC is formed. It accumulates in S and G2 phase cells to inactivate Cdt1 (McGarry & Kirschner, 1998) preventing its renewed association to chromatin until the next mitosis.

Pre-RC formation occurs as Mcm2-7 is loaded as a double hexamer, which upon activation mediates bi-directional progression of the replication machinery (Gambus et al, 2006; Remus et al, 2009). Formation of the pre-RC complex does not ensure the activation of an origin, as it has been shown that only 10% of

licensed origins fire, where 90% remain dormant under normal conditions, with dormant origins fired in cases of replication stress, serving as a sort of back up system (Ge et al, 2007; Ibarra et al, 2008). Origins of replication seem to be organised into so-called "replication domains" comprised of adjacent clusters of 5-10 origins which fire almost simultaneously (Alabert & Groth, 2012). A possible explanation for this phenomenon is the three dimensional structure of these regions, with origins of replication brought into close proximity via the formation of chromatin loops (Buongiorno-Nardelli et al, 1982; Courbet et al, 2008), possibly mediated by encircling of chromatin fibres by the cohesin protein complex (Alabert & Groth, 2012; Guillou et al, 2010). Indeed cohesin itself is enriched at origins and depletion of the RAD21 cohesin subunit increases the size of chromatin loops and reduces the number of active origins of replication (Guillou et al, 2010) (Figure 2). Origins of replication fire in a sequential manner, with megabases of DNA termed "timing domains" replicating at similar times and the timing of origin firing correlates well with the local chromatin environment (Alabert & Groth, 2012). DNA replication in

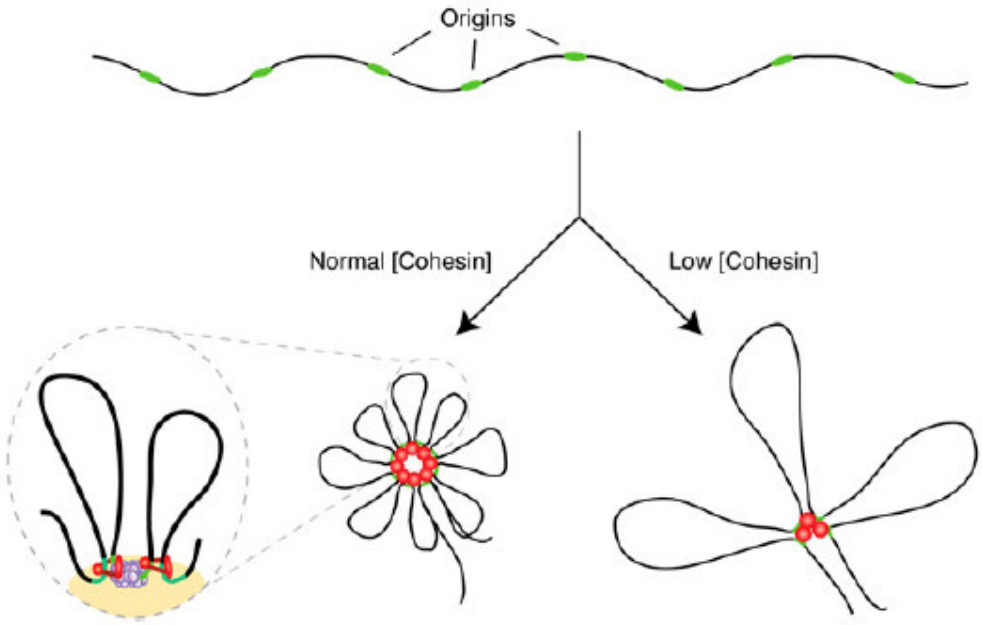

Figure 2: Chromatin loop model for origin firing
Origins of replication are brought into close spatial proximity via cohesin-mediated formation of chromatin loops. (Figure adapted from (Guillou et al, 2010))

early S phase correlates with DNA accessibility (Bell et al, 2010; Hansen et al, 2010) and with histone H4K16 acetylation (Schwaiger et al, 2009) with more heterochromatic regions replicating later in S phase (Alabert & Groth, 2012).

Activation of the pre-RC is mediated by CDKs and DDK which act in a cell cycle-dependent manner to allow the binding of Cdc45 and the GINS (go-ichi-ni-san (five-one-two-three)) complex to the Mcm2-7 proteins (Blow & Dutta, 2005; Nasheuer et al, 2006), with Cdc45 recruitment to the preRC dependent on Cdc7-Dbf4 and Cdk2-cyclin E (Chou et al, 2002). Formation of the CMG (Cdc45-MCM-GINS) complex occurs in a Ctf4/And-1-, RecQL4-, and Mcm10-dependent manner (Im et al, 2009) and the formation of this complex is essential for full MCM helicase function and the initiation of DNA replication (Blow & Dutta, 2005; Nasheuer et al, 2006). Activation of the helicase function of MCM complex allows for the formation of a larger multi-subunit protein machinery which mediates the elongation phase of DNA replication (Nasheuer et al, 2006) (Figure 3). Activation of this helicase complex mediates origin "firing" and mediates the formation of a replication fork, in which the protein machinery that mediates DNA replication progresses away from the origin of replication in a bi-directional manner (Alabert & Groth, 2012). Activation of the replicative helicase creates single-stranded DNA (ssDNA) which is coated by RPA (Replication Protein A) while the RNA primer for DNA replication is synthesised by Pol-prim (DNA Polymerase α-primase), which are recruited to chromatin in an Mcm10 and Ctf4-And-1-dependent manner (Zhu et al, 2007).

The RNA primer is then elongated by the DNA polymerase activity of Pol-prim with RNA–DNA recognized by RFC (replication factor C) which loads PCNA (proliferating-cell nuclear antigen) (Blow & Dutta, 2005; Nasheuer et al, 2006). RFC and PCNA, together with RPA, allow a polymerase switch from Pol-prim to Pol ε and δ (DNA polymerase ε or δ), to mediate continuous DNA synthesis on the leading strand and discontinuous DNA synthesis on the lagging strand, respectively (Blow & Dutta, 2005; Nasheuer et al, 2006). On the lagging strand the elongating DNA polymerases cause the formation of Okazaki fragments, which form continuous new strand via the actions of RNAse H, Fen1 (flap endonuclease 1), Dna2, Pol δ and DNA ligase 1 (Blow & Dutta, 2005; Nasheuer et al, 2006). In addition to these factors, recent studies show that other proteins including

topoisomerase 1, which is recruited to sites ahead of the replication fork to relieve tortional stress on the DNA caused by super-coiling (Takeda & Dutta, 2005) form part of the RPC, as well as Claspin/Timeless/Tipin and And1 complex, which form the so-called "fork protection complex", play important roles in determining replication rates, checkpoint responses and fork-stabilizing (Errico et al, 2009; Szyjka et al, 2005) with unloading of the MCM helicase at late S phase regulated by MCM-binding proteins (Nishiyama et al, 2010).

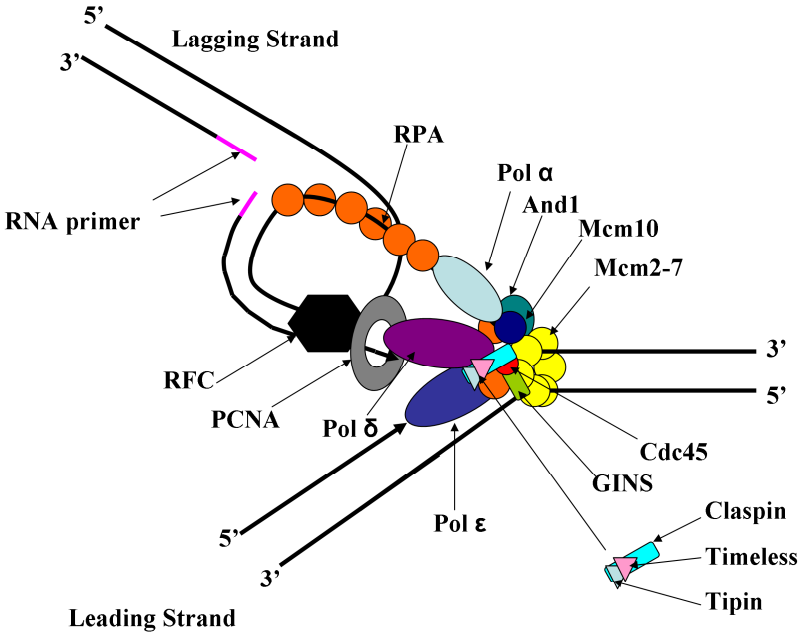

Figure 3: Schematic diagram of the main components of the RPC
Represented diagrammatically is a simplified depiction of the various proteins which work in concert as part of the RPC to mediate continuous and discontinuous DNA replication on the leading and lagging strands, respectively. (Figure adapted from (Broderick & Nasheuer, 2009))

1.3 The role of Cdc45 in DNA replication

The Cdc45 protein plays a key role in the initiation and elongation phases of DNA replication, with chromatin association of Cdc45 corresponding well with origin activation (Masuda et al, 2003). Cdc45 is a part of the CMG complex at replication origins shortly before the onset of S phase and forms the core of the RPC after

initiation (Aparicio et al, 2009). It has been demonstrated that chromatin association of Cdc45 is dependent on Cdc7-mediated phosphorylation of Mcm4 protein (Masai et al, 2006) As this only occurs in late G1- and S-phase, this regulation of Cdc45 protein may then finally control the initiation of DNA replication (Broderick & Nasheuer, 2009). This implies that Cdc45 may represent a 'limiting factor' in the imitation of DNA replication (Broderick & Nasheuer, 2009). Recent data indicate that Cdc45 progresses from formation of the CMG complex at the onset of S phase to a larger RPC complex present at the elongation phase of DNA replication during S phase. (Gambus et al, 2006). Another recent study has elucidated the structure of the CMG complex, giving a structural basis for its helicase function (Costa et al, 2011). Protein-protein interaction studies lend credence to this model, with human Cdc45 shown to interact with Mcm5, Mcm7 and members of the GINS complex (Bauerschmidt et al, 2007), with interactions between Cdc45 and the replicative Pols δ and ε observed only in S-phase cells (Bauerschmidt et al, 2007). Cdc45 is also shown to interact with Claspin, a member of the fork protection complex, which forms part of the RPC at S phase (Uno & Masai, 2011). The current model suggests that in the RPC, Cdc45 forms a molecular bridge between the helicase and DNA polymerase components of the complex (Broderick & Nasheuer, 2009).

1.4 Subcellular localisation of Cdc45

Initial Studies in *Saccharomyces cerevisiae* expressing GFP-Cdc45 show a clearly nuclear localisation of the yeast fusion protein (Hopwood & Dalton, 1996). The authors also use a bioinformatic approach to identify a putative bipartite NLS in yeast Cdc45 KRGNSSIGPNDLSKRKQKKK at aa 209-228. Studies in other model organisms confirm this nuclear localisation, with Cdc45 C-terminally tagged with 3 x HA tag in trypanosomes showing an apparently nucleoplasmic localisation during inter-phase (Dang & Li, 2011). At mitosis in these organisms

Cdc45 is found in the cytoplasm with apparent nuclear export of Cdc45 at this stage of the cell cycle, as this localisation is abrogated and nuclear localisation restored by treatment with leptomycin-B treatment (Dang & Li, 2011). A study of the interactions of MCP1 protein with components of the replication machinery in human MO59K cells using an antibody raised against Cdc45 shows nucleoplasmic

localisation of Cdc45 in interphase cells with no clear exclusion of Cdc45 from the nucleolus (Bronze-da-Rocha et al, 2011).

In a study by Bauerschmidt and colleagues (Bauerschmidt et al, 2007), HeLa S3 cells synchronised at various cell cycle stages by consecutive thymidine block, and using the C45-3G10 monoclonal antibody for Cdc45 show a diffuse nucleoplasmic localisation in G1 phase with no clear nucleolar exclusion, a punctuate nucleoplasmic localisation in S phase cells with clear nucleolar exclusion and a less punctate signal in G2 cells with no clear nucleolar exclusion. Mitotic cells show that Cdc45 signal is still present but is distinct from DNA (Bauerschmidt et al, 2007). In the case of S phase cells observed, HCl denaturation was employed to visualise incorporated BrdU. It is of note to observe that in this study no immunofluoresence data are provided from asynchonous cells instead of thymidine-treated, HCl denaturated or detergent extracted.

1.5 Bioinformatic analyses of Cdc45

Bioinformatic analyses of Cdc45 identify several D-box and KEN box motifs, which are consensus sequences for substrates of the APC/C indicating that Cdc45 may be a novel substrate for this complex (Pollok & Grosse, 2007). These motifs are commonly ubiquitinylated (Pollok & Grosse, 2007). Initial evidence suggests that Cdc45 is degraded via the ubiquitin-mediated proteasome although no evidence of direct ubiquitinylation of Cdc45 is yet known. Another bioinformatic analysis of Cdc45 shows that Cdc45 is the ortholog of the *E. coli* RecJ protein, with similarities in sequence between the N-terminal region of RecJ and of Cdc45 observed (Sanchez-Pulido & Ponting, 2011). This region of RecJ has exonuclease activity, though the authors fail to demonstrate that Cdc45 has any activity *in vitro* or *in vivo* as an exonuclease (Sanchez-Pulido & Ponting, 2011). These findings have recently been corroborated, with another bioinformatic analysis showing that a relationship among eukaryotic Cdc45 proteins and a large family of phosphoesterases, the DHH family, including inorganic pyrophosphatases and RecJ ssDNA exonucleases exists (Krastanova et al, 2011). These enzymes catalyse the hydrolysis of phosphodiester bonds via a mechanism involving two Mn2+ ions and only a subset of the amino acids that coordinate Mn2+ are conserved in Cdc45 (Krastanova et al, 2011). The authors also demonstrate that like RecJ exonucleases, recombinant human Cdc45 protein is able to bind single-stranded, but not double-stranded DNA but the authors

do not report that Cdc45 has exonuclease activity (Krastanova et al, 2011). The authors suggest that Cdc45 originated from an ancestral 5'-3' exonuclease which during evolution lost its catalytic activity and only retained the ability to bind single-stranded DNA. Bioinformatic analyses of Cdc45 to date all fail to find any conserved helicase or DNA binding domains, suggesting that Cdc45 itself lacks catalytic activity in DNA replication and in all likelihood exsists as a helicase co-factor.

1.6 Cdc45 as a therapeutic target in cancer cells

Cdc45 has been demonstrated to be a proliferation associated antigen, with western blot analyses demonstrating that hat Cdc45 protein is absent from long-term quiescent, terminally differentiated and senescent human cells, although it is present throughout the cell cycle of proliferating cells (Pollok et al, 2007). Cdc45 protein level was shown to be higher in human cancer-derived cells compared with primary human cells and the authors demonstrated that tumour tissue was preferentially stained using Cdc45-specific antibodies (Pollok et al, 2007). Indeed, Cdc45 has recently been demonstrated to be a novel tumour associated antigen (TAA) and therapeutic target in lung cancer immunotherapy with potential immunogenic peptides of Cdc45 generated (Tomita et al, 2011). In this study, Cdc45 was expressed in the majority of lung cancer tissues, but not in the adjacent non-cancerous tissues or in many normal adult tissues (Tomita et al, 2011). The authors examined the *in vitro* and *in vivo* anti-tumour effects of cytotoxic T-lymphocytes (CTL) specific to Cdc45-derived peptides and identified three peptides that could reproducibly induce Cdc45-specific CTL from both healthy donors and lung cancer patients (Tomita et al, 2011). These Cdc45-derived peptides were shown to be highly immunogenic epitopes that might be a useful target for lung cancer immunotherapy (Tomita et al, 2011). Lung cancer itself is the most common form of cancer and is the leading cause of death from cancer-associated disease, accounting for 1.18 million of the 6.7 million cancer-related deaths worldwide. (Tomita et al, 2011). Therefore, novel therapeutic drugs in this field have a great potential.

1.7 Protein-protein interactions of Cdc45

Cdc45 forms part of the CMG complex, and has been found to co-IP in human cells with Mcm5, Mcm7, members of the GINS complex and to interact with the replicative Pols δ and ε only in S-phase cells (Bauerschmidt et al, 2007). In human cells, Cdc45 has also been shown to interact with the DUE-B protein in pre-initiation complex formation (Chowdhury et al, 2010), and with TopBP1 at the G1/S-transition (Schmidt et al, 2008). Using bimolecular fluorescence complementation assays in HeLa cells it was suggested that Cdc45 may interact with human Mcm2, Mcm6 and Sld5 (Im et al, 2009). Studies in yeast demonstrate that CDC45 interacts with Sld3 (Kamimura et al, 2001) Mcm2, RPA, Pol ε (Zou & Stillman, 2000), Mcm5 (Hopwood & Dalton, 1996), Mcm7 (Dalton & Hopwood, 1997), Mcm10 (Araki et al, 2003) and Mrc1 (Zhao & Russell, 2004) protein. The latter is the yeast homologue for human Claspin. Cdc45 has been shown to interact *in vivo* with Claspin in Xenopus egg extracts. *In vitro* assays report that aa265–605 of Claspin associates with Cdc45, Pol ε, RPA, and two RFC complexes on chromatin (Lee et al, 2005). In a recent study, Claspin was also shown to interact with Cdc45 *in vivo* in human cells. Additional *in vitro* experiments show that human Claspin interacts with Cdc45 via its aa1-851 and that Cdc45 functionally interacts with RPA in human cells (Nakaya et al, 2010; Sercin & Kemp, 2011).

1.8 DNA damage and DNA-damage checkpoint respone

Genomic DNA can become damaged via exogenous sources (UV light, which induces abberant DNA structures, or ionising radiation, which induces DNA double strand breaks) or endogenous sources (reactive oxygen species and free radicals) (Nasheuer et al, 2002). UV light with a wavelength of 254nm (UVC) can cause covalent cross-linking between adjacent pyrimidines on the same strand of genomic DNA, with the predominant UV photoproducts being the cyclobutane pyrimidine dimer (CPD), the most common of which are the thymine dimer and the 6-4 photoproduct (6-4PP), which occurs between adjacent thymine and cytosine (Friedberg et al, 2006; Mitchell & Nairn, 1989).

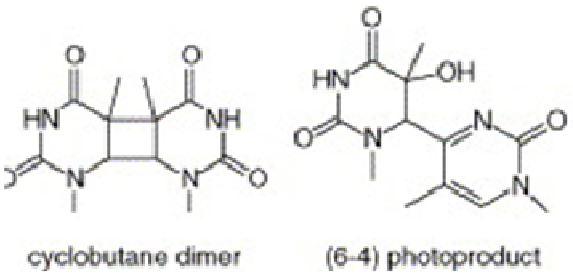

Figure 4: Lewis structures of UVC photoproducts
Depicted are the cycobutane pyrimidine dimer (CPD) and the (6-4) photoproduct. (Figure adapted from (Cadet et al, 2005))

In order to maintain genome stability after DNA damage, eukaryotic cells have established various processes to repair DNA lesions and posses mechanisms to initiate DNA damage-dependent signalling pathways and to establish DNA damage-dependent checkpoints throughout the cell cycle, which arrest cells in certain cell cycle phases to facilitate repair of damaged DNA or apoptosis of the cell (Levy et al, 2009). These checkpoint pathways are essential to diminish genome instability of eukaryotic cells and tumour development in humans (Bartkova et al, 2006; Di Micco et al, 2006; Levy et al, 2009). Cell cycle checkpoints perform at least two important functions. Firstly, they ensure that essential events are completed in the cell cycle before subsequent downstream events are initiated (Kaufmann, 2007). For example it is detrimental to the cell to initiate mitosis before DNA replication and chromatin condensation are completed in S and G2, respectively (Kaufmann, 2007). Checkpoints block the progression into mitosis when DNA replication is incomplete or chromatin condensation is insufficient (Kaufmann, 2007). Failures of such checkpoints can cause allelic deletions and chromatid mis-segregation (Kaufmann, 2007). Secondly, DNA damage checkpoints recognize the presence of damage to genomic DNA and subsequently delay or arrest DNA replication and mitosis to facilitate repair of the damage (Kaufmann, 2007). For example, it is detrimental to the cell to initiate DNA synthesis when template strands are damaged, as this may induce mutations and chromosomal aberrations via the replication of damaged DNA (Kaufmann, 2007). These checkpoints mediate a cells progression through the cell cycle via active, enzyme-mediated signalling pathways (Kaufmann, 2007). Cells activate signal transduction pathways mediated by sensor, transducer and effector proteins in response to DNA damage. These

pathways control a wide variety of processes including cell-cycle arrest, DNA repair pathways, modulate transcriptional activity and may lead to programmed cell death via apoptosis in some cell types (Zhou & Elledge, 2000).

One class of signal transducers are the phosphatidylinositiol-3 kinase (PIK)-like kinase family, which include the ATM (ataxia telangiectasia mutated) and ATR (ATM-Rad3-related) proteins in mammals and their homologues in yeast (Zhou & Elledge, 2000). In addition, these transducers act upstream in the regulation of two checkpoint kinases Chk1 and Chk2, which act in a sub-set of the damage response involved in cell-cycle regulation (Zhou & Elledge, 2000).

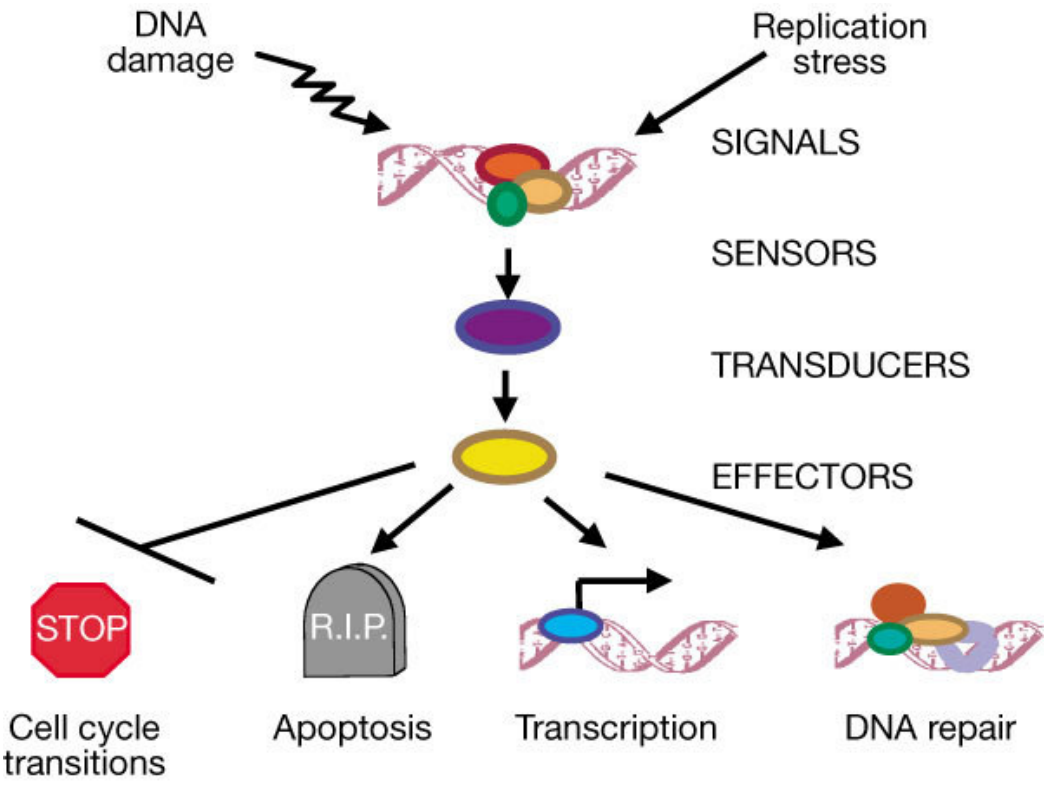

Figure 5: Hierarchical model of the DNA damage reponse
Depicted is the hierarchical model of DNA damage response, whereby DNA damage detected by sensor proteins triggers an amplifying signalling cascade mediated by transducer and effector proteins, culminating in various outcomes for the cell. (Figure adapted from (Zhou & Elledge, 2000))

1.9 The intra-S-phase checkpoint response to ionising radiation.

Studies have established an intra-S-phase signalling pathway from sites of DNA damage through the checkpoint kinases ATM and ATR to p53 and then from p53 to the CDK inhibitor p21 in response to DNA double strand breaks (Kaufmann, 2007). While p21 is required for the G1 checkpoint response to IR, there are many other genes which are induced by p53 following DNA damage which affect cell proliferation, including CEBP-a, BTG2, PLK2, PLK3, GADD and PLAB (Kaufmann, 2007). The intra-S-phase checkpoint response to IR-induced DNA double strand breaks (DSBs) requires ATM, MRE-11 and NBS1, and appears to signal through apparently two separate branches to inhibit replicon initiation (Falck et al, 2002; Yazdi et al, 2002). One branch involves activation of Chk1 and Chk2 that mediate the phosphorylation of Cdc25A. Studies using *Xenopus* egg extracts demonstrated that this is a p53-independent mechanism of G1 arrest in response to IR (Costanzo et al, 2000) and showed that kinase activity of cyclin E/Cdk2 is rapidly inhibited after IR through a p53-independent mechanism. This pathway involves ATM signalling through Chk1 and Chk2 to phosphorylate Cdc25A and stimulate its proteolytic degradation. As Cdc25A phosphatase activates cyclin E/Cdk2, degradation of Cdc25A leads to inhibition of the latter. This pathway for inactivation of Cdc25A and inhibition of cyclin E/Cdk2 appears to account for a major component of the intra-S checkpoint response to IR that slows the rate of replicon initiation in S phase cells (Falck et al, 2001).

A second arm of the ATM-dependent intra-S-phase checkpoint response proceeds through the cohesin subunits, Smc1 and Smc3 (Kim et al, 2002; Luo et al, 2008; Yazdi et al, 2002). Smc1 forms a heterotetrameric complex with Smc3, Scc1 and SA1 or SA2 to form cohesin. Cohesin is a ring-like protein complex that can encircle the two DNA duplexes. The chromatin loading of cohesin is dependent upon DNA replication and is loaded onto newly replicated DNA (Onn et al, 2008). Cohesion between daughter duplexes as enforced by cohesin acts to enhance recombinational repair of DNA double strand breaks (Strom et al, 2007; Unal et al, 2007). It is thought that cohesin maintains daughter duplexes in spatial proximity and sequence alignment (Kaufmann, 2009). In this model, damage in one chromatid and the other undamaged chromatid are proximal and

are aligned to facilitate error-free recombinational repair of the double-strand break (Kaufmann, 2009).

1.10 The intra-S-phase checkpoint response to UVC.

The intra-S-phase DNA damage checkpoints slow down the rate of replicon initiation following UVC-mediated DNA damage to allow DNA repair and also to stabilise stalled DNA replication forks (Kaufmann, 2009). When intra-S-phase checkpoint function is disabled, stalled replication forks are prone to collapse leading to DNA double strand breaks and gene deletions or rearrangements (Kaufmann, 2009). Replication fork stalling occurs when RPCs encounter UV-induced lesions in DNA or in cases where dNTP abundance has been compromised, such as following treatment with hydroxyurea (Smith et al, 2009; Van et al, 2010). The helicase component of the RPC continues to unwind the DNA whereas the replicative DNA polymerases are stalled by the encounter of abnormal DNA structures or the lack of available dNTPs (Smith et al, 2009; Van et al, 2010). This causes an excess of ssDNA which is coated by RPA and leads to the recruitment of ATR by ATRIP (Kaufmann, 2009). Junctions of duplex and ssDNA also recruit an alternative form of the RFC complex, in which RFC1 is replaced by Rad17 (Kaufmann, 2009). The Rad17-RFC complex loads the 9-1-1 checkpoint clamp at the stalled replication fork with phosphorylation of Rad9 creating a binding site for TopBP1, an activating cofactor for ATR, which stimulates ATR phosphorylation and leads to subsequent activation of Chk1 which then transduces the checkpoint signal throughout the cell (Kaufmann, 2009). In this checkpoint, the fork protection complex, comprised of Claspin, Tim and Tipin acts as a mediator of Chk1 phosphorylation (Kaufmann, 2009).

1.11 The role of Cdc45 in the intra-S-phase checkpoint.

Cdc45 is the main target of a Chk1-mediated S-phase checkpoint, which operates via a Cdc25A/CDK2- independent mechanism (Liu et al, 2006). In this study DNA damage induced by BPDE (benzo[a]pyrene dihydrodiol epoxide), a UVC-mimetic drug, caused a reduction in the affinity for chromatin of Cdc45 as assayed by biochemical fractionation and western blotting (Liu et al, 2006). This was accompanied by Chk1 activation and the inhibition of DNA synthesis with a

reduction of the association between Cdc45 and Mcm7 observed in the chromatin-associated fraction generated, with no change in co-IP observed in the detergent-soluble fraction (Liu et al, 2006). Moreover, Cdc45 was shown to dissociate from a known origin of replication after BPDE treatment by ChIP assay (Liu et al, 2006). These effects were ablated by inhibition or RNAi interference of Chk1 protein (Liu et al, 2006).

1.12 The role of Claspin in the intra-S-phase checkpoint and in DNA replication.

Claspin mediates the intra-S-phase checkpoint response to replication stress by facilitating phosphorylation of Chk1 by ATR (Petermann et al, 2008). Human Claspin is constitutively associated with ATR, and phosphorylation of Claspin facilitates its interaction with Chk1 (Chini & Chen, 2003) Claspin is required for the promotion of Chk1 phosphorylation (Lee et al, 2005) and Chk1 has been shown to stabilise Claspin in HeLa cells (Chini & Chen, 2006). A recent study shows that the replication fork interaction domain (RFID) of Claspin in Xenopus contains two basic patches (BP1 and BP2) at aa 265–331 and 470–600 with deletion of either BP1 or BP2 compromising optimal binding of Claspin to chromatin and that removal of BP2 caused a large reduction in the Chk1-activating potency of Claspin (Lee et al, 2005). Xenopus Claspin contains a small Chk1-activating domain (aa 776–905) that does not bind stably to chromatin, but it is fully effective in the activation of Chk1 if present in high concentration. Moreover, Xenopus Claspin interacts via aa265-605 with Cdc45 (Lee et al, 2005). A functional characterisation of human Claspin corroborates these data, and it was demonstrated that the interaction between Claspin and Cdc45 is mediated by aa1-851 of Claspin, with Chk1, Pol ε and Rad17-RFC interaction mediated by the C-terminus of Claspin.

Claspin also functions in controlling the rates of DNA replication during the normal cell cycle. Claspin has been shown to be a ring-shaped protein that binds to replication fork structures (Sar et al, 2004) with Xenopus Claspin binding to chromatin in a pre-replicative complex and in a Cdc45-dependent manner (Lee et al, 2005). Chk1 is also required for high rates of global replication fork progression, and Claspin-depleted human cells display reduced rates of replication fork progression similar to those observed in Chk1-depleted cells but lower reduction of

fork progression was observed in primary human 1BR3 fibroblasts (Petermann et al, 2008). This reduction of fork progression did not depend on a lack of Chk1 phosphorylation since Claspin-depleted cells retained significant levels of Chk1 phosphorylation at both Ser317 and Ser345 (Petermann et al, 2008).

1.13 Intra-S-phase checkpoint signalling and translesion DNA synthesis.

In higher eukaryotic cells, translesion synthesis (TLS) is mediated by Y family DNA polymerases including the polymerases η, ι and κ and the Rev1 protein.. The DNA polymerase ζ, a member of the B family of polymerases is also involved in TLS (Prakash et al, 2005). In contrast to the replicative DNA polymerases, which replicate the eukaryotic genome with very few errors but cannot replicate through CPDs or 6-4PPs, the enzymes that mediate TLS are comparatively error prone but are able to incorporate nucleotides opposite these lesions (Prakash et al, 2005). In TLS, PCNA provides a role as a scaffolding protein, allowing the various TLS DNA polymerases to gain access to the DNA replication machinery at stalled replication forks in order to carry out efficient TLS (Prakash et al, 2005). Although there is little data available on how the replicative polymerases are disengaged at stalled replication forks, and how the loading and unloading of TLS polymerases are regulated recent studies identify that Rad6-Rad18-mediated ubiquitinylation of PCNA plays a crucial role in this process (Prakash et al, 2005).

Activation of the intra-S-phase checkpoint and polymerase-switching mechanisms at stalled replication forks are tightly linked, as Rad6, a ubiquitin-conjugating enzyme and Rad18, a ssDNA-binding protein, form a ubiquitin ligase complex that mono-ubiquitylates PCNA at lysine 164 in response to UVC-induced DNA damage are required for this process (Kannouche et al, 2004; Watanabe et al, 2004). This ubiquitylation of PCNA appears to be required for pol η-dependent bypass of CPDs (Kannouche et al, 2004; Watanabe et al, 2004). Rad18-dependent PCNA mono-ubiquitylation also may also be required for switching of DNA polymerase κ with replicative DNA polymerases in the bypassing of BPDE–DNA adducts (Bi et al, 2005). Inactivation of ATR and Chk1 reduced the mono-ubiquitylation of PCNA by 50% in H1299 cells, demonstrating a connection between the intra-S-phase checkpoint response to

replication fork stalling and ubiquitin-mediated polymerase switch for efficient bypass of BPDE–DNA adducts (Heffernan et al, 2007).

Interestingly, Chk1 protein but not its catalytic activity is required for PCNA ubiquitylation in HeLa cells (Yang et al, 2008). As depletion of Claspin and Timeless also lead to a reduction in PCNA ubiquitinylation (Yang et al, 2008), and the depletion of Chk1 destabilises Claspin (Chini et al, 2006; Yang et al, 2008), it is reasonable to deduce that that Claspin and Timeless must both be present for the Rad6–Rad18 complex to monoubiquitylate PCNA at stalled replication forks. These data suggest a close link between proteins which mediate the intra-S-phase checkpoint response and TLS.

1.14 Differential activation of the intra-S-phase checkpoint by CPDs and 6-4PPs.

By blocking DNA polymerization, UV-induced photoproducts (CPDs and 6-4PPs) cause discontinuities in newly replicated DNA strands that are subsequently processed by translesion DNA synthesis and by nucleotide excision repair (NER) (Kaufmann, 2009). Analysis of the kinetics of Chk1 phosphorylation in UVC-damaged human fibroblasts suggests that 6-4PPs and not CPDs are the lesion that activates the intra-S-phase checkpoint (Chen et al, 2009). In this study, quantification of UVC-induced CPDs and 6-4PPs showed that 80% of the 6-4PPs were removed from DNA within 3 h after irradiation with 12 J/m^2 UVC whereas 75% of CPDs remained in the DNA. Analysis of Chk1 phosphorylation showed that rapid removal of 6-4PPs by NER was associated with subsidence of the phospho-Chk1 detection. At a time (6 h post- UVC) when the signal of phosphorylated Chk1 had decreased to background levels the majority of the UVC-induced CPDs still remained in DNA. This result implies that the CPDs that remain in S phase cells do not activate the intra-S checkpoint.

It is therefore conceivable that the processing of CPDs by TLS occurs so rapidly that insufficient uncoupling of helicase and polymerase and therefore insufficient amounts of RPA-coated ssDNA occur to activate the intra-S-phase checkpoint (Kaufmann, 2009). The 6-4PP photoproduct itself cannot be processed only by polymerase eta during TLS. Here, bypass requires a more complicated process of polymerase switching requiring other factors, for example hREV3 protein has

been shown to be required for efficient TLS in human fibroblast cells (Li et al, 2002). This less efficient TLS at 6-4PP may then generate sufficient fork stalling and hence ssDNA coated by RPA to cause the activation of the intra-S-phase checkpoint. A second independent analysis is consistent with this model. XP variant cells lacking polymerase eta-dependent TLS across TT CPDs display the consequences of fork stalling at both CPDs and 6-4PPs (Boyer et al, 1990).

1.15 Nucleotide excision repair.

The nucleotide excision repair (NER) pathway consists of a series of enzymatic reactions by which DNA damage caused by UVC-induced photoproducts or similar DNA lesions induced by certain chemicals or reactive oxygen species are recognized and repaired (Cleaver et al, 2009). Depending upon whether DNA damage occurs in a transcriptionally active or inactive region of the genome, repair can be mediated by two different pathways: global genomic repair (GGR) or transcription-coupled repair (TCR) (Cleaver et al, 2009). Damage in transcriptionally active regions is detected via arrest of transcription machinery by stalling of RNA polymerase (RNA Pol) I or II (Cleaver et al, 2009). Transcriptional arrest is enhanced by binding of Cockayne syndrome A (CSA) and CSB proteins, both of which are required for ubiquitylation of the carboxy-terminal domain of RNA Pol II. This polyubiquitylated RNA Pol II at sites of stalled transcription is subsequently removed and degraded via the proteasome (Cleaver et al, 2009).

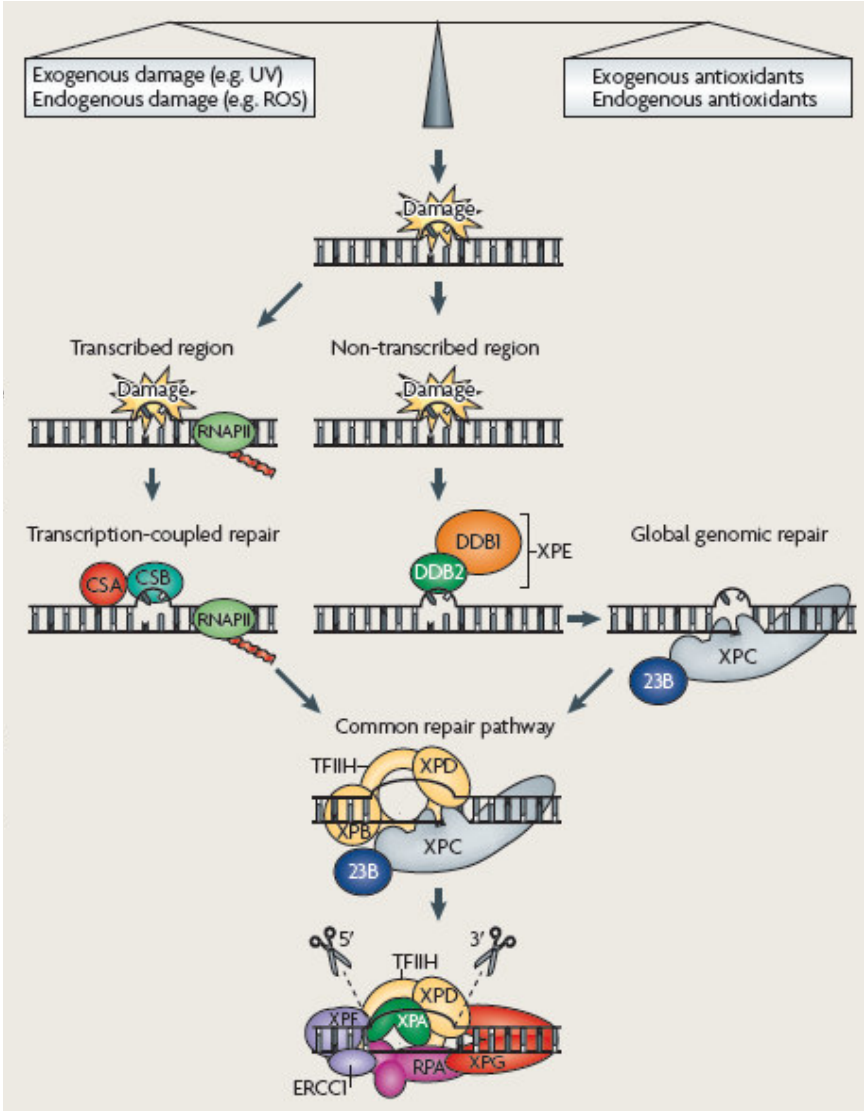

Figure 6: Summary of nucleotide excision repair
Diagram representing NER via the global genome repair (GGR) and transcription-coupled repair (TCR) pathways. (Figure adapted from (Cleaver et al, 2009))

Damage in transcriptionally inactive regions is detected by the DNA damage-binding protein XPC complex and XPE complex, consisting of DNA damage binding proteins 1 and 2, thereby mediating global genomic repair (Cleaver et al, 2009). Damage recognition then allows the binding of a ten-subunit basal transcription factor TFIIH through interaction with either XPC in GGR or the arrested transcription apparatus in TCR (Cleaver et al, 2009). XPD (also known as ERCC2) is a component of TFIIH and is a DNA helicase which acts in a 5′ to 3′ manner, unwinding of the DNA in the vicinity of a damaged base (Cleaver et al, 2009). ATP hydrolysis by the XPB component of TFIIH then allows binding

of the NER complex to the site of DNA damage (Cleaver et al, 2009). The DNA around the damaged site is then cleaved by the XPG 3′ nuclease, and the XPF–ERCC1 5′ nuclease (Cleaver et al, 2009). XPG is bound through interaction with XPC and TFIIH and both nucleases are held in place by XPA–RPA complexes bound to the exposed ssDNA, which defines the cleavage sites and denotes strand specificity (Cleaver et al, 2009). Once the damaged oligonucleotide is removed, re-synthesis of the excised region occurs, mediated by PCNA, Pols δ, ε or κ and a DNA ligase, which in quiescent cells requires the X-ray repair cross-complementing protein 1 (XRCC1) and in proliferating cells DNA ligase I (Cleaver et al, 2009)

1.16 Overlap of NER and intra-S-phase checkpoint signalling

Initial studies suggested that human fibroblasts lacking XPA protein had an efficient intra-S-phase checkpoint response when challenged with low fluences of UVC (Kaufmann & Schwartz, 1981). These results were interpreted that NER was not required for the inhibition of replicon initiation and the activation and downstream signalling of the intra-S-phase checkpoint (Kaufmann, 2009). However, recent reports showed a role for XPA, a protein involved in NER, in the activation of the intra-S-phase checkpoint (Bomgarden et al, 2006). XPA-deficient human fibroblasts have reduced activation of Chk1 when compared to isogenic cells where the XPA gene had been re-integrated at 1h and 2h post-UVC treatment, but not at time points after 4h (Bomgarden et al, 2006). The authors also showed that XPA was needed for rapid recruitment or ATR/ATRIP to nuclear foci following UVC treatment. These results suggest that although the presence of XPA was not necessary for Chk1 activation, it affected the kinetics of activation of the intra-S-phase checkpoint (Kaufmann, 2009).

Examination of the requirement of NER factors for activation of the intra-S-phase checkpoint revealed that no other NER proteins are needed for efficient activation of the intra-S-phase checkpoint or effect the kinetics of its activation in any way (Kaufmann, 2009). This implies that XPA itself has a role separate from NER in the activation of the intra-S-phase checkpoint and suggests that as XPA can bind to UVC-induced DNA damage and in some way enhances the phosphorylation of Chk1 by ATR (Kaufmann, 2009). Given that XPA and RPA have a high affinity for

one another (Reardon & Sancar, 2004) and that both proteins have a higher binding affinity to 6-4PPs than to undamaged DNA (Reardon & Sancar, 2003), it is reasonable to assume that these proteins work in concert to enhance assembly of intra-S-phase signalling machinery at sites of stalled replication forks caused by 6-4PPs.

Cep164, a protein involved in primary cilia formation, has also been shown to have a role in activation of the intra-S-phase checkpoint (Pan & Lee, 2009; Sivasubramaniam et al, 2008). siRNA-mediated depletion of Cep164 caused a severely reduced activation of Chk1 following UVC treatment (Pan & Lee, 2009). Cep164 was phosphorylated by ATR and interacted with XPA with higher affinity following UVC treatment than in mock-treated cells (Pan & Lee, 2009). These data support a hypothesis that the XPA-Cep164 complex may mediate the phosphorylation of Chk1 by ATR.

Given the high affinity of XPA and RPA for ssDNA with 6-4PPs (Reardon & Sancar, 2004) it is reasonable to propose that S phase cells suppress the assembly of the NER machinery on this lesion when it occurs within a stalled replication fork. The assembly the NER machinery on template strands could interfere with the polymerase-switch mechanism of post-replication repair, and could lead to strand scission and formation of a DNA double strand break. The reduction in 6-4PP repair in ATR-depleted S phase cells provides evidence that ATR may regulate a factor that regulates NER in S phase. Cep164 provides an attractive candidate for this factor, as it is phosphorylated by ATR and interacts with XPA, a component of the NER machinery (Kaufmann, 2009).

1.17 **Objectives**

The Cdc45 protein has been shown to be crucial for the initiation and elongation of DNA replication, and plays a role in the intra-S-phase checkpoint following DNA damage. Its physical interactions with cellular proteins have been analysed in model systems from yeast to humans, yielding some contradictions in these studies which need clarification. Moreover, the timing of the interaction of Cdc45 with other replication factors in the cell cycle, and the regulation of these interactions following activation of the intra-S-phase checkpoint are poorly understood.

An aim of this work was to characterise the protein-protein interactions of Cdc45, focusing on novel interactors or proteins whose association with Cdc45 has not been shown in a human model system. These characterisations would include an analysis of the timing of these interactions in the cell cycle and following activation of the intra-S-phase checkpoint. In addition, deletion mutants of Cdc45 would allow us to characterise the regions of Cdc45 that mediate its interactions with these proteins, adding to the current understanding of how the replication machinery operates.

The subcellular localisation of Cdc45 following activation of the intra-S-phase checkpoint is important for the regulation of the protein and, therefore, changes in distribution of Cdc45 following damage should be studied including the characterisation of the regions of Cdc45 that mediate its localisation to the nucleus using deletion mutagenesis.

As the model for how Cdc45 operates as part of the RPC has been put forward on the basis of biochemical and cell biological experiments, an aim of this thesis work was to use *in vitro* and *in vivo* methods to study this model. To this end, fluorescence correlation spectroscopy performed on eGFP-Cdc45 in living cells would examine the mobility and complex formation of Cdc45 in the cell cycle and following checkpoint activation. This would both validate our understanding of Cdc45's role in DNA replication and provide the technical means to study DNA replication in living cells.

Chapter 2

Cell cycle-dependent formation of Cdc45-Claspin complexes in human cells are compromized by UV-mediated DNA damage

2.1 Abstract

The replication factor Cdc45 has essential functions in the initiation and elongation steps of eukaryotic DNA replication and plays a role in the intra-S-phase checkpoint. Its interactions with other replication proteins during the cell cycle and after intra-S-phase checkpoint activation remain to be fully characterized. We find that the C terminal part of Cdc45 is important for its interactions with Claspin. The interactions of human Cdc45 with the three replication factors Claspin, replication protein A (RPA) and DNA polymerase δ are maximal during S phase. Following UVC-mediated DNA damage, Cdc45-Claspin complex formation is reduced whereas the binding of Cdc45 to RPA is not affected. We also show that treatment of cells with UCN-01, Caffeine or Wortmannin does not rescue the UV-mediated destabilisation of Cdc45-Claspin interactions, suggesting that the loss of interaction between Cdc45 and Claspin occurs independently of ATR activation in the intra-S-phase checkpoint.

2.2 Introduction

In eukaryotic cells the replication of the genome is strictly controlled and occurs only once per cell cycle (Nasheuer et al, 2002; Zegerman & Diffley, 2009). Errors in replication of chromosomal DNA lead to mutations in the genome and create the possibility of transformation of the cell to a malignant state (Hoeijmakers, 2001; Zegerman & Diffley, 2009). Eukaryotic DNA replication begins with the binding of the origin recognition complex (ORC) to origins of replication in early G1 phase of the cell cycle (Blow & Dutta, 2005; Masai et al, 2010). This allows Cdc6 (cell division cycle protein 6) and Cdt1 (Cdc10-dependent target) to associate with ORC on chromatin, which in turn is the base for the recruitment of other factors such as the Mcm2–7 (mini-chromosome maintenance 2 to 7) complex, forming the pre-replicative complex (preRC). Subsequently Cdc45 and the GINS [go-ichi-ni-san (five-one-two-three)] complex bind to the Mcm2-7 proteins and form the CMG complex (Cdc45-Mcm2-7-GINS), which is the replicative helicase in eukaryotes (Aparicio et al, 2009; Masai et al, 2010; Moyer et al, 2006; Nasheuer et al, 2006; Pospiech et al, 2010; Tsakraklides & Bell, 2010). Early in S phase the CMG helicase unwinds DNA at origins creating bi-directional replication forks and single-stranded DNA (ssDNA), which is subsequently bound by replication protein

A (RPA). Following this, DNA polymerase α-primase (Pol-prim) synthesizes the RNA primer at the origin of replication (Blow & Dutta, 2005; Ilves et al, 2010; Masai et al, 2010; Zhu et al, 2007). The binding of these proteins and additional factors outlined below allow the formation of the replisome progression complex (RPC) (Gambus et al, 2006) which facilitates continuous DNA synthesis on the leading strand and discontinuous DNA synthesis on the lagging strand (Blow & Dutta, 2005; Masai et al, 2010; Nasheuer et al, 2006). The Claspin/Timeless/Tipin and And1 complex, which form the so-called "fork protection complex" bind to RPCs and controls replication rates, checkpoint responses and fork-stabilizing (Errico et al, 2009; Szyjka et al, 2005).

The role of Cdc45 in DNA replication as a part of the CMG complex is regulated by the intra-S-phase DNA damage checkpoint and its expression is tightly regulating in quiescent cells and when the latter re-enter the cell cycle (Ilves et al, 2010; Liu et al, 2006; Masai et al, 2010; Pollok et al, 2007). In human cells Cdc45 has been shown to interact only in S phase cells with Mcm5, Mcm7, members of the GINS complex and the replicative Pols δ and ε (Aparicio et al, 2009; Bauerschmidt et al, 2007). Cdc45 has also been determined to interact with the DUE-B protein in pre-initiation complex formation, and with TopBP1 at the G1/S-transition in human cells (Chowdhury et al, 2010; Schmidt et al, 2008). Studies in yeast have revealed that Cdc45 interacts with Mcm2, Mcm5, Mcm7, Mcm10, Pol ε, RPA, Sld3 and Mrc1 protein, which is the yeast homologue for human Claspin (Araki et al, 2003; Dalton & Hopwood, 1997; Hopwood & Dalton, 1996; Kamimura et al, 2001; Zegerman & Diffley, 2009; Zhao & Russell, 2004; Zou & Stillman, 2000). Cdc45 has also been shown to interact with Claspin in Xenopus egg extracts (Lee et al, 2005) and recently in human cells (Uno & Masai, 2011).

Claspin is a mediator of the ATR- (Ataxia telangiectasia and Rad 3–related) dependent intra-S-phase checkpoint in human cells and also promotes DNA replication fork progression and stability (Sercin & Kemp, 2011). When the RPC encounters DNA lesions or reductions of dNTP levels, such as after cell treatment with hydroxyurea, the Mcm2-7 helicase continues to unwind the DNA whereas the replicative DNA polymerases are stalled by their encounter with abnormal DNA structures or by the lack of free dNTPs (Smith et al, 2009; Van et

al, 2010). This causes an excess formation of ssDNA, which is coated by RPA, and leads to the recruitment of ATR by ATRIP (ATR-interacting protein) (Broderick et al, 2010; Kaufmann, 2009). The Rad17-RFC2-5 complex loads the 9-1-1 checkpoint clamp (Rad9-Rad1-Hus1) at stalled replication forks. The phosphorylation of Rad9 creates a binding site for TopBP1, an activating cofactor for ATR, which stimulates ATR phosphorylation and leads to subsequent activation of Chk1 kinase, which then transduces the checkpoint signal further throughout the cell (Kaufmann, 2009; Nasheuer et al, 2002). In this checkpoint control system, the fork protection complex, comprised of Claspin, Tim and Tipin, acts as a mediator of Chk1 phosphorylation (Kaufmann, 2009).

Claspin has been shown to be a ring-shaped protein that binds to replication fork structures (Sar et al, 2004) with *Xenopus* Claspin binding to chromatin in a pre-replicative complex (preRC) and Cdc45-dependent manner (Lee et al, 2005). Currently it is hypothesized that Claspin mediates this checkpoint response to replication stress by facilitating the phosphorylation of Chk1 by ATR (Petermann et al, 2008). Human Claspin constitutively associates with ATR, and phosphorylation of Claspin facilitates its interaction with Chk1 (Chini & Chen, 2003). The latter is required for the phosphorylation of Chk1 and the kinase has been shown to stabilize Claspin in HeLa cells (Chini & Chen, 2006; Lee et al, 2005). The replication fork interaction domain of Claspin in Xenopus contains two basic patches (BP1 and BP2). Deletion of either BP1 or BP2 compromizes the optimal binding of Claspin to chromatin and removal of BP2 caused a reduction in Claspin-mediated Chk1-activation (Lee et al, 2005). Xenopus Claspin contains a small Chk1-activating domain that does not bind stably to chromatin but is fully effective at high concentrations for mediating activation of Chk1 (Lee et al, 2005). In addition to its role in mediating the intra-S-phase checkpoint, Claspin also functions in controlling the rates of DNA replication during the normal cell cycle (Petermann et al, 2008). A recent study shows that Claspin is required for normal rates of global replication fork progression (Petermann et al, 2008). In this study Claspin-depleted HeLa and HCT116 cells had replication fork progression rates which were slower than wild type cells and were similar to those observed in Chk1-depleted cells (Petermann et al, 2008).

As illustrated above, the protein-protein interactions of Cdc45 as part of the RPC are numerous, and in some cases the functional significance and timing in the cell cycle of these interactors are poorly understood. Therefore, it is important to know how the protein-protein interactions of Cdc45 are regulated after the activation of the intra-S-phase checkpoint, as the RPC encounters lesions which stall the replicative DNA polymerases, or after dNTP depletion. In addition, the question remains as to which regions of Cdc45 are involved in these protein-protein interactions. In this study, we show that Cdc45 reciprocally co-immuno-precipitates with both, Claspin and RPA, in human cells. Here, we found that the C-terminus of Cdc45 is important for its interaction with Claspin. We showed that these Cdc45-Claspin interactions are maximal during S phase. Following UVC-mediated DNA damage and dNTP depletion by hyrdroxyurea treatment, Cdc45-Claspin interactions are reduced whereas the binding of Cdc45 to RPA is not reduced. We also show that treatment of cells with UCN-01, Caffeine or Wortmannin does not rescue the UVC-mediated reduction of Cdc45-Claspin interactions, suggesting that this process is independently of ATR activation in the intra-S-phase checkpoint.

2.3 Results

2.3.1 Claspin and RPA32 co-immunoprecipitate with ectopically-expressed and endogenous Cdc45.

Human Cdc45 protein was transiently expressed in HeLa S3 cells carrying a single FLAG tag at its C-terminus to a level that was on average up to 3-fold higher than endogenous Cdc45 as determined by quantitative western blotting (data not shown). The affinity-purified recombinant FLAG-Cdc45 co-immunoprecipitated Claspin and RPA32 (Figure 1A and 1C). The levels of Claspin binding to Cdc45 were low but above background. (Figure 1A, compare lane 6 with lane 4 of the upper panel (marked with Claspin)). The reciprocal immunoprecipitation for each interactor was carried out from HeLa S3 cell extracts using antibodies that recognise endogenous Claspin or RPA32 and demonstrated that endogenous Cdc45 co-immunopreci-pitated with Claspin and RPA32 (Figure 1B and 1D, respectively). These results show that human Cdc45 forms complexes with the replication factors Claspin and RPA *in vivo*.

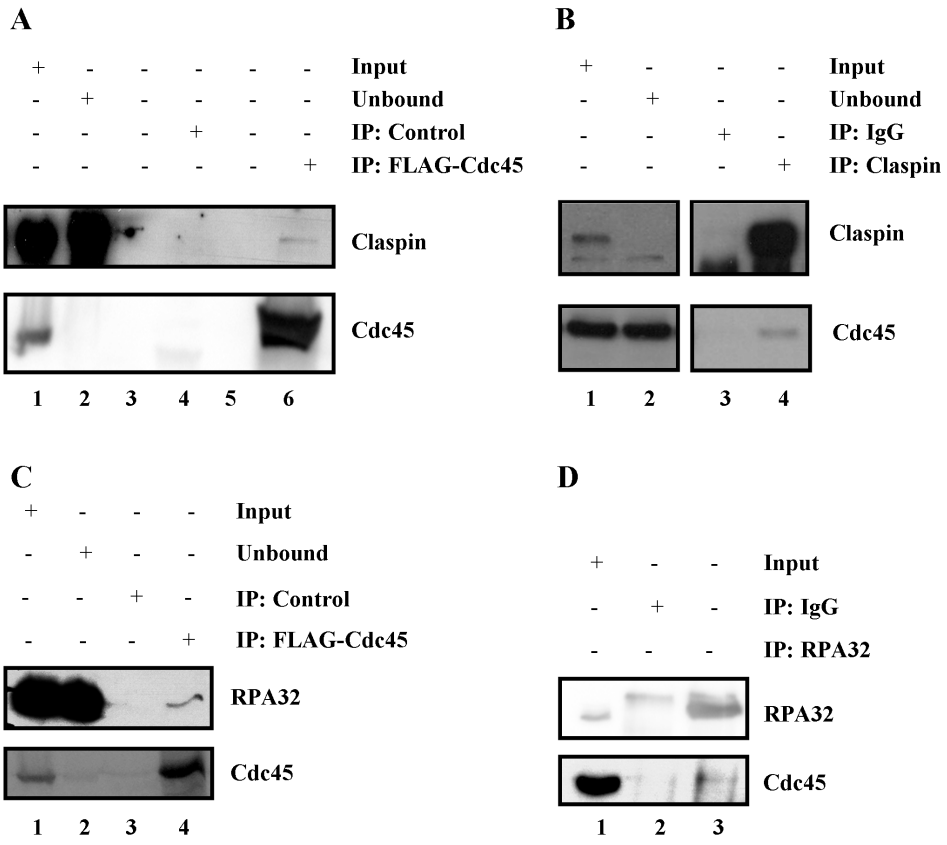

Figure 1: Claspin and RPA32 interact with Cdc45 in human cells
HeLa S3 cells transiently expressing FLAG-Cdc45 (IP:FLAG-Cdc45), or mock transfected control cells (IP: Control) were lysed, normalized for protein content and subjected to IP using anti-FLAG antibody M2 resin (panels A and C), antibody resin specific for Claspin (panel B; (IP: Claspin)) or RPA (panel D; (IP: RPA32)). The co-immunoprecipitation of Claspin and RPA with FLAG-Cdc45 was assayed by western blotting using Claspin-specific polyclonal antibody, the monoclonal antibody RBF-4E4 recognizing the second largest RPA subunit RPA32, and the Cdc45-recognizing monoclonal antibody C45-3G10. Equal amounts of input (Input) and unbound (Unbound) (2% of total) were loaded, indicating efficiency of the immunoprecipitation. Panels A and C: FLAG-bound proteins were eluted with FLAG peptide-containing buffer at 4℃. Equal amounts of eluate from FLAG resin performed with cells expressing FLAG-Cdc45 (IP: FLAG-Cdc45) and mock transfected control cells (IP: Control) were loaded to assay Claspin interacting with Cdc45. In panels B and D, proteins bound to non-specific IgG (IP: IgG) or an antibody specific to Claspin or RPA (IP: Claspin or IP: RPA32) were eluted with gel electrophoresis loading buffer and analysed by western blotting as indicated.

2.3.2 Cdc45-Claspin interaction *in vivo* is deficient upon deletion of Cdc45 C-terminus

To determine the regions of Cdc45 important for the *in vivo* interaction of proteins with FLAG-Cdc45, deletion mutants of FLAG-Cdc45 were generated (Figure 2A). These deletion mutants were transiently expressed in HeLa S3 cells to similar levels (data not shown) and localized in the nucleus with the exemption of Cdc45-Δ(aa101-190) (Supplementary Figure 1). To direct the deletion mutant Cdc45-Δ(aa101-190) into the nucleus the SV40 L-TAg NLS was added to this polypeptide and the fusion protein was expressed and found in the nucleus (Supplementary Figure 1).

The association of these deletion mutants with Claspin and RPA32 were tested (Figure 2B). Deletion of the C-terminal part of Cdc45 (ΔCT mutant) resulted in a reduced association of Claspin with Cdc45 and the detection of Claspin was hardly above background (Figure 2B, top panel, second last lane). In contrast, none of the Cdc45 deletion mutants tested showed a strongly decreased physical interaction with RPA. The relative efficiency of the Claspin interactions with FLAG-Cdc45 mutants in comparison to full length Cdc45 was densitometrically analyzed (Supplementary Figure 2A). The Cdc45-ΔCT mutant bound about 20 times less efficiently to Claspin than the full length Cdc45 protein (0.04 AU and 1.0 AU, respectively), and also had a reduced affinity to Claspin in comparison to the other Cdc45 deletion mutants (Supplementary Figure 2A). These findings indicate that the last 78 aa of Cdc45 are crucial for Cdc45 binding to Claspin. The overall reduced binding of Cdc45 deletion mutants Δ(aa191-290), Δ(aa291-390) and Δ(aa391-488) to Claspin suggests that several parts of Cdc45 may contribute to the complex formation of Cdc45 with Claspin but that the C terminus of Cdc45 is the most important part for this interaction. The similar affinity of all Cdc45 deletion mutants to RPA, Mcm7, Pol δ and Pol ε suggests that the C terminal deletion mutant Cdc45-ΔCT is specifically defective in its interaction with Claspin (Figure 2B, lower panel, and Supplementary Figures 2B and 2C).

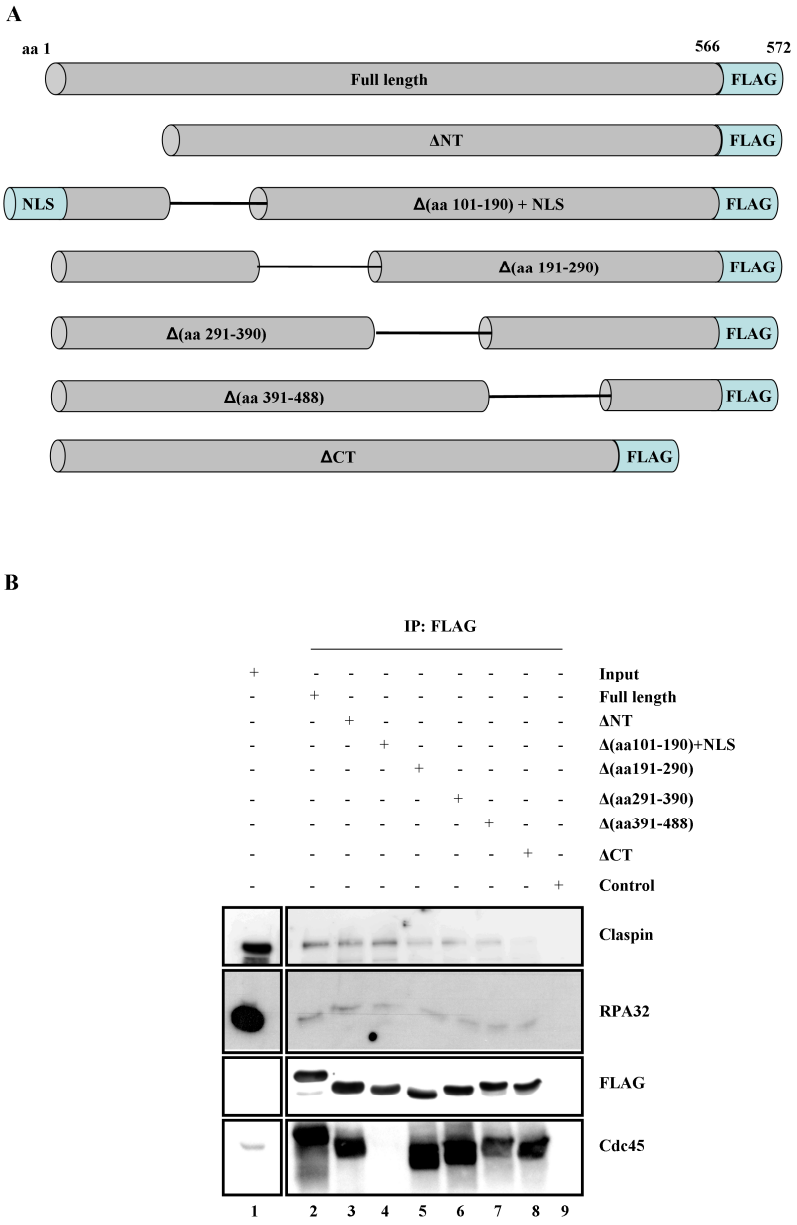

Figure 2: Interaction of replication proteins with regions of Cdc45
A) Schematic diagram of full length FLAG-Cdc45 fusion protein and deletion mutants. Theoretical fusion protein products for plasmids coding for full length FLAG-Cdc45 (Full Length), and deletion mutants lacking amino acids (aa) 1-100 (ΔNT), aa 101-190 and with the addition of the SV40 large T-Antigen NLS (PKKKRKVG) to the N-terminus (Δ(aa101-190)+NLS), aa 191-290 (Δ(aa191-290)), aa 291-390 (Δ(aa291-390)), aa 391-488 (Δ(aa391-488)) and aa 488-566 (ΔCT) are depicted (panel A). **B**) HeLa S3 cells transiently expressing FLAG-Cdc45, ΔNT, Δ(aa101-190)+NLS, Δ(aa191-290), Δ(aa291-390), Δ(aa391-488), ΔCT or mock transfected control cells (IP: Control) were lysed and subjected to FLAG immunoprecipitation. Eluates from each immunoprecipitation were subjected to SDS-PAGE and western blotting using antibodies specific to Claspin, RPA32, FLAG and Cdc45.

2.3.3 Claspin and RPA32 interact with Cdc45 maximally at S phase

To analyse the interactions of Cdc45 with Claspin and RPA during the cell cycle, of K562 cells transiently expressing FLAG-Cdc45 were elutriated and the binding of proteins to FLAG-Cdc45 was tested. The elutriated cells were enriched at various cell cycle stages as confirmed by flow cytometry (Figure 3A). The elutriation yielded cells enriched in G1, S and G2 (summarized in Supplementary Figure 3A). Subsequently the fractionated cells were lysed, protein concentrations were determined and equal amounts of proteins were subjected to SDS-PAGE. After the separation by SDS PAGE, the levels of replication proteins in these extracts throughout the cell cycle were analysed by western blotting (Figure 3B).

Cdc45, Pol δ and RPA32 were expressed at similar levels throughout the cell cycle whereas Claspin showed a reduced expression level in G1 cells. If one takes into account that the G1-enriched cell fraction contained approx. 30% S phase cells (Supplementary Figure 3B), which is a normal level of S phase cells in such an early elutriation fraction, these S phase cells in the G1 cell-enriched fraction could at least in part explain the residual expression level of Claspin in this fraction (Figure 3B, top panel, lane 2). In parallel, equal amounts of FLAG-Cdc45 were immunoprecipitated from extracts of these elutriated cells (Figure 3C, lowest panel, lanes 2 to 5) whereas no Cdc45 was immunoprecipitated from cells which do not express FLAG-Cdc45 (Figure 3C, lowest panel, lane 7). From these elutriated cells, FLAG-Cdc45 bound a maximal amount of p125 of Pol δ from extracts of cells enriched in S phase (Figure 3C, second lowest panel, lane 3), which is consistent with previously described findings using thymidine-arrested and released cells (Bauerschmidt et al, 2007). These results supported the functional activity of the FLAG-Cdc45. The western blots of the FLAG-affinity pull-downs showed that FLAG-Cdc45 co-immunoprecipitated Claspin and RPA32 maximally from cells enriched in S phase of the cell cycle (Figure 3C, top and second highest panel, respectively, lane 3). The densitometry analyses of western blots of immunoprecipitation experiments from two independently elutriated cell populations showed maximal association between Cdc45 and Claspin in S phase (Supplementary Figure 3B). The presence of S phase cells in G1-enriched cell fraction reaching about 30% (Supplementary Figure 3B) could explain the residual

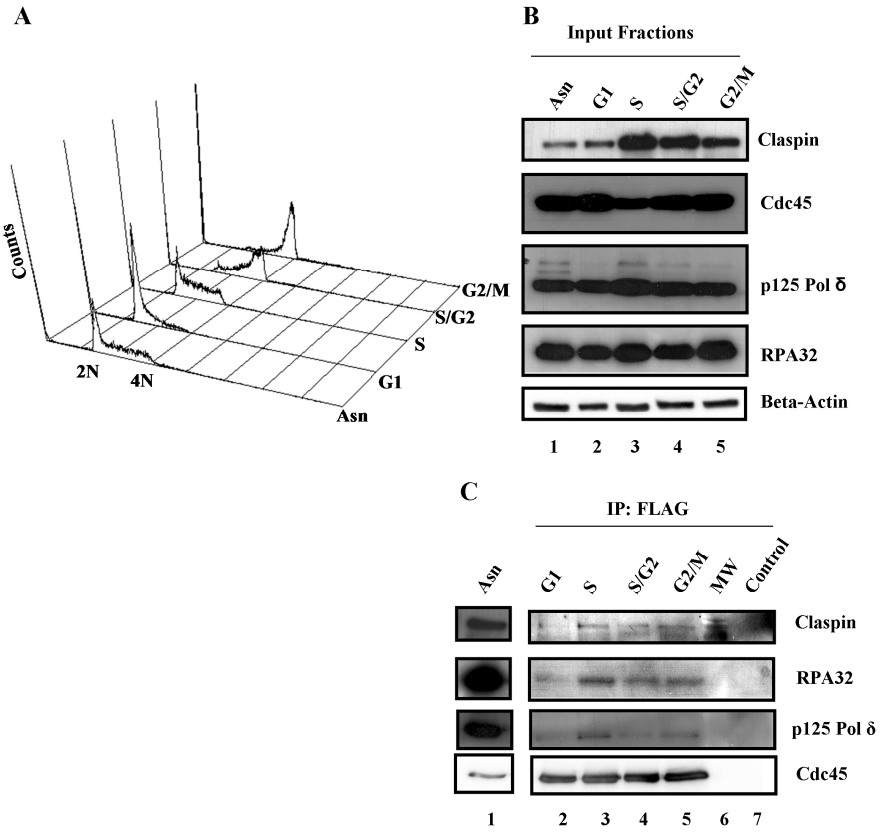

Figure 3: Claspin and RPA32 interact with Cdc45 maximally in S phase
$1.5x10^8$ K562 cells transiently expressing FLAG-Cdc45 were elutriated, collected and fractions were analysed by FACS for cell cycle-enriched cells (panel A). Asynchronous control cells (Asn) and cells enriched in G1 phase, S phase, late S/G2 phase and G2/M phase were lysed, normalized for protein content, subjected to SDS-PAGE and western blotting using antibodies raised against Cdc45, Claspin, RPA32, and the p125 subunit of Pol δ. Detection of β-Actin serves as a loading control (panel B). Co-immunoprecipitation of FLAG Cdc45 with Claspin, RPA32 and p125 subunit of Pol δ through the cell cycle was assayed. Extracts of fractions of the elutriation experiment and of asynchronous control cells (IP: Control) were subjected to FLAG-immunoprecipitation. Bound proteins were separated by SDS PAGE and determined by western blotting using antibodies recognising the indicated proteins (panel C). Asn = asynchronous cells, MW = molecular weight marker.

level of Claspin found in these cells (Figure 3B, top panel, lane 2) and Cdc45-Claspin complexes determined in cells of this fraction (Figure 3C, top panel lane 2). The fractions enriched in S/G2 and G2/M cells also contained late S phase cells (Supplementary Figure 2B), which could explain the presence of Claspin and Cdc45-Claspin complexes. The amounts of Claspin and the Claspin-containing complexes decreased in these cell fractions, and they closely followed the reduced

levels of S phase cells (Figure 3B and 3C, top panel, compare lane 3 with lanes 4 and 5).

2.3.4 Modulation of Cdc45 interactions with Claspin by UV and HU treatment

The maximal Cdc45-Claspin and Cdc45-RPA interactions observed at S phase raised the question whether the binding of Cdc45 to Claspin may be modulated by DNA damage and activation of the intra-S-phase checkpoint. To test the modulation of these interactions after DNA damage HeLa S3 cells transiently expressing FLAG-Cdc45 were exposed to doses of 5 J/m^2 and 30 J/m^2 of UVC and the physical interactions of both endogenous Claspin or RPA32 with Cdc45 were studied 2h post-treatment by co-immunoprecipitations. Protein levels in these cell extracts were analysed by SDS-PAGE and western blotting (Figure 4A). Treatment with UV did not influence the protein levels of Cdc45, Claspin and Chk1 in comparison to β-Actin, which served as the loading control. To verify the induction of DNA damage checkpoint pathways in these UV-treated cells, the phosphorylation of checkpoint kinase Chk1 was monitored (Figure 4A, third last panel of western blots from the bottom, lanes 4 and 5). Both UV treatments resulted in the phosphorylation of the Chk1 protein.

In parallel, FLAG-Cdc45 was immunoprecipitated from these cell extracts and the Cdc45-associated proteins were determined. Claspin showed a reduction in its co-immunoprecipitation with Cdc45 following 30 J/m^2 of UVC but not at the dose of 5 J/m^2 of UVC two hours after UVC treatment compared to the untreated control immunoprecipitation of Cdc45 (Figure 4B, compare lane 3 (UT: untreated) with lanes 4 and 7, 5 J/m^2 and 30 J/m^2, respectively). The decrease in association between Claspin and Cdc45 following UVC treatment was also verified by densitometry of western blots of these co-immunoprecipitation experiments (Supplementary Figure 4). In contrast, neither dose of UVC decreased the co-immunoprecipitation of RPA32 with FLAG-Cdc45 compared to the untreated control immunoprecipitation (Figure 4C).

These findings were verified by reciprocal immunoprecipitation with an antibody recognising endogenous Claspin. Treating cells with 30 J/m^2 UVC or 2 mM hydroxyurea (HU) did not influence the expression level of Claspin and Cdc45 (Figure 4D, the two top panels) whereas the DNA damage signal transduction was

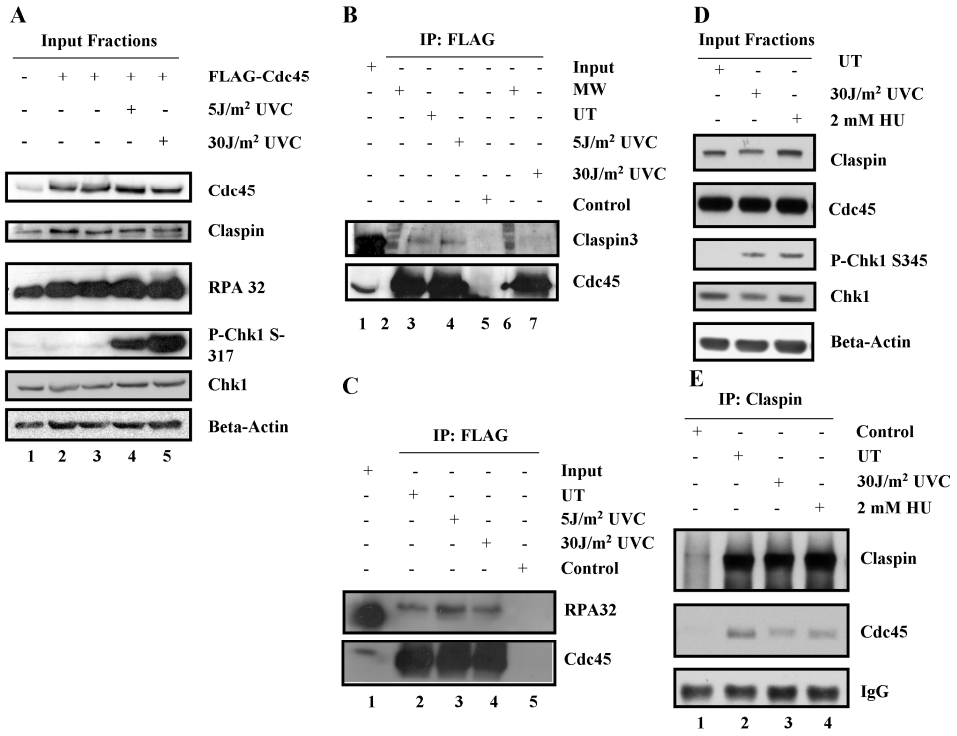

Figure 4: The effects of UVC and HU treatment on the interactions of Claspin and RPA32 with Cdc45.
HeLa S3 cells transiently expressing FLAG-Cdc45 or mock-transfected control cells were treated with a dose of 5 J/m^2 or 30 J/m^2 of UVC and were harvested 2h post-treatment. Cells were lysed and subjected to SDS-PAGE and western blotting using antibodies raised against Cdc45, Claspin, RPA32, P-Chk1 S-317, and Chk1. Detection of Beta-Actin acts as a loading control (panel A). Input from mock-transfected control cells (Input) and eluates of FLAG immunoprecipitated from lysates of cells expressing FLAG-Cdc45 (IP: UT), which were exposed to 5 J/m^2 UVC (IP: 5 J/m^2), exposed to 30 J/m^2 UVC (IP: 30 J/m^2) or mock-transfected control cells (IP: Control) were analysed by SDS-PAGE and western blotting. Antibodies raised against Cdc45, Claspin and RPA were employed to detect Cdc45 and associated Claspin (panel B) and RPA (panel C). In panel D, asynchronous HeLa S3 cells (UT) or cells treated with 30 J/m^2 of UVC (30 J/m^2) or 2 mM hydroxyurea (2 mM HU) were harvested 2h post-treatment and lysed. Input lysates were normalized for protein content and subjected to SDS-PAGE and western blotting, using antibodies raised against Claspin, Cdc45, P-Chk1 S-345, and Chk1. Detection of β-Actin served as a loading control. In panel E, Claspin was immunoprecipitated as indicated with binding to a control IgG serving as negative control (lane 1, IP: IgG). Eluates from each IP were subjected to SDS-PAGE and western blotting using antibodies specific to Claspin, Cdc45 or IgG.

activated in these cells as determined by the phosphorylation of Chk1 (Figure 4D, third panel from the top). Using an antibody specific to Claspin (Figure 4E), Claspin co-immunoprecipitation with Cdc45 was reduced following a UVC

treatment of 30 J/m^2 (Figure 4E, compare lanes 2 and 3). After HU treatment of cells, an antibody specific to endogenous Claspin reproducibly co-immunoprecipitated less Cdc45 from cell extracts than from extracts prepared from cells grown in the absence of HU (Figure 4E, compare lane 2 with lane 4). These results suggest that the binding of Cdc45 and Claspin is regulated by DNA damage caused by UV or HU.

2.3.5 The reduction in binding of Claspin to FLAG-Cdc45 is insensitive to UCN-01, Wortmannin and Caffeine treatment

In order to investigate whether loss of co-immunoprecipitation between FLAG-Cdc45 and Claspin depends on replication checkpoint signal transduction, small molecule inhibitors UCN01, known to inhibit Chk1 kinase (Zhao et al, 2002), and the PI-3-kinase inhibitors Caffeine and Wortmannin, inhibiting ATM, ATR and DNA-PK, were used (Sarkaria et al, 1999; Sarkaria et al, 1998).

After treatment of HeLa S3 cells transiently expressing FLAG-Cdc45 with 30 J/m^2 - UVC in the presence or absence of 100 nM UCN-01, extracts were prepared and input fractions were subjected to SDS-PAGE and western blotting (Figure 5A). In parallel, proteins associating with Cdc45 were tested. After treatment of cells with 30 J/m^2 UVC, FLAG-Cdc45 co-immunoprecipitated reduced amounts of Claspin compared to control cells but treatment of cells with UV in the presence of UCN-01 did not abolish the decrease in interaction of Cdc45 with Claspin after DNA damage (Figure 5B). Treatment of cells with UCN-01 inhibitor alone, however, slightly increased the co-immunoprecipitation of Claspin with FLAG-Cdc45 (Supplementary Figure 5). In addition, validation of activity of the UCN-01 drug used by analysing its ability to abrogate Cdk1 phosphorylation in IR-treated HeLa S3 cells arrested at mitosis by nocodazole, agrees with previously published validation experiments (Wang et al, 1996) (Supplementary Figure 6).

To test whether the loss of Claspin-Cdc45 association was regulated by PIKK activity cells were treated with PIKK inhibitors, Caffeine and Wortmannin, and were exposed to 30 J/m^2 UVC in the presence or absence of 5 mM Caffeine or 100 μM Wortmannin. Neither Caffeine nor Wortmannin treatment affected the amounts of Cdc45, Claspin or RPA 32 present in input fractions (Figure 6A and 6C). Treatment with Caffeine or Wortmannin also did not affect the co-immunoprecipi-

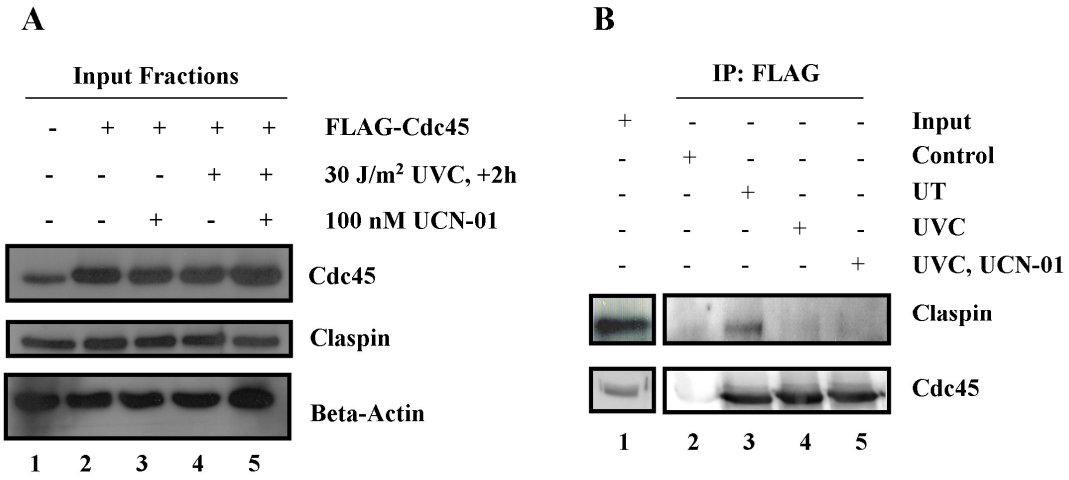

Figure 5: Inhibition of Chk1 by UCN-01 does not recover Cdc45-Claspin interaction after UV damage.
HeLa S3 cells transiently expressing FLAG-Cdc45, or mock-transfected control cells were treated with 30 J/m^2 of UVC with or without a 1h pre-treatment with 100 nM UCN-01, a Chk1 inhibitor. Cells were harvested 2h post UVC treatment in the presence or absence of UCN-01, lysed and then proteins were subjected to SDS-PAGE and western blotting using antibodies specific to Cdc45 and Claspin. Detection of β-Actin acts as a loading control (panel A). The influence of UCN-01 on the interaction of Cdc45 and Claspin after UV treatment was tested by co-immunoprecipitation using FLAG resin as indicated in panel B. Detection of bound proteins occurred after SDS-PAGE and western blotting of peptide eluates using antibodies specific to Claspin and Cdc45.

tation of Claspin with FLAG-Cdc45 or the reduction in their co-immunoprecipitation following UVC treatment (Figure 6B and 6D). Please note that in the presence of Wortmannin, a slight increase in the co-immunoprecipitation of Claspin with FLAG-Cdc45 was observed following drug treatment alone (Figure 6D, top panel, lane 5). The efficacy of the Caffeine used was demonstrated by the ability of the drug to abrogate the G2/M checkpoint as determined by pS10-Histone H3 FACS analysis (Supplementary Figure 7) whereas the efficacy of the Wortmannin was determined by the loss of RPA32 S4/S8 phosphorylation following UVC-treatment in the presence of the drug (Figure 6C, third lowest panel, compare lanes 4 and 5).

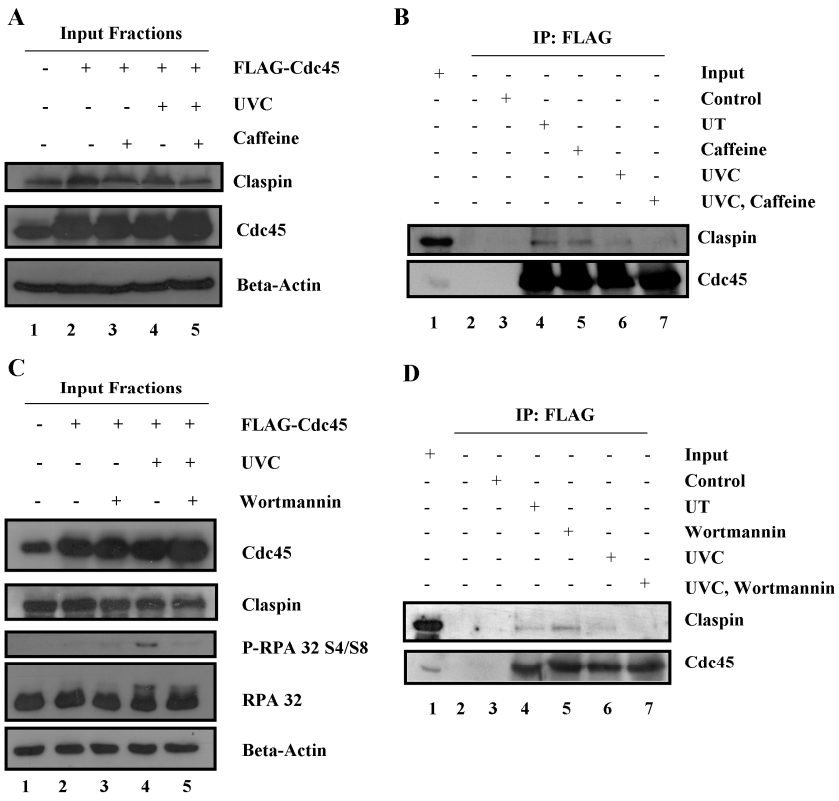

Figure 6: Inhibition of DNA damage signalling by Caffeine or Wortmannin does not recover Cdc45-Claspin interaction after UV damage.
HeLa S3 cells transiently expressing FLAG-Cdc45, or mock-transfected control cells were treated with 30 J/m^2 of UVC with or without a 1h pre-treatment with 5 mM Caffeine and were harvested 2h post-UVC treatment in the presence or absence of Caffeine as indicated. Cells were lysed and subjected to SDS-PAGE using antibodies specific to Cdc45 and Claspin. Detection of β-Actin acts as a loading control (panel A). To determine the influence of Caffeine, FLAG-IP was performed with lysates of untreated HeLa S3 cells expressing FLAG-Cdc45 (IP: UT), with HeLa S3 cells expressing FLAG-Cdc45 exposed to a 1h pre-treatment with 5 mM Caffeine (IP: Caffeine), expressing FLAG-Cdc45 exposed to 30 J/m^2 of UVC in the absence of Caffeine (IP: UVC) and in the presence of 5 mM Caffeine plus Caffeine pre-treatment (IP: UVC, Caffeine) as described above. Both UVC-exposed cell populations were harvested 2h post-UVC treatment whereas Caffeine-only incubated cells were collected after 3h of the addition of Caffeine. Eluted proteins were separated by SDS-PAGE and analysed by western blotting using antibodies specific to Claspin and Cdc45 as shown in panel B. In addition, HeLa S3 cells transiently expressing FLAG-Cdc45, expressing FLAG-Cdc45 exposed to a 1h pre-treatment with 100 μM Wortmannin or mock-transfected control cells were treated with 30 J/m^2 of UVC with or without a 1h pre-treatment with 100 μM Wortmannin and were harvested 2h post-UVC treatment in the presence or absence of Wortmannin. Cells were lysed and subjected to SDS-PAGE using antibodies specific to Cdc45, Claspin and P-RPA32 S4/S8. Detection of β-Actin acts as a loading control (panel A/C). Panel B/D presents the FLAG-immunoprecipitation performed with lysates HeLa S3 cells after SDS-PAGE and western blotting.

2.4 Discussion

In order to investigate the interaction of Cdc45 with Claspin and RPA32, C-terminally FLAG-tagged Cdc45 was transiently expressed in HeLa S3 cells. FLAG-Cdc45 co-immunoprecipitated Claspin and RPA32. In addition, interactions with previously characterized interaction partners of Cdc45, namely Mcm7, Pols δ and ε were observed. The detection of these previously identified interactors demonstrates the functionality of the FLAG-Cdc45 fusion protein. The association of Claspin and RPA with endogenous Cdc45 was also confirmed using antibodies specific for Claspin and RPA32. These results are in agreement with recent reports that Claspin co-immunoprecipitates with Cdc45 (Uno & Masai, 2011). These findings also show that Cdc45 and RPA associate with each other in human cells, supporting recent reports about their interaction *in vitro* (Nakaya et al, 2010).

To determine the regions of Cdc45 that mediate its interactions with Claspin, RPA32 and other interacting proteins, deletion mutants of Cdc45 were generated and their nuclear localisation and association with other proteins were analyzed (Figure 2, Supplementary Figures 1 and 2). All Cdc45 deletion mutants tested expressed at comparable levels to each other. This allowed the determination of the efficiency of interactions of proteins with each mutant (Figure 2B and Supplementary Figure 2). The addition of the SV40 large T-Antigen nuclear localisation sequence (NLS: PKKKRKVG) to the Δ(aa101-190) mutant stabilized its expression in HeLa S3 cells (Supplementary Figure 2C) and mediated its localisation to the nucleus (Supplementary Figure 1). All other Cdc45 deletion mutants had nuclear localisation as shown by immunofluorescence microscopy (Supplementary Figure 1). Interestingly, the monoclonal C45-3G10 antibody used for these experiments did not recognize the Δ(aa101-190+NLS) deletion mutant demonstrating that this epitope is necessary for the binding of the antibody. In the case of RPA32, no Cdc45 deletion mutant showed a deficient association with this protein. The co-immunoprecipitation of p125 of Pol δ, p261 of Pol ε and Mcm7 with Cdc45 deletion mutants were also investigated but no deletion mutants deficient for association with these proteins were identified (Supplementary Figure 2B and 2C). These findings suggest that either multiple regions of Cdc45 interact

with these proteins, or that these interactions are mediated by other proteins whose binding to Cdc45 is not disturbed by these mutations.

Interestingly, the co-immunoprecipitation of Claspin with the Cdc45 ΔCT deletion mutant was strongly diminished, which suggests that the C-terminal region of Cdc45 is important for the *in vivo* interaction of Cdc45 with Claspin (Figure 2B). Recent data obtained using small angle X-ray scattering has generated a putative structure for Cdc45 (Krastanova et al, 2011). Here the predicted structure of Cdc45 resembles the TthRecJ core structure, with the N- and C-termini of the protein arranged on one site of the molecule spacially close to each other. The regions of Claspin which interact with Cdc45 *in vitro* in Xenopus and human cells have been characterized, with Xenopus Claspin interacting via aa 265-605 with Xenopus Cdc45 (Lee et al, 2005) and human Cdc45 shown to interact with aa 1-851 of Claspin (Sercin & Kemp, 2011). Our data support a model whereby the C-terminus of Cdc45 and the N-terminus of Claspin mediate the interaction between the two proteins *in vivo.*

In order to study the regulation of these interactions through the cell cycle, the co-immunoprecipitation of FLAG-Cdc45 with Claspin, RPA32 and p125 of Pol δ was analysed in elutriated human K562 cells. Claspin and RPA32 interact maximally with FLAG-Cdc45 in S phase of the cell cycle. Pol δ served as a positive control in this experiment. In agreement with a previous report, which showed endogenous Cdc45 co-immunoprecipitated with Pol δ in S phase cells released from a double thymidine block (Bauerschmidt et al, 2007), FLAG-Cdc45 maximally interacted with Pol δ in elutriated, S phase-enriched cells. Maximal co-immunoprecipitations of Claspin, RPA32 and p125 with Cdc45 during S phase suggests that these interactions of Cdc45 are part of the DNA replication machinery. Previous characterisations of the interaction partners of Cdc45 throughout the cell cycle have used either drug-based methods to synchronize cells, such as double thymidine block (Bauerschmidt et al, 2007), serum depletion (Pollok et al, 2007) or contact inhibition (Aparicio et al, 2009). These synchronisation methods may induce replication stress or other stresses on cells (Darzynkiewicz et al, 2011; Gaballah et al, 2012). Elutriation is a stress-free method to obtain cells enriched in various cell cycle stages and does not need any drug treatment or pre-treatment of cells. Therefore, our data are likely to represent the *in vivo* interactions of replication

factors throughout the cell cycle (Dehde et al, 2001; Nasheuer et al, 1991; Zhang et al, 2011).

Previous results showed that the expression of Claspin is proliferation-controlled, with a similar pattern seen for Mcm proteins and Pol-prim (Chini & Chen, 2003; Pollok et al, 2007). Importantly, the elutriation experiments presented here revealed that Claspin appears to be expressed in a cell cycle-dependent manner with its levels being low in G1-enriched cells and maximal in S phase cells. In contrast, Cdc45 and RPA32 are constantly expressed throughout the cell cycle at similar levels, which is comparable to the findings previously observed for Pol-prim and RPA in elutriated human cells (Dehde et al, 2001; Din et al, 1990), and for Cdc45 in cells released from double thymidine block (Pollok et al, 2007). The p125 subunit of Pol δ shows a similar expression pattern with a slight up-regulation in S phase cells which is consistent with previously published elutriation analyses (Zeng et al, 1994). In the normal cell cycle the levels of these replication proteins do not oscillate whereas Claspin is clearly variable throughout the cell cycle, having an expression pattern reminiscent of Cyclin A (Dehde et al, 2001). This expression pattern of Claspin may explain its maximal association with Cdc45 in S phase since the expression levels of Claspin in the cell correlate well with the Claspin-Cdc45 complex formation.

The treatment of HeLa S3 cells with UVC did not abrogate the Cdc45-RPA interactions at any dose tested whereas the binding of Cdc45 to Claspin is diminished by UVC in a dose-dependent manner. In contrast to treatment with 5 J/m^2 UVC or mock treatment, HeLa S3 cells exposed to 30 J/m^2 of UVC showed a reduction in this co-immunoprecipitation. The decreased Cdc45-Claspin interaction with 30 J/m^2 UVC of UVC suggests a mechanism whereby lower doses of UVC cause less replication fork stalling, while higher doses induce more stalled forks, possibly contributing to the reduction of the observed physical interactions. Treatment of HeLa S3 cells with hydroxyurea, which induces replication stress by dNTP depletion, caused a reduction in the interaction between endogenous Claspin and Cdc45 (Figure 4E). These data also suggest that replication fork stalling may cause the reduction of the interaction between Cdc45 and Claspin.

To better understand the mechanism and the control of Cdc45-Claspin interactions it was investigated if the decreased complex formation of Cdc45 and Claspin

following UVC treatment was mediated by the activation or downstream signalling of the intra-S-phase checkpoint. Therefore, co-immunoprecipitations of Claspin with FLAG-Cdc45 were analysed in the presence or absence of drugs which would inhibit different facets of this checkpoint. Neither the compound UCN01, which is known to inhibit Chk1, nor Caffeine or Wortmannin, which inhibit the upstream PIKKs, restored the complex formation of Cdc45 and Claspin at 30 J/m^2 UVC. The use of Caffeine and Wortmannin also makes it less likely that other branches of the DNA damage response modulate the interactions between Cdc45 and Claspin following UVC damage, such as ATM and DNA-PK. In all experiments performed, the concentrations of Caffeine and Wortmannin were sufficient to effectively inhibit ATM, DNA-PK and ATR kinases (Sarkaria et al, 1999; Sarkaria et al, 1998). Taken together, these results suggest that the reduction in the interaction between Cdc45 and Claspin may occur up-stream of ATR-recruitment and Chk1 activation in the intra-S-phase checkpoint or are independent ways to regulate DNA replication. This regulatory pathway may depend on a change in conformation in the RPC when the replication machinery becomes stalled which is independent of ATR activation in the intra-S-phase checkpoint. Conversely, the reduction in interaction may be mediated by another factor, which is Caffeine, Wortmannin and UCN-01 insensitive.

2.5 Materials and Methods

2.5.1 Cell Culture

HeLa S3 cells were cultured in Dulbecco's modified Eagle's medium (Sigma) supplemented with 10% foetal calf serum (Sigma), 100 units/ml penicillin (Lonza) and streptomycin (Lonza). K562 cells were cultured in RPMI media (Sigma) supplemented with 5% foetal calf serum (Sigma), 100 units/ml penicillin (Lonza) and streptomycin (Lonza).

2.5.2 Antibodies

Antibodies recognizing Cdc45 (C45-3G10) (Bauerschmidt et al, 2007), p125 of Pol δ (PGD-5E1) (Pollok et al, 2007) and RPA32 (RBF-4E4) (Pestryakov et al, 2003; Stephan et al, 2009). Antibody raised against p261 of Pol ε was obtained from BD Biosciences (611238). RPA32 pS4/S8 was obtained from Bethyl Laboratories (800-338-9579). Mcm7 antibody was obtained from Neomarkers (47DC141). Antibody raised against β-Actin (A5441) and FLAG (F1804) were obtained from Sigma. Antibody raised against Cdk1 (sc54) was obtained from Santa Cruz. Antibody raised against Chk1 pS-317 (#2344) and P-Chk1 pS-345 (#2341) were obtained from Cell Signalling Tech. Antibody raised against Chk1 (DCS-300) and RPA32 (9H8) were obtained from Neomarkers. A rabbit polyclonal anti-Claspin antibody was generated in collaboration with Pocono Rabbit Farm and Laboratory (Supplementary Figure 8).

2.5.3 Generation of plasmid constructs for FLAG-Cdc45 and FLAG-Cdc45 deletion mutants.

CDC45L ORF and deletion mutants were amplified by PCR or fusion PCR using KOD DNA polymerase and PCR kit (Novagen) according to the manufacturer's recommendations. PCR products were cloned into the Gateway entry vector pENTR3C (Invitrogen) in frame between the BamH1 and EcoR1 restriction sites and recombined into the Gateway destination vector pT-Rex-DEST30 (Invitrogen) using the LR-Clonase II enzyme mix (Invitrogen) according to the manufacturers recommendations.

2.5.4 Cell treatment

Cells were treated with UVC by removing media from cells, washing once in PBS at 37ºC, removing excess PBS and exposing cells to UVC for precise amounts of time to control dose using a UVC lamp (Benda, Germany) at room temperature (Stephan et al, 2009). Wortmannin, Caffeine and UCN-01 (Sigma) were dissolved as stock solutions in DMSO and added to cells at the indicated final concentrations. For experiments using these inhibitors and UVC treatment, cells were pre-treated for 1h in the presence of 5 mM Caffeine, 100 μM Wortmannin or 100 nM UCN-01 before treatment with UVC, with drug containing media put back onto cells until harvesting for experiments at later time-points. Hydroxyurea (HU (Sigma)) was dissolved as a stock solution in ddH_20. Cells were treated with 2 mM HU for 2h and harvested for subsequent experiments.

2.5.5 Cell lysis and immunoblotting

Lysates were prepared in TGN buffer (50 mM Tris-HCl pH 7.5, 200 mM NaCl, 50 mM sodium β-glycerophosphate, 50 mM Sodium Fluoride, 1% Tween-20, 0.2% NP-40) supplemented with phosphatase inhibitor cocktail II (Sigma) and ETDA free protease inhibitor cocktail (Roche Applied Sciences). Briefly, cells were lysed for 20 min on ice and centrifuged for 10 min at 13,000 x g at 4°C. Supernatant fractions were collected and used as input for immunoprecipitation experiments.

2.5.6 Quantitative western blotting

For quantitative western blotting, images of western blots were acquired using a LAS3000 imaging system and software (Fuji). Images were analysed quantitatively using densitometry analysis software (Multi Gauge V2.2 (Fuji)) to determine the relative signal intensities of distinct bands.

2.5.7 Immunoprecipitation

FLAG immunoprecipitation experiments were carried out using FLAG M2 resin and purification kit (Sigma) in line with the manufacturer's recommendations. Briefly, $2x10^7$ HeLa S3 cells were transfected with 20 μg of plasmid coding for FLAG-Cdc45 fusion protein using Fugene/X-treme GENE HP transfection reagent

(Roche Applied Sciences), harvested 24h post-transfection and lysed in TGN buffer. Protein G-Sepharose resin (GE Healthcare) was washed 3 times in 500 µl TGN buffer, yielding 20 µl packed resin and 5 mg of lysate was incubated with this resin for 30 min at 4°C to pre-clear. 20 µl packed FLAG resin was washed 3 times in TGN buffer and incubated with 5 mg pre-cleared lysate from cells transfected with FLAG-Cdc45 plasmid or from mock-transfected control cells. Lysates were incubated with the resin for 2h at 4°C and washed 4 times with 1 ml of TGN buffer. Bound proteins were eluted by incubation of the FLAG beads in 40 µl TGN buffer supplemented with 400 µg/ml 3x FLAG peptide (Sigma).

For IP experiments using antibodies raised against Claspin and RPA32, 5 mg of lysate from cells lysed in TGN buffer was incubated with 20 µl protein A/G Agarose (Calbiochem) which had been washed 3 times in 500 µl TGN buffer for 30 min to pre-clear. Either 2 or 5 µg of IgG specific to Claspin or RPA 32 respectively, or an equal amount of non-specific control IgG was incubated for 2h at 4 °C with 20 µl A/G Agarose (Calbiochem) which had been washed 3 x in 500 µl TGN buffer to couple the IgG to the beads. IgG-coupled beads were washed 3 x in 500 µl TGN buffer and incubated with 5 mg of pre-cleared lysate for 2h at 4 °C. These beads were then washed 4 times in 1 ml TGN buffer before bound proteins were solubilized by boiling the beads in 40 µl of 2x Laemmli buffer.

2.5.8 Electroporation

Electroporation of K562 cells was carried out using a procedure adapted from (Delgado-Canedo et al, 2006). Briefly, 1 x 10^7 K562 cells were resuspended in 500 µl serum- and antibiotic-free RPMI media in a 0.4mm diameter Gene Pulser® cuvette (BioRad). 30 µg of plasmid coding for FLAG-Cdc45 was added to the cuvette and the cells were incubated for 15 min at room temperature. Electroporation was carried out using a Gene Pulser® II electroporation unit and capacitance extender at a voltage of 875 V/cm^2 and set to high capacitance. Cells were then reususpended in 10 mls RPMI media containing FCS and antibiotic, placed back in the incubator and were harvested for experiments 24h post-electroporation.

2.5.9 Elutriation

$1.5x10^8$ K562 cells collected 24h post-electroporation were elutriated using a JE-5.0 elutriation system (Beckman Coulter) in an Avanti J-26 XP high-performance centrifuge (Beckman Coulter) as previously described (Dehde et al, 2001; Nasheuer et al, 1991). Briefly, the elutriation system was rotated at a constant speed of 1200 rpm at 8℃. RPMI media supplemented with 5% FCS was injected into the elutriation system using a peristaltic pump (Masterflex ® L/S, Cole Parmer Instrument Company) at a constant initial flow-rate. $1.5x10^8$ K562 cells were re-suspended in 10 ml RPMI medium supplemented with 5% FCS and a single cell-suspension state was ensured by pipetting cells through a syringe tip (Beckton Dickinson, Microlance 3 syringe tip). These cells were then introduced into the system and loaded into the elutriation chamber using a constant flow-rate. The flow rate was gradually increased and 100 ml fractions at each different flow-rate were collected, yielding fractions enriched in G1-, S-, late S/G2- and G2/M-phase cells. Cell synchrony was assayed by FACS analysis for each experiment and appropriately synchronized fractions were used for subsequent immunoprecipitation experiments.

2.5.10 Flow cytometry and FACS analysis.

$1x10^6$ HeLa S3 cells were trypsinized, washed in PBS at 4 °C and re-suspended in 1 ml PBS. Ice-cold ethanol was added to a final concentration of 75% to fix samples for flow cytometry as previously described (Broderick et al, 2012). For propidium iodide staining, samples were then centrifuged at 1500 x g, the supernatant was removed, and the cell pellet was re-suspended in 1 ml propidium iodide with RNAse solution (BD Biosciences) and incubated overnight at 4°C on an overhead rocker. Cells positive for PI staining were acquired on a FACS Canto flow cytometer (BD Biosciences) with data analysed using WinMDi software.

2.6 Supplementary information:

Validation of Caffeine activity was carried out as previously described (Rainey et al, 2008). Briefly HeLa S3 cells were pre-treated with 5 mM Caffeine for 1h before irradiation with 2 Gy I.R. and cells were harvested 1h post-irradiation. Cells were treated with ionizing radiation (IR) in the presence of serum-containing medium, using a gamma irradiator (Mainance Engineering Ltd, UK) at room temperature.

Cells positive for p-S10 on histone H3 were determined by FACS analysis. For analysis of pS10-Histone H3 staining, 1 x 10^6 cells were fixed as normal, centrifuged at 1500 x g for 5 min at 4 °C and re-suspended in 50 µl of PBS supplemented with 1% BSA, 0.5% Triton X-100 and pS10-Histone H3 antibody at a dilution of 1:50, with cells incubated with primary antibody for 2h at room temperature. Cell were then washed 2 x with 1 ml PBS supplemented with 1% BSA before re-suspension in 50 µl of PBS supplemented with 1% BSA, 0.5% Triton 100x and anti-rabbit-FITC antibody at a dilution of 1:50, incubating for 1h with secondary antibody at room temperature in the dark. Cells were then centrifuged and washed 2 x in 1 ml PBS supplemented with 1% BSA before re-suspended in 1 ml propidium iodide with RNase solution (BD Biosciences) for 1h at room temperature in the dark on an overhead rocker. Cells positive for PI staining and/or for pS10-Histone H3 staining were acquired on a FACS canto flow cytometer (BD Biosciences) with data analysed using WinMDi software. Antibody recognising pS10-Histone H3 (06-570) was obtained from Upstate. Goat-anti-rabbit-FITC (111-096-042) was obtained from Jackson Immunoresearch.

Validation of UCN-01 activity was carried out as previously described (Wang et al, 1996). Briefly, HeLa S3 cells were irradiated with 6.3 Gy IR and nocodazole (Sigma) was added to cells at a dose of 400 ng/ml for 17h to synchronise cells in mitosis. 6h before the end of the nocodazole block, UCN-01 was added at a concentration of 100 nM to cells in media containing nocodazole. Cells were harvested for SDS-PAGE and western blotting with Cdk1 phosphorylation assessed using an antibody against total Cdk1. Total cell lysates were prepared in RIPA buffer (1% Triton X-100, 0.5% deoxycholate, 1% Sodium Dodecyl Sulphate (SDS) in PBS, pH 7.4) supplemented with phosphatase inhibitor cocktail II (Sigma) and ETDA free protease inhibitor cocktail (Roche Applied Sciences). Briefly, cells

were lysed for 20 min at room temperature and centrifuged at 18,000 x g for 10 min at 4°C. Supernatants were collected and used for subsequent experiments

Validation of Wortmannin activity was carried out by analysing RPA32 S4/S8 phosphorylation by SDS-PAGE and western blotting as previously described (Stephan et al, 2009).

Immunofluorescence microscopy was carried out as follows. Cells were grown on glass coverslips (Alpha-Hartenstein, Germany) in culture, were washed twice in PBS and fixed using 4% paraformaldehyde (PFA) in PBS for 10 mins at 37℃ and rinsed 3 times in PBS. Cells were permeabilised with 0.2% Triton-X100 in PBS for 10 mins at 37℃ and rinsed 3 times in PBS and transferred to a humidified chamber. Fixed cells were blocked using blocking solution (5% BSA, 10% Goat Serum in PBS-T (0.025% Tween)). Primary antibodies were diluted in blocking solution and blocked cells were incubated for 1h at 37℃ with primary antibody.

Coverslips were then washed 3 times for 5 min in PBS-T (0.025% Tween) before incubation with secondary antibodies. Secondary antibodies were appropriately diluted in blocking solution and coverslips were incubated with secondary antibody for 1h at 37℃. Coverslips were washed 3 times for 5 min with PBS-T (0.025% Tween) before mounting on glass slides (Alpha-Hartenstein, Germany) using Vectashield mounting medium with DAPI (Vector Laboratories). Images were acquired using an Olympus IX51 Brightfield microscope and Cell R software.

2.7 Supplementary Figures

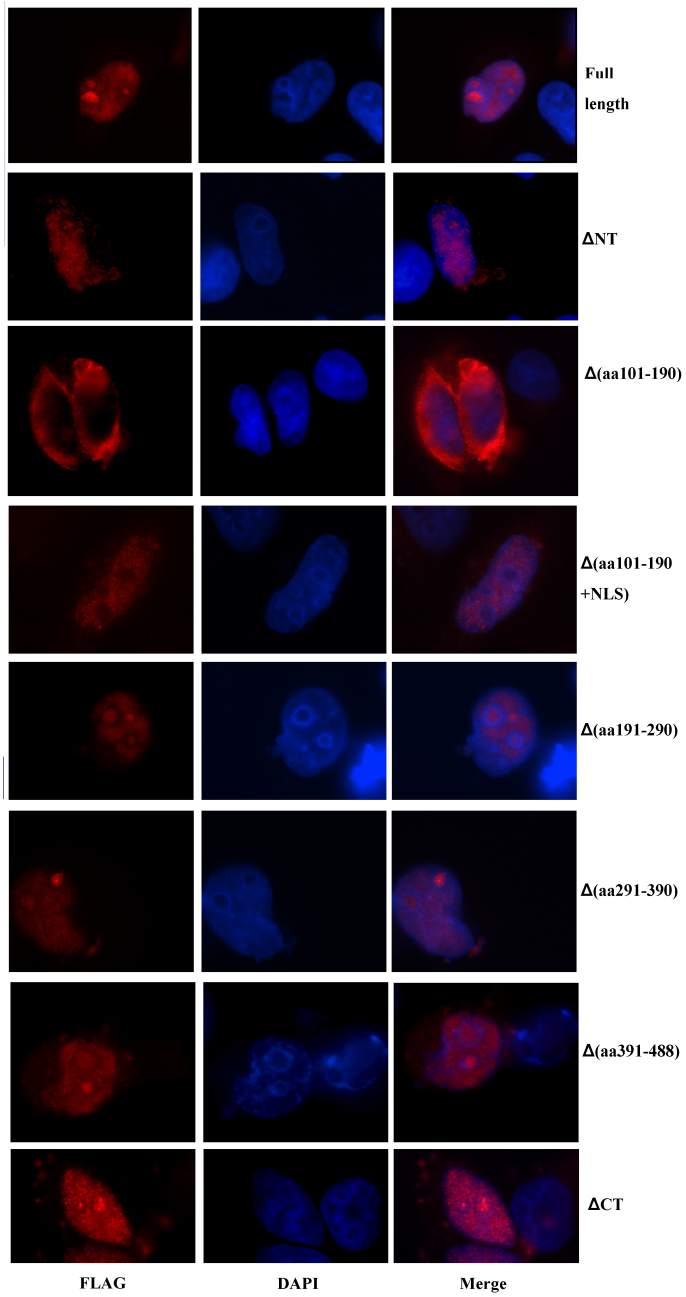

Supplementary Figure 1: Localisation of FLAG-Cdc45 and FLAG-Cdc45 mutants. HeLa S3 cells were transfected with plasmid encoding C-terminally FLAG-tagged Cdc45 (Full length) or with plasmids encoding C-terminally FLAG-tagged deletion mutants (ΔNT, Δ(aa101-190), Δ(aa101-190+NLS), Δ(aa191-290), Δ(aa291-390), Δ(aa 391-488) and ΔCT). Cells were harvested, fixed and subjected to immunofluorescence microscopy using an antibody specific for FLAG and Cy3-conjugated secondary antibodies for detection. DAPI staining acts as a marker for the nucleus.

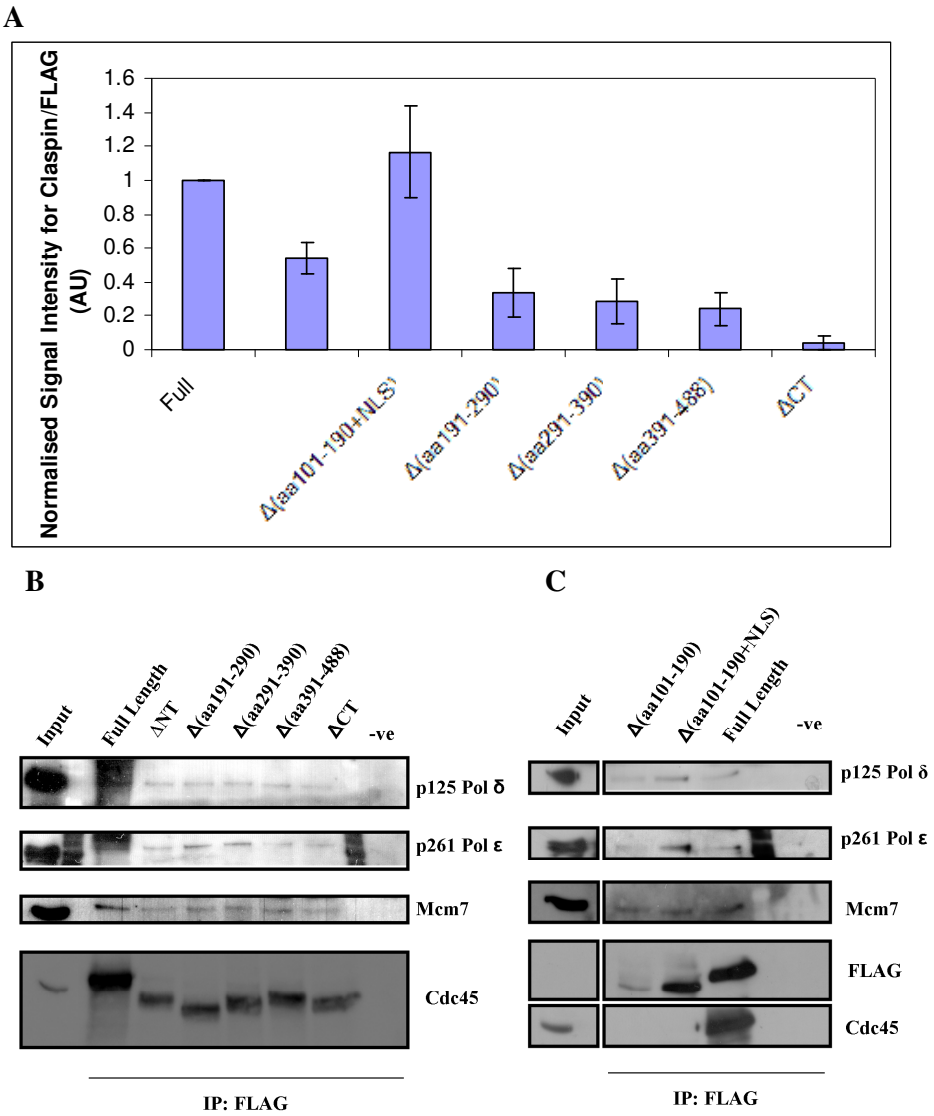

Supplementary Figure 2: Co-IP of FLAG-Cdc45 deletion mutants with replication proteins. A. The ratios of signal intensities for Claspin (minus background)/FLAG (minus background) from three immunoprecipitation experiments of FLAG-Cdc45 and mutant FLAG-Cdc45 from HeLa S3 cells were determined by densitometry. Signal intensities minus background for Claspin in each experiment were determined by densitometry. The ratio of Claspin signal to immunoprecipitated full length FLAG-Cdc45 (Full) was arbitrarily set to 1. Ratio of signal for Claspin/FLAG for full length FLAG-Cdc45 (Full), ΔNT, Δ(aa101-190+NLS), Δ(aa191-290), Δ(aa291-390), Δ(aa391-488) and ΔCT are depicted with standard deviation from the mean indicated by error bars. AU = Arbitrary Units. **B.** HeLa S3 cells transiently expressing full length FLAG-Cdc45 (Full Length), ΔNT, Δ(aa191-290), Δ(aa291-390), Δ(aa391-488), ΔCT or mock transfected control cells (-ve) (panel A) or FLAG-Cdc45 (full length), Δ(aa101-190), Δ(aa101-190+NLS) or mock transfected control cells (-ve) (panel B) were lysed and subjected to FLAG IP. Eluates from each IP were subjected to SDS-PAGE and western blotting using antibodies specific to p125 of Pol δ, p261 of Pol ε, Mcm7 and Cdc45 to determine co-IP for each interactor with FLAG-Cdc45.

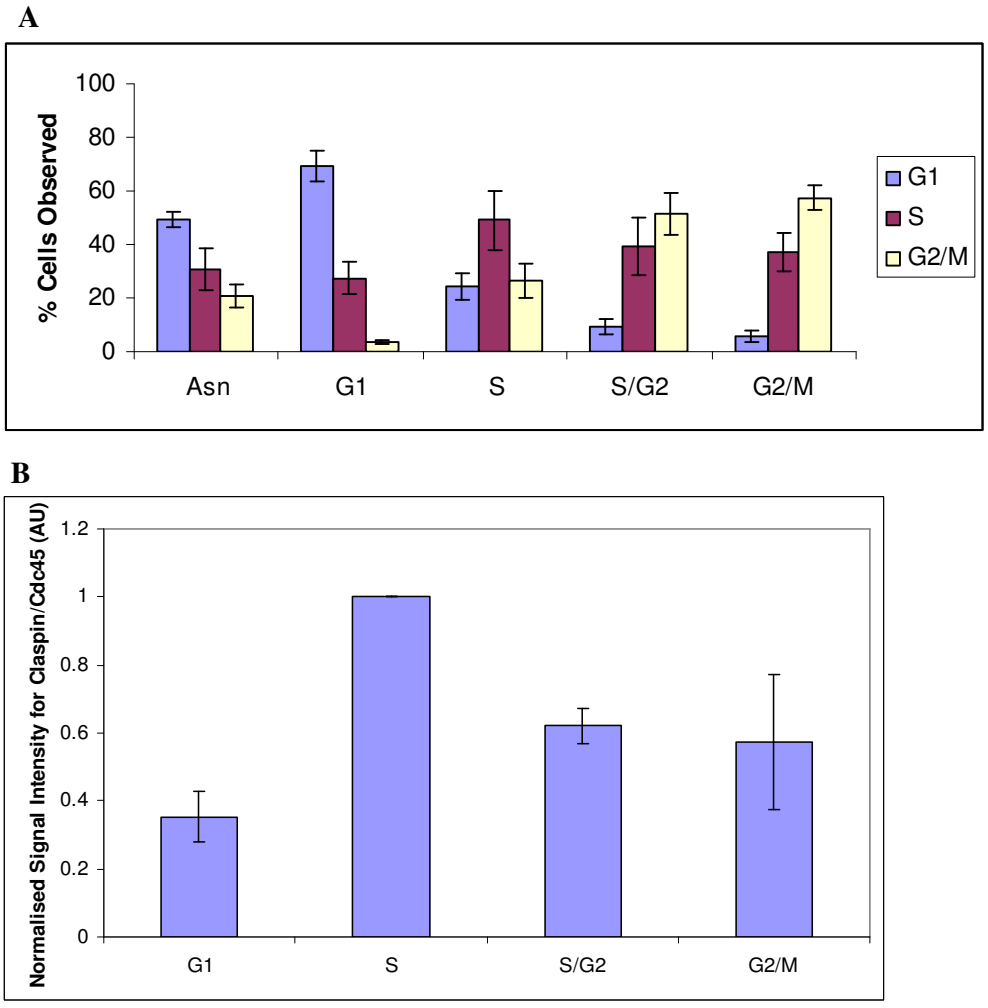

Supplementary Figure 3: Densitometry analysis of Cdc45-Claspin interaction in the cell cycle. A. Human exponentially growing K562 cells were separated by elutriation into four fractions, which were named G1, S, S/G2 and G2/M following the main population of cells in these fractions. The numbers presented are the average and standard deviation of two independent elutriation experiments from an asynchronous control cells (Asn) or from cells enriched at the G1, S, S/G2 or G2/M stages of the cell cycle were measured by flow cytometry after propidim iodide staining. **B.** The ratios of signal intensities for Claspin (minus background) and Cdc45 of two independent immunoprecipitation experiments of FLAG-Cdc45 from elutriated K562 cells were determined by densitometry. Signal intensities minus background for Cdc45 and Claspin in each experiment were determined by densitometry (G1 signal for Cdc45 and S phase Claspin signal were normalised to 1). Ratio of signal for Claspin/Cdc45 for G1, S, S/G2 and G2/M cells are depicted with standard deviation from the mean indicated by error bars. AU = Arbitrary Units

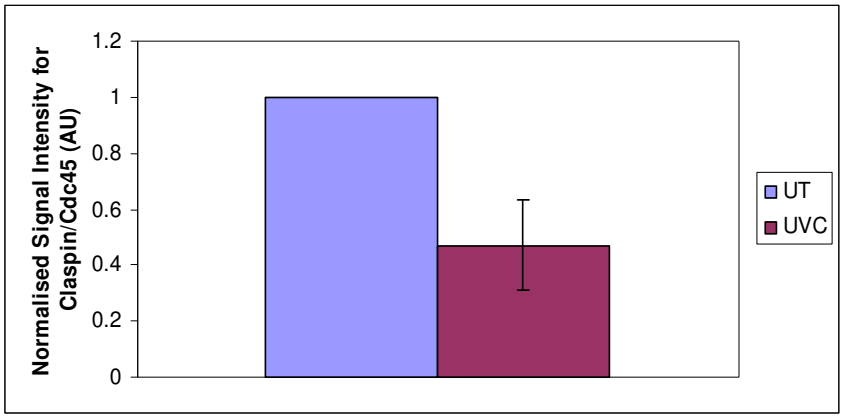

Supplementary Figure 4: Densitometry analysis of Cdc45-Claspin interaction after UVC treatment. The ratios of signal intensities for Claspin (minus background)/Cdc45 (minus background) from 4 different immunoprecipitation experiments of FLAG-Cdc45 from HeLa S3 cells were determined by densitometry. The difference in ratio between untreated (UT, arbitrarily normalised to 1) and UVC-treated (UVC) cells with standard deviation from the mean indicated by error bars are depicted. AU = Arbitrary Units

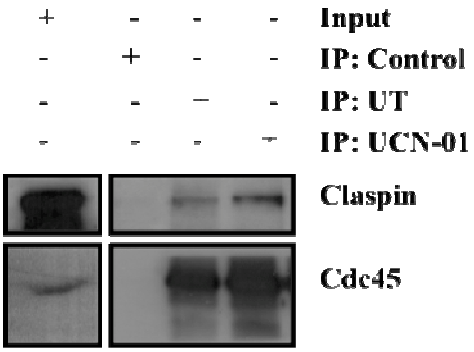

Supplementary Figure 5: Effect of UCN-01 treatment on Cdc45-Claspin interaction. HeLa S3 cells transiently expressing FLAG-Cdc45 or mock-transfected control cells were left untreated or treated for 1h in the presence of 100 nM UCN-01. Cell lysates were normalised for protein content and subjected to FLAG immunoprecipitation. HeLa S3 lysate (Input), and eluates from immunoprecipitations of control cells (IP: Control), cells expressing FLAG-Cdc45 (IP: UT) and cells expressing FLAG-Cdc45 in the presence of UCN-01 (IP: UCN-01) were separated by SDS-PAGE and the co-immunoprecipitation of Claspin with FLAG-Cdc45 was assayed using antibodies raised against Cdc45 and Claspin.

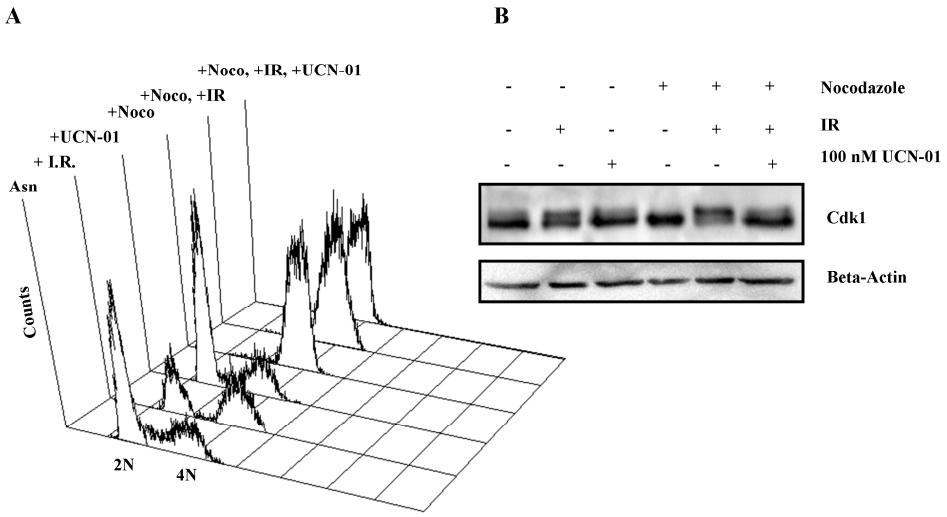

Supplementary Figure 6: Validation of UCN-01 efficacy. HeLa S3 cells were irradiated with 6.3 Gy IR and then incubated in the presence or absence of 400 ng/ml nocodazole for 17h. 11h post-irradiation, UCN-01 was added at a concentration of 100 nM as indicated. Asynchronous (Asn), irradiated (+IR), UCN-01 treated (+UCN-01), nocodazole treated (+Noc) cells, and cells given a combination of treatments (+Noc, +IR) and (+Noc, +IR, +UCN-01) were fixed and subjected to propidium iodide staining and FACS analysis (panel A). **B.** Cells were TGN-lysed, normalised for protein content and subjected to SDS-PAGE and western blotting using antibodies specific to Cdk1 kinase and β-Actin. The former validates UCN-01 efficacy and the latter acts as a loading control, respectively.

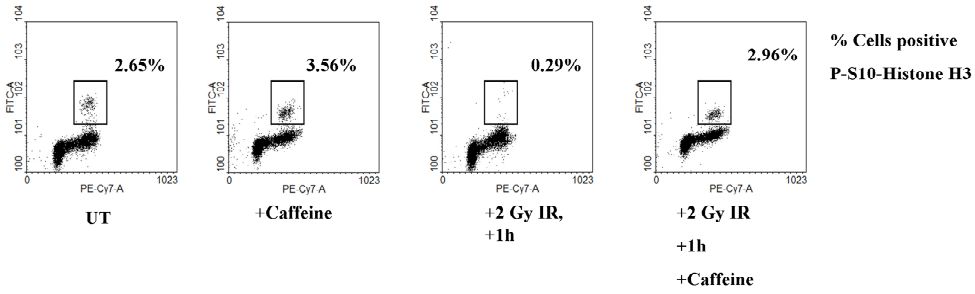

Supplementary Figure 7: Validation of Caffeine efficacy. Asynchronous HeLa S3 cells (UT), cells incubated with 5 mM Caffeine for 2h (+Caffeine), cells exposed to 2 Gy ionizing radiation (IR) and harvested 1h post-treatment (+2 Gy IR, + 1h) or cells pre-treated for 1h with Caffeine, exposed to 2 Gy IR and harvested after 1h in the presence of Caffeine (+2Gy I.R., +1h, +Caffeine) were fixed and harvested for FACS analysis. pS-10-Histone H3 staining was employed and used to determine the % of cells positive for staining.

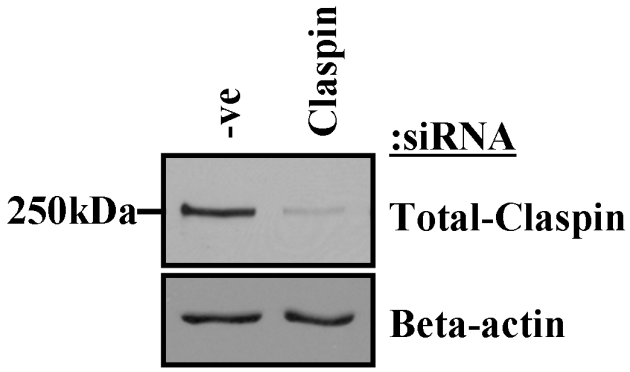

Supplementary Figure 8: Validation of anti-Claspin antibody. A rabbit polyclonal anti-Claspin antiserum was produced against a recombinant N-terminal fragment of Claspin (amino acids 1-237). The antibodies utilized in the experiments were enriched by affinity purification. Validation of this antibody for western blotting was carried out using an siRNA generated against Claspin as previously described (Semple et al, 2007). Briefly, HeLa S3 cells were transfected with siRNA oligonucleotides using siPORT NeoFX (Ambion) and harvested after 48h post transfection for analysis. Cells were lysed in RIPA buffer, normalised for protein content and subjected to SDS PAGE and western blotting using antibody specific to Claspin. Detection of β-Actin serves as a loading control.

Chapter 3

Sub-cellular localisation of Cdc45 in the cell cycle and following DNA damage.

3.1 Abstract

The Cdc45 protein has a central role in the regulation of the initiation and elongation stages of eukaryotic chromosomal DNA replication. In addition, it is the main target for a Chk1-dependent Cdc25A/CDK2-independent checkpoint signal transduction pathway as part of the intra-S-phase checkpoint. The subcellular localisation of Cdc45 following activation of this checkpoint and the regions of Cdc45 which mediate its localisation to the nucleus remain to be determined. Here, we demonstrate the sub-cellular localisation of Cdc45 in the cell cycle and following activation of the intra-S-phase checkpoint. Cdc45 showed a specific nuclear and nucleolar localisation and Cdc45 association with nucleoli was reversively abolished following UV damage and inhibiting nucleolar transcription. Determination of the regions of Cdc45 needed for its localisation to nuclear compartments showed that aa101-155 and aa156-169 are required for recruitment of Cdc45 to the nucleus and nucleolus, respectively.

3.2 Introduction

3.2.1 The role of Cdc45 in DNA replication

The Cdc45 protein plays a key role in the initiation and elongation phases of DNA replication. (Masuda et al, 2003). Cdc45 forms part of the CMG a complex at replication origins shortly before the onset of S phase, mediating the intiation of DNA replication and travelling with the RPC (Replisome Progession Complex) after initiation (Aparicio et al, 2009). Here, it is thought that in the RPC, Cdc45 forms a molecular bridge between the helicase and DNA polymerase components of the complex (Broderick & Nasheuer, 2009). Cdc45 is also the main target of a Chk1-mediated DNA S-phase checkpoint, which operates via a Cdc25A/CDK2-independent mechanism (Liu et al, 2006).

The subcellular localisation of Cdc45 has been characterised in several model systems. Initial studies in *Saccharomyces cerevisiae* expressing GFP-Cdc45 show a nuclear localisation of the yeast fusion protein in many cells observed (Hopwood & Dalton, 1996). The authors also use a bioinformatic approach to identify a putative bipartite NLS in yeast Cdc45 KRGNSSIGPNDLSKRKQKKK at aa 209-228. Studies with Cdc45 C-terminally tagged with 3 x HA in trypanosomes confirm the nuclear localisation of Cdc45 which localised

nucleoplasm during interphase but no noticeable enrichment in the nucleolus of cells was observed (Dang & Li, 2011). At mitosis in these organisms Cdc45 is seen to be in the cytoplasm with apparent cytosolic localisation of Cdc45 at this stage of the cell cycle, as this localisation is abrogated and nuclear localisation restored by treatment with leptomycin-B (Dang & Li, 2011). A study of the interactions of MCP1 protein with components of the replication machinery in human MO59K cells using an antibody raised against Cdc45 shows nucleoplasmic localisation of Cdc45 in interphase cells with no clear exclusion of Cdc45 from the nucleolus (Bronze-da-Rocha et al, 2011). In a study by Bauerschmidt and colleagues (Bauerschmidt et al, 2007), HeLa S3 cells synchronised at various cell cycle stages by consecutive thymidine block stained for Cdc45 show a diffuse nucleoplasmic localisation in G1 phase with no clear nucleolar exclusion, a punctuate nucleoplasmic localisation in S phase cells with clear nucleolar exclusion and a less punctate signal in G2 cells with no clear nucleolar exclusion. Mitotic cells show that Cdc45 is still present but is distinct from DNA (Bauerschmidt et al, 2007).

3.2.2 Cellular functions of nucleoli in eukaryotic cells

The nucleolus is a sub-nuclear organelle whose primary function was originally identified as ribosome biogenesis, (Dellaire & Bazett-Jones, 2007). Nucleoli form at the end of mitosis around tandem repeats of ribosomal DNA (rDNA) genes which are arranged in arrays of head-to-tail repeats, termed nucleolar organizer regions (NORs) located on acrocentric chromosomes (Boisvert et al, 2007). Nucleoli have recently been demonstrated to have other functions distinct from ribosome biogenesis, including the maturation of non nucleolar RNAs and ribonucleoproteins, mRNA export and nonsense-mediated decay, regulation of cell-senescence, control of viral infection, the regulation of telomerase activity and interestingly, control of cell-cycle progression, tumour suppression, DNA repair and the cell stress response (Dellaire & Bazett-Jones, 2007). Several proteomic analyses have been undertaken to characterize the nucleolar proteome in human and plant cells which have identified more than 200 plant proteins and over 700 human proteins that stably co-purify with isolated nucleoli, and that only 30% of all of the proteins detected have a function that is related to the production of ribosome subunits (Boisvert et al, 2007). Recent studies have characterized

dynamic changes in the proteome of the nucleolus under different metabolic conditions, such as inhibition of transcription following treatment of cells with Actinomycin D, a Pol I inhibitor (Boisvert et al, 2007). The protein dynamics and composition of the nucleolus can change dramatically in response to cellular stress such as transcriptional and proteosomal inhibition, aberrant ribosome biogenesis, heat shock, hypoxia and DNA damage indicating that in addition to ribosome biogenesis the nucleolus may serve a central role in regulating the cell stress response by integrating the control of both cellular protein levels and the cell cycle (Dellaire & Bazett-Jones, 2007). DNA damage caused by UV-irradiation or induction of DNA DSBs by topoisomerase II inhibitors causes nucleolar segregation, with separation of the nucleolar compartments and the appearance of "nucleolar caps" around what appears to be a nucleolar remnant (Dellaire & Bazett-Jones, 2007). Formation of these "nucleolar caps" also occurs after inhibition of Pol I by Actinomycin D treatment (Reynolds et al, 1964). Morphological changes induced by UV-irradiation are also accompanied by the redistribution of nucleolar proteins such as Ki-67, nucleolin, RNA pol I, and nucleophosmin (B23) (Dellaire & Bazett-Jones, 2007). Other DNA damaging agents such as cisplatin, which induce DNA cross-links, disrupt nucleoli by the redistribution of upstream-binding factor (UBF) and RNA pol I, resulting in inhibition of rRNA synthesis (Dellaire & Bazett-Jones, 2007).

The rDNA is replicated in a biphasic manner with active genes (60%) replicating early and silent ones (40%) replicating late in S-phase (Li et al, 2005). The ATP-dependent chromatin remodelling complex NoRC also plays a role in replication timing of rDNA (Li et al, 2005). NoRC is exclusively associated with late-replicating rDNA arrays with overexpression of NoRC silencing rDNA transcription, reducing the size and number of nucleoli and impairing cell proliferation and changing replication timing of rDNA regions from early to late replicating (Li et al, 2005). A replication fork barrier (RFB) at the 3′ end of eukaryotic ribosomal RNA genes blocks bidirectional fork progression and limits DNA replication to the same direction as transcription (Gerber et al, 1997). Depletion of the RNA polymerase I–specific transcription termination factor TTF-I, or deletion of the termination domain of TTF-I abolishes this RFB activity demonstrating that the same factor that blocks elongating RNA polymerase I

prevents head-on collision between the DNA replication apparatus and the transcription machinery (Gerber et al, 1997). In HeLa cells it has been demonstrated that early replicating rDNA is localised to the nucleolar periphery and more rarely outside nucleoli (Dimitrova, 2011). Early-replicated rDNA relocates to the nucleolar interior and reassociates with the transcription factor UBF, implying that it predominantly represents expressed rDNA units (Dimitrova, 2011). Silent rDNA copies appear to replicate inside the nucleoli during mid and late S phase (Dimitrova, 2011). At this stage of the cell cycle replication origins are fired preferentially within the non-transcribed intergenic spacers (NTSs) of the rDNA repeats and ongoing rDNA transcription is required to maintain this specific initiation pattern (Dimitrova, 2011).

3.2.3 Cdc45 and replication of rDNA

The sub-cellular localisation of Cdc45 in the cell cycle and and after the induction of replication stress remains to be fully examined. In this study, we examined the localisation of Cdc45 in asynchronous HeLa S3 and U20S cells and determined a nuclear localisaion with some nucleolar localisation. This nucleolar pool of Cdc45 was also observed via isolation of nucleoli followed by SDS-PAGE and western blotting. The localisation pattern of Cdc45 is modulated by replication stress, with cells treated with UVC, Actinomycin D or thymidine having less pronounced nucleolar localisation than untreated cells. Deletion mutants of Cdc45 reveal the regions of the protein necessary for its nuclear and nucleolar localisation. Sequestering of Cdc45 to the nucleolus, and analysis of the sizes of Cdc45-containing complexes suggest that Cdc45 present in the nucleolus of cells has no alternative function besides that of replication of the rDNA. Taken together, these results support a model whereby non-exclusion of Cdc45 from the nucleolus may facilitate its role in DNA replication of the rDNA repeats.

3.3 Results

3.3.1 Cdc45 localisation in asynchronous cells, after UV damage and inhibition of RNA Polymerase I transcription

To analyse the function of human Cdc45 *in vivo* a detailed investigation of the sub-cellular localisation in expontially growing human cells was carried out. Immunofluorescence staining of asynchronous HeLa S3 cells using C45-3G10 antibody shows localisation of Cdc45 in the nucleoplasm and in the nucleolus of interphase cells (Figure 1). Nucleolar localisation of Cdc45 was also observed in other human cell lines such as U20S cells (Figure 2). Detergent pre-extraction of HeLa S3 cells results in loss of this nucleolar localisation and in a dot like localisation of Cdc45 observed in the nucleolplasm (Figure 3). Following treatment of HeLa S3 cells with UVC or inhibition of Pol I transcription with Actinomycin D, nucleolar enrichment of Cdc45 is reduced as assayed by immunofluorescence microscopy (summarised in Figures 4 and 5). The loss of nucleolar localisation following UVC treatment occurs in a dose and time-dependent manner (Figure 4). HeLa S3 cells treated with 5 or 30 J/m^2 UVC also showed a loss of nucleolar enrichment at 2 h post-treatment with recovery of nucleolar enrichment observed 8 h post-treatment in cells treated with 5 J/m^2. Conversely no recovery of localisation was observed in cells treated with 30 J/m^2 (Figure 4). The inhibition of rDNA transcription caused a loss of Cdc45 association with nucleoli (Figure 5) which suggests that ongoing transcription in nucleoli is necessary for the nucleolar localisation of Cdc45. These findings suggest that Cdc45 is not excluded from the nucleolar compartment and that this localisation is sensitive to reagents which cause replication stress and Pol I inhibiton.

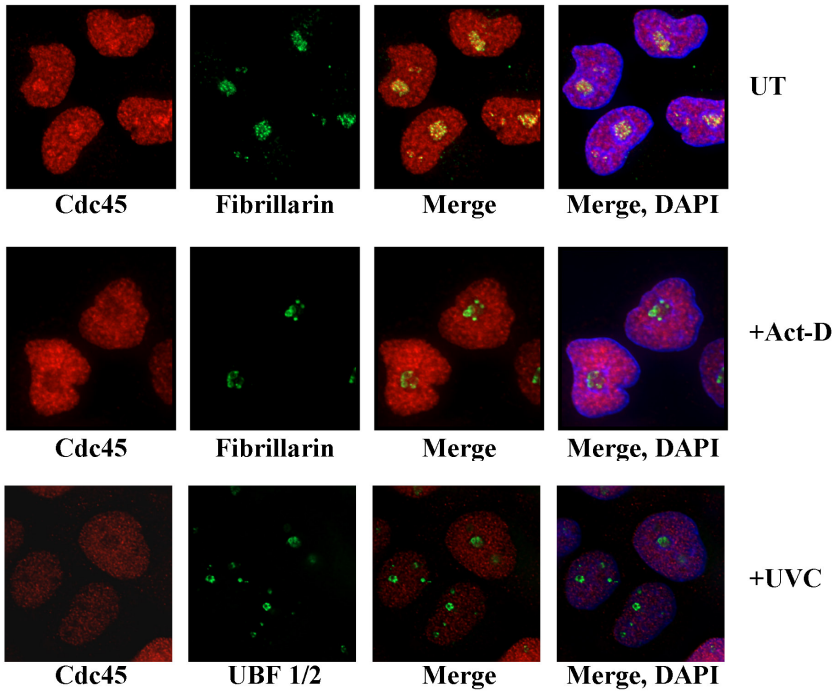

Figure 1: Subcellular localisation of Cdc45 in asynchronous cells and following UVC and Actinomycin D treatment.
Asynchronus HeLa S3 cells untreated (UT), treated with 30J/m^2 of UVC (+UVC) or with 0.1 µg/ml of Actinomycin D (+Act-D) and harvested 2h post-treatment were analysed by immunofluorescence microscopy using antibodies against Cdc45, UBF 1/2 or Fibrillarin. UBF1/2 or Fibrillarin act as a markers for the nucleolus. DAPI staining acts as a marker for the nucleus and nucleolus. DyLight 594-labelled secondary antibody was employed for red staining, and Cy2-labelled secondary antibody was used for green staining.

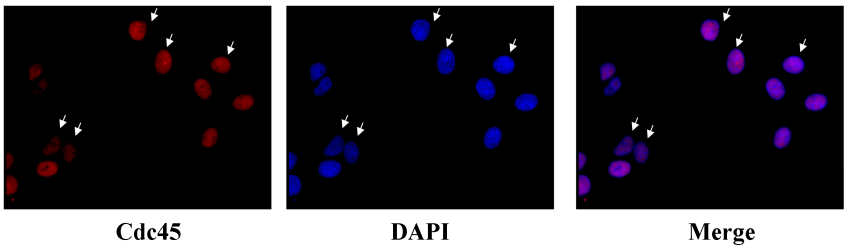

Figure 2: Sub-cellular localisation of Cdc45 in U20S cells.
Asynchronus U20S cells were analysed by immunofluorescence microscopy using antibody raised against Cdc45. White arrows indicate cells with nucleolar localisation. DAPI staining serves as a marker for the nucleus and nucleolus. DyLight 594-labelled secondary antibody was used for red staining.

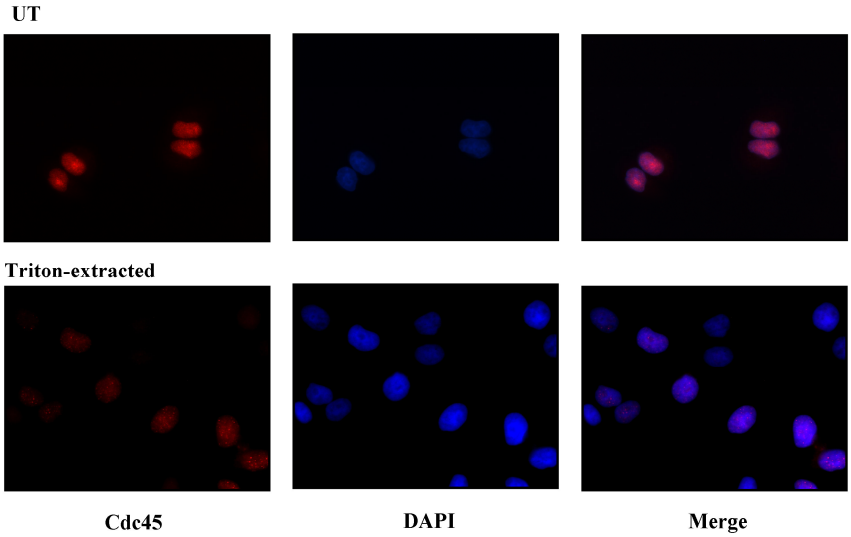

Figure 3: Detergent pre-extraction ablates nucleolar localisation of Cdc45
Asynchronus HeLa S3 cells (UT) or cells which were pre-extracted with 0.1% Triton in CSK buffer were fixed and analysed by immunofluorescence microscopy using antibody specific to Cdc45. DAPI staining acts as a marker for the nucleus and nucleolus. DyLight 594-labelled 594 antibody was used for red staining.

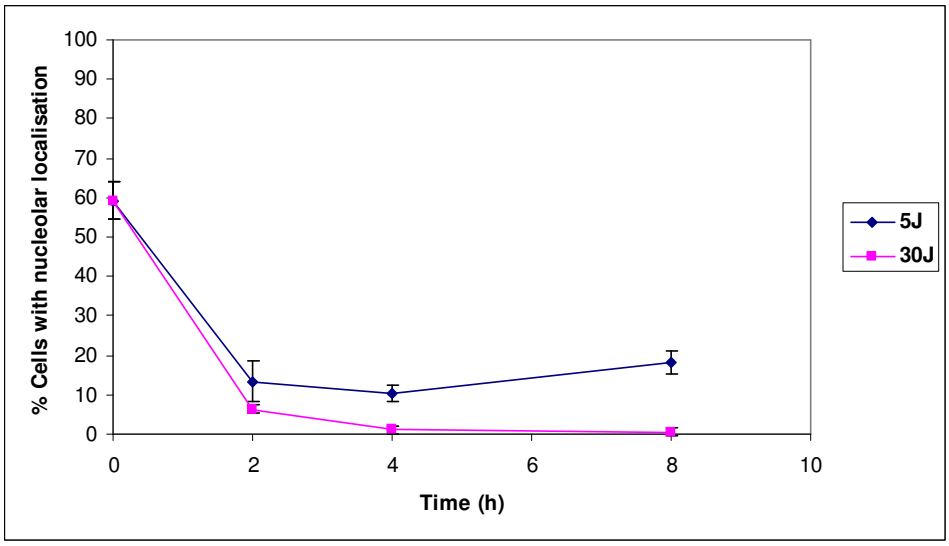

Figure 4: Nucleolar localisation of Cdc45 following UVC treatment
Asynchronous HeLa S3 cells were treated with 5 or 30 J/m^2 UVC, harvested at the indicated time points and subjected to immunofluoresence microscopy using antibody raised against Cdc45. 100 cells at each time point were counted and the % of cells with clear nucleolar localisation of Cdc45 was determined. Error bars represent standard deviation from the mean of 3 independent experiments.

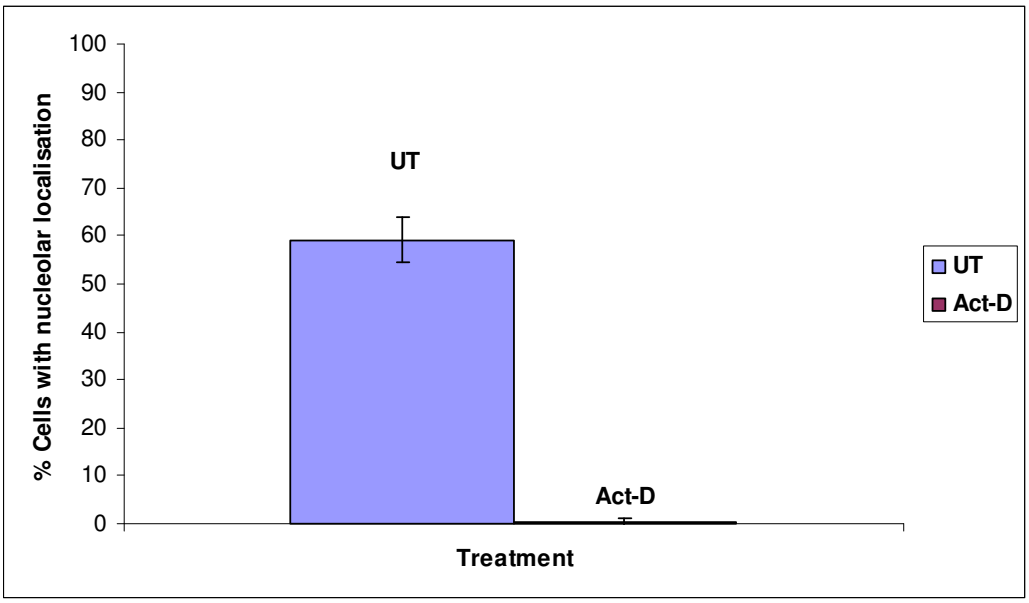

Figure 5: Subcellular localisation of Cdc45 following Actinomycin D treatment
Asynchronous HeLa S3 cells were untreated (UT) or treated with 0.1 µg/ml of Actinomycin D (Act-D) and harvested 2h post treatment and were analysed by immunofluorescence microscopy using antibody against Cdc45. 100 cells at each point were counted and the % of cells with clear nucleolar localisation of Cdc45 was determined. Error bars represent standard deviation from the mean of 3 independent experiments.

3.3.2 Analysis of nucleolar Cdc45 by isolation of nucleoli and quantitative western blotting

To biochemically analyse the localisation of Cdc45 within nucleoli exponetially growing HeLa S3 cells were lysed and nucleoli were isolated following standard procedures. The nucleoli purified from these cells did not show an enriched association of Cdc45 (Figure 6). Asynchronous HeLa S3 cells or cells crosslinked with PFA were harvested, normalised to cell number and the nucleoli from these cells were isolated (Figure 6). Assuming equal yields from these preparations, equal numbers of nucleoli were lysed in Laemmli buffer and sonicated to solubilise all proteins present and were analysed by SDS PAGE and quantitative western blotting. It was determined that Cdc45 was present in nucleoli at a level above background contaminantions, and at a level greater than other proteins involved in DNA replication such as RPA since no enrichment of the RPA subunit RPA32 has been demonstrated in the nucleolus by localisation studies. Following crosslinking with PFA levels of Cdc45 determined in isolated nucleoli were markedly increased

whereas no increase in signal for β-Actin was observed (Figure 6). In contrast, a slight decrease in the levels of PAF53, a nucleolar protein which is tightly associated with Pol I, was observed following crosslinking (Figure 6). In crosslinked nucleoli RPA32 showed a slight increase (Figure 6) but this was significantly less than that of Cdc45 and was just above the level of detection with this highly sensitive antibody. These results suggest that only a small amount of Cdc45 is retained in isolated nucleoli with more Cdc45 retained after PFA crosslinking of proteins and nucleic acids.

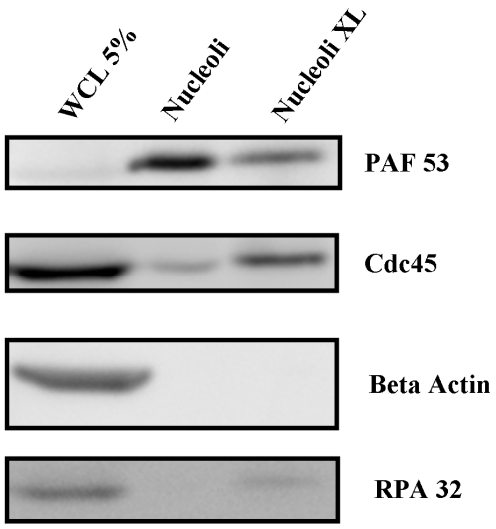

Figure 6: Characterisation of Cdc45 in isolated nucleoli
Asynchronus HeLa S3 cells were untreated or cross-linked (XL) with 1% paraformaldeyde to prevent loss of Cdc45 protein and subjected to nucleolar purification. Nucleoli were isolated and samples were boiled in 1x Laemmli buffer, sonicated and subjected to SDS-PAGE (10% gel, $1.2x10^6$ cells/lane or 1/20 this number of whole cell lysate (WCL) as indicated). Antibodies raised against PAF53 (RNA Pol I-associated protein) acts as a marker for proteins enriched within the nucleolus. Antibodies raised against β-Actin and RPA32 act as controls for cytoplasmic, cytoskeletal and chromatin contaminants, respectively.

To determine wether the regulation of Cdc45 localisation could be biochemically analysed, untreated, asynchronous HeLa S3 cells or cells treated with UVC or Actinomycin D were harvested 2h post-treatment and cross-linked with PFA (Figure 7). Nucleoli were isolated, lysed and subjected to SDS PAGE and western blotting. The levels of Cdc45 in UVC-treated cells were 50% of that in untreated control cells using quantitative western blotting whereas the levels of Cdc45 in Actinomycin D-treated cells were 10% of the control cells (Figure 7). Equal loading

of nucleolar preparations was confirmed by western blotting and detection of PAF53 serving as a positive control, whereas purity of the preparations was assayed by detection β-Actin as a negative control in parallel.

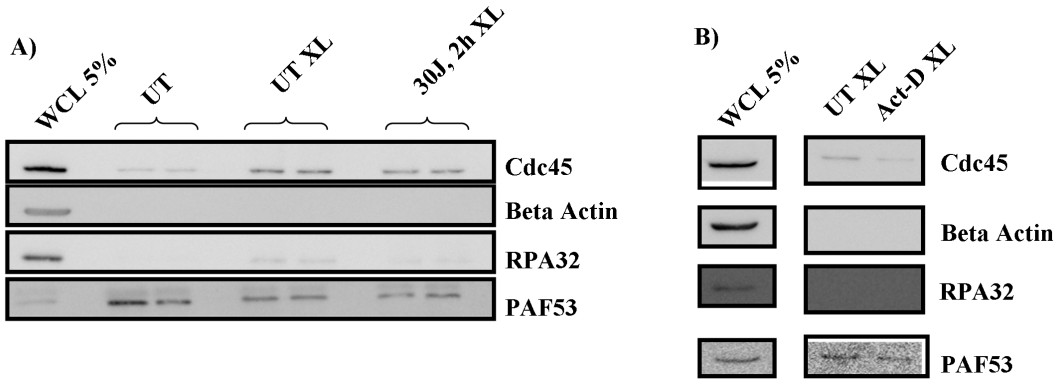

Figure 7: Characterisation of Cdc45 in isolated nucleoli following UVC and Actinomycin D treatment
HeLa S3 cells were treated with 30J/m2 UV or 0.1μg/ml Actinomycin D and cross-linked (XL) to prevent loss of Cdc45 protein and subjected to nucleolar purification. Samples were boiled in 1x Laemmli, sonicated and subjected to SDS-PAGE (10% gel, $1.2x10^6$ cells/lane or 1/20 this number of whole cell lysate (WCL) as indicated). Antibodies raised against RPA43 and Paf 53 (RNA Pol I subunit and associated protein, respectively) act as markers for proteins enriched within the nucleolus. Antibodies raised against β-Actin and RPA32 act as controls for cytoplasmic, cytoskeletal and chromatin contaminants, respectively.

3.3.3 Localisation of Cdc45 throughout the cell cycle

After determining that Cdc45 had nuclear and nucleolar localisation in an asynchronous population of cells, we sought to characterise the localisation of Cdc45 throughout the cell cycle. HeLa S3 cells were synchronised at the G1/S transition by two consecutive thymidine blocks and cells were then released from thymidine treatment and progressed in synchrony through the cell cycle. The cells were fixed and Cdc45 localisation was assayed by immunofluorescence microscopy (Figure 8). Here nucleoplasmic and nucleolar localisation are observed in untreated, asynchronous control cells (Figure 8). In cells synchronised at the G1/S transition Cdc45 localises in the nucleoplasm but does not have any nucleolar enrichment. A similar localisation pattern is seen in S phase and G2 phase cells after release from the double thymidine block. In mitotic cells, Cdc45 is present but distinct from condensed chromatin. Asynchronous HeLa S3 cells treated with thymidine showed

a time-dependent loss of nucleolar enrichment, which took place within 24 h post-treatment (Figure 9).

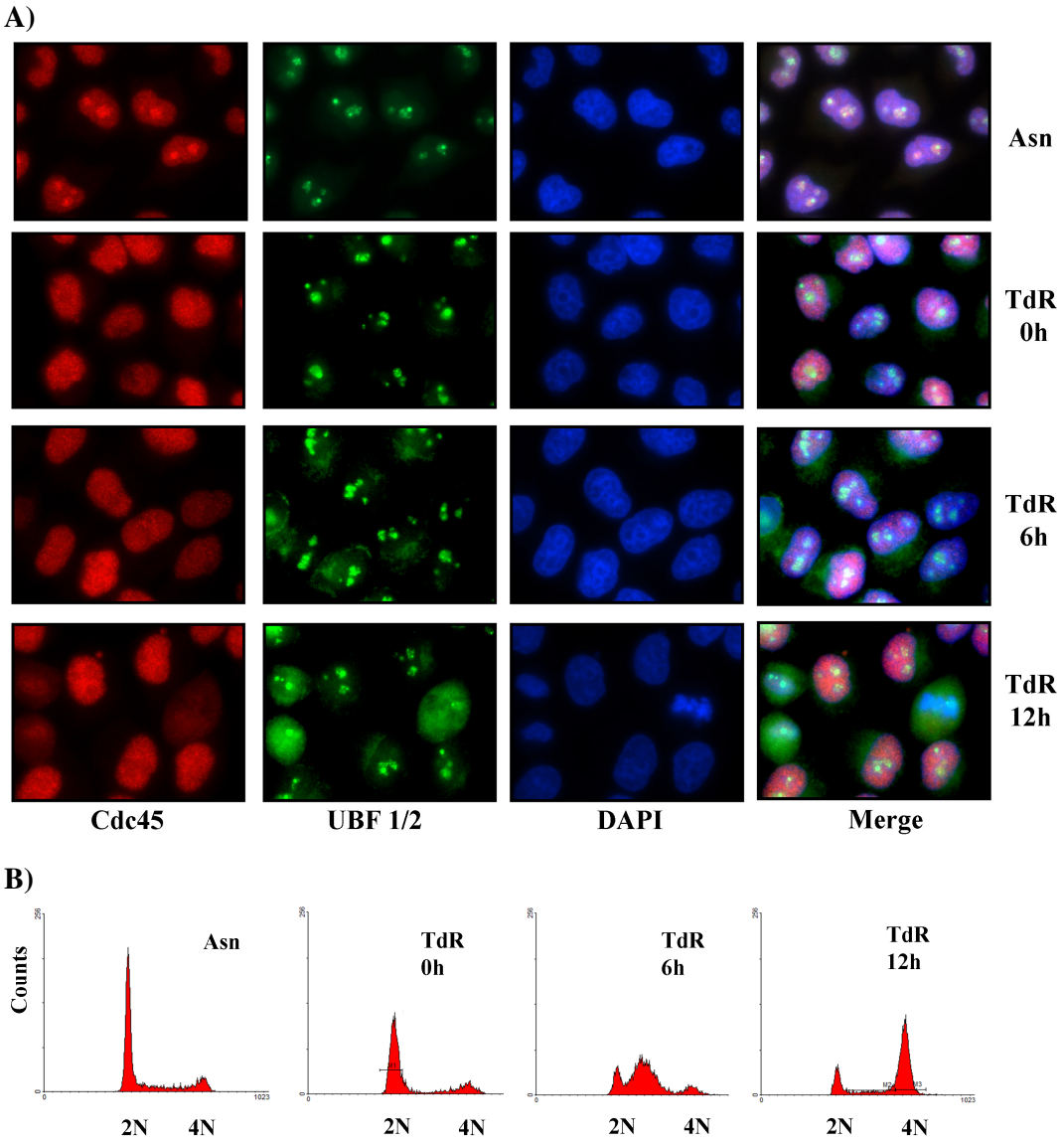

Figure 8: Sub-cellular localisation of Cdc45 following release from double thymidine block and release procedure

A Asynchronous HeLa S3 cells (Asn) or cells synchronised by sequential thymidine block and harvested at various timepoints post release from the second thymidine block (TdR 0h to TdR 12h) were fixed for immunofluorescence microscopy using antibodies specific to Cdc45 and UBF 1/2. UBF 1/2 acts as a marker for the nucleolus and DAPI staining acts as a marker for the nucleus and nucleolus. Cell synchrony was confirmed by fixing cells for FACS analysis and propidium iodide staining (Panel B).

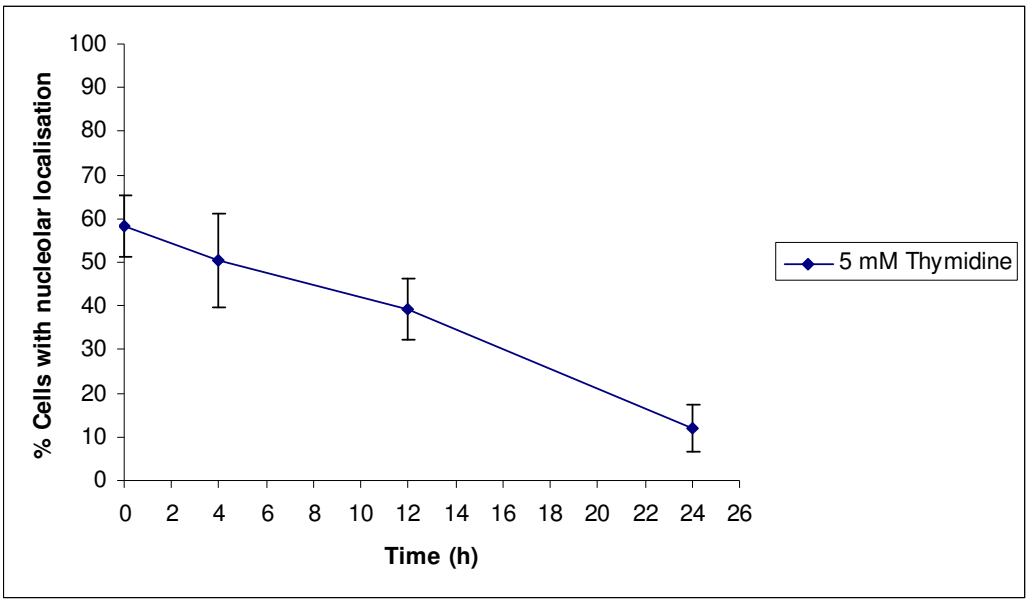

Figure 9: Nucleolar localisation of Cdc45 is thymidine sensitive
Asynchronous HeLa S3 cells were treated 5 mM Thymidine (5, mM Thymidine) and harvested at various time points post treatment (Time (h)) and were analysed by immunofluorescence microscopy using antibody against Cdc45. 100 cells from each point were counted and the % of cells with clear nucleolar localisation of Cdc45 was determined. Error bars represent standard deviation from the mean of 3 independent experiments.

To further characterise the localisation of Cdc45 through the cell cycle without thymidine arrest, cellular distribution of Cdc45 in asynchronous cells was determined in parallel with cell phase-specific markers. Labelling of cells with BrdU during DNA replication could not be utilized since the determination of incorporated BrdU required a denaturing step, which itself altered the staining obtained for Cdc45 by immunofluorescence microscopy (data not shown). Asynchronous HeLa S3 cells were pulse labelled with EdU, fixed and stained for immunofluorescence microscopy using antibodies for Cdc45, pS10 of Histone H3 and/or labelled for EdU incorporation (Figure 10). Here nucleolar enrichment is seen in interphase cells, in cells labelled with EdU (S phase cells) and in cells staining for pS10 of Histone H3, a marker for late G2 phase and mitosis. Single and double labelling of Cdc45 with each of these markers revealed cells with nucleoplasmic and nucleolar localisation in EdU-labelled and pS10 H3-labelled cells, and in cells not labelled with either marker, suggesting that this localisation

occurs in all interphase cells. In mitotic cells Cdc45 is seen to be present but distinct from condensed chromatin.

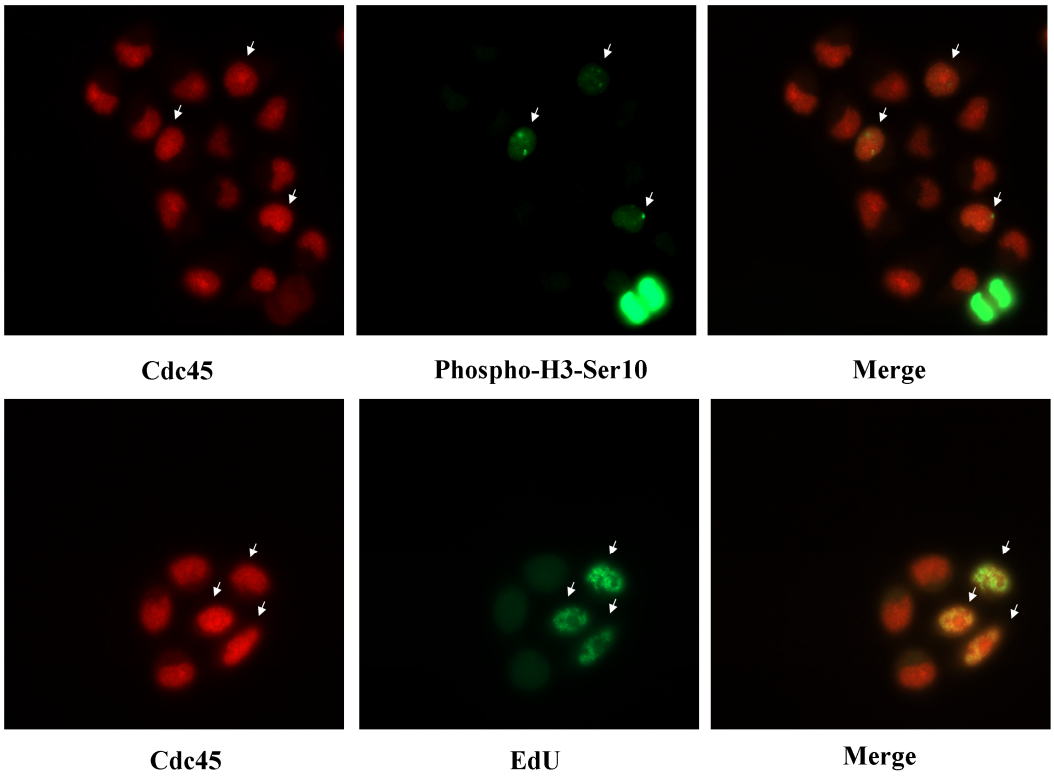

Figure 10: Cdc45 localisation in EdU and pS-10 Histone H3 labelled cells
Asynchronous HeLa cells were pulse-labelled with EdU, fixed and stained for EdU and for immunofluoresence microscopy using antbodies against Cdc45 or Phospho-Histone H3 Serine 10 (Phospho-H3-Ser10). Cells with clear nucleolar localisation are indicated by white arrows. DyLight 594-labelled secondary antibody was employed for red staining, and Cy2-labelled secondary antibody was used for green staining.

3.3.4 Ectopic expression and localisation of Cdc45 fusion proteins

In order to generate tools for the further biochemical characterisation of Cdc45 function in human cells, Cdc45 fusion proteins were generated and their expression and localisation characterised. HeLa S3 cells transiently expressing CFP-Cdc45, GFP-Cdc45 or FLAG-tagged Cdc45, with a single FLAG tag added to either the N- or C-terminus were lysed, normalised for protein content and subjected to SDS PAGE and western blotting. (Figures 11 to 13). Antibodies against FLAG, GFP or Cdc45 confirmed expression of all fusion proteins and β-Actin serves as a loading control in all cases (Figures 11 to 13).

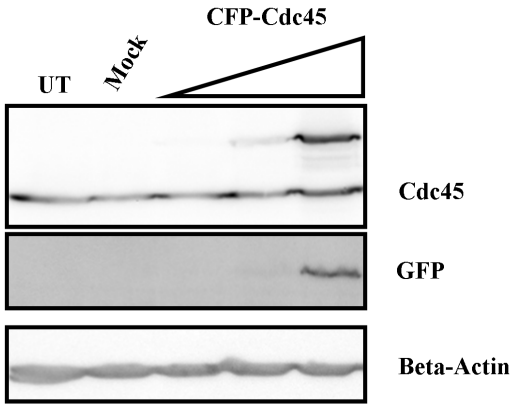

Figure 11: Ectopic expression of CFP-Cdc45
HeLa S3 cells were untransfected (UT), mock transfected (Mock) or transfected with plasmid encoding CFP-Cdc45 and varying amounts of transfection reagent (indicated by wedge) and were harvested 24h post-transfection and lysed in RIPA buffer. Lysates were normalised for protein content and subjected to SDS-PAGE and western blotting using antibodies specific to Cdc45, GFP and β-Actin, with β-Actin acting as a loading control.

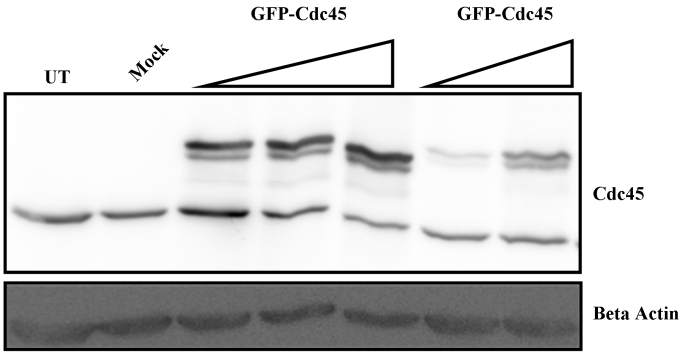

Figure 12: Extopic expression of GFP-Cdc45
HeLa S3 cells were un-transfected (UT) or mock transfected (Mock) or transfected with plasmid ecoding GFP-Cdc45 and varying amounts of transfection reagent (indi-cated by wedge) were harvested 24 hours post-transfection and lysed in RIPA buffer. Lysates were normalised for protein content and subjected to SDS-PAGE and western blotting using antibodies specific to Cdc45 and β-Actin, with β-Actin acting as a loading control.

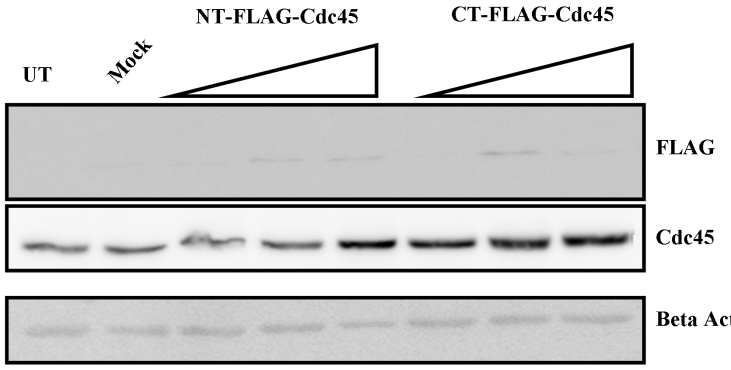

Figure 13: Ectopic expression of FLAG-Cdc45
HeLa S3 cells were untransfected (UT) or mock transfected (Mock) or transfected with plasmid ecoding N- or C-terminally FLAG-tagged Cdc45 and varying amounts of transfection reagent (indicated by wedge) were harvested 24 hours post-transfection and lysed in RIPA buffer. Lysates were normalised for protein content and subjected to SDS-PAGE and western blotting using antibodies specific to FLAG, Cdc45 and β-Actin, which served as a loading control.

In addition, immunofluorescence microscopy was performed with HeLa S3 cells transiently expressing CFP-Cdc45, GFP-Cdc45, N-terminal FLAG or C-terminal FLAG-Cdc45 or using antibody raised against Cdc45 in untransfected control cells (Figure 14). In all cases nuclear localisation in interphase cells was observed. In asynchronous control cells endogenous Cdc45 showed a nucleolar enrichment (Figure 14). Cells expressing CFP-Cdc45 also had nucleolar localisation of the fusion protein in a sub-set of cells (Figure 14). Here a globular, spot-like localisation is found within nucleoli, which is distinct from the more uniform nucleolar enrichment of endogenous Cdc45 seen in control cells (Figure 14, compare panels A and C). This globular localisation in a sub-set of cells is also observed in cells expressing GFP-Cdc45 (with the GFP tagged to the N-terminus of Cdc45) and in N-terminally FLAG-tagged Cdc45 for the recombinant Cdc45 fusion protein (Figure 14). In contrast, cells expressing C-terminally FLAG-tagged Cdc45

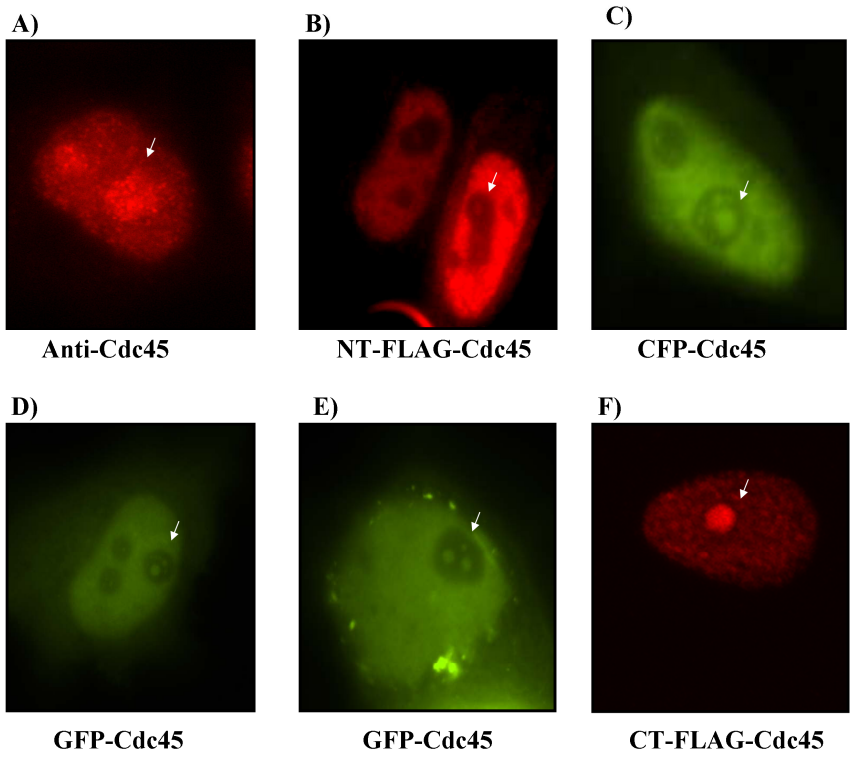

Figure 14: Subcellular localisation of ectopically expressed Cdc45
Asynchronus HeLa S3 cells were stained for immunofluorescence with antibody raised againsed Cdc45, or transiently transfected with N-terminal or C-terminal FLAG-tagged Cdc45 in pTRExDEST30 vector and stained for immuno-fluorescence with anti-FLAG antibody (Sigma M2 anti-FLAG). HeLa S3 cells transiently transfected with plasmid constructs coding for CFP- or GFP- Cdc45 fusion proteins. Nucleolar localisation is indicated by arrows. Independent secondary antibodies were used for red staining

showed a subcellular localisation of the recombinant Cdc45 which is the most similar to that obtained when endogenous Cdc45 (Figure 14 compare panel A with panel F, respectively).

3.3.5 Generation of HeLa S3 cells stably expressing GFP-Cdc45 or N-terminally tagged FLAG-Cdc45

In order to generate stable cell lines to study the biochemical functions and localisation of Cdc45 in the cell cycle and after DNA damage, HeLa S3 cells were transfected with plasmid encoding GFP-Cdc45 or N-terminally FLAG-tagged Cdc45 and cultured in the presence of G-418. Stable clones were isolated and screened by SDS PAGE and western blotting using antibodies raised against Cdc45 or FLAG, with β-Actin serving as a loading control in all cases (Figures 15 and 16, respectively)

Several positive clones expressing GFP-Cdc45 fusion proteins were isolated and in all cases the level of expression of GFP-Cdc45 was less than that of endogenous Cdc45 as determined by quantitative western blotting (Figure 15). Clone number 21 was chosen for further experiments due to its lack of any apparent abnormal phenotype.

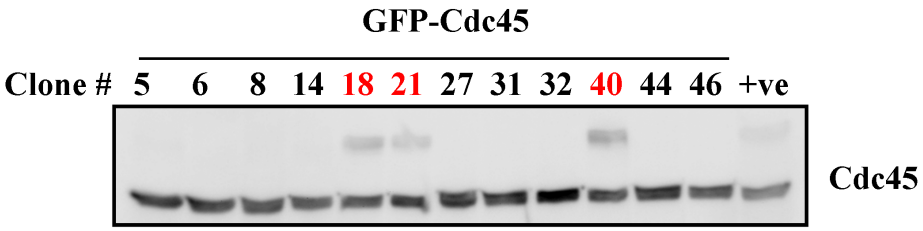

Figure 15: Characterisation of expression levels of HeLa S3 cells stably expressing GFP-Cdc45
HeLa S3 cells were transfected with plasmid encoding GFP-Cdc45 fusion protein and stable clones were selected using G418 treatment and clonal selection. Lysates from different clones were normalised for protein content and subjected to SDS-PAGE and western blotting using antibody specific for Cdc45. Clone number is indicated with clones clearly positive for GFP-Cdc45 highlighted in red. Lysate from a transient transfection of HeLa S3 cells expressing GFP-Cdc45 was loaded in each case as a positive control (+ve).

Several positive clones expressing N-terminally FLAG-tagged Cdc45 were isolated and confirmed by quantitative western blotting (Figure 16). Antibody raised against FLAG confirms expression of the fusion protein. Due to the small size of the single FLAG tag added to the N-terminus of Cdc45 it was not possible to distinguish the endogenous Cdc45 from the fusion protein. Clone number 24 was chosen due to its lack of multi-nuclear cells and its level of expression, which was estimated to be equal to the endogenous Cdc45 (Figure 16). The expression levels of Cdc45 in all cell lines generated proved to be too low to carry out live cell imaging or most biochemical assays but they were suitable for fluorescence correlation spectroscopy and are further analysed in Chapter 4.

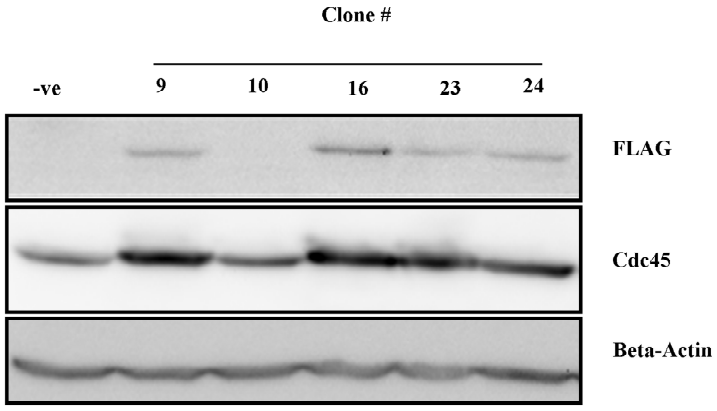

Figure 16: Characterisation of expression levels of HeLa S3 cells stably expressing FLAG-Cdc45
HeLa S3 cells were transfected with plasmid encoding N-terminally FLAG-tagged Cdc45 in pT-RexDest30 plasmid and stable clones were selected using G418 treatment and clonal selection. Lysates from different clones were normalised for protein content and subjected to SDS-PAGE and western blotting using antibody specific for FLAG, Cdc45 and β-Actin. β-Actin acts as a loading control. Clone number is indicated with un-transfected HeLa S3 cells used as a negative control (-ve).

3.3.6 Cdc45 is sequestered to the nucleolus using a NoLS tag and remains sequestered following UVC treatment and inhibition of RNA Polymerase I transcription

In order to determine if the Cdc45 localising to the nucleolus has any essential function within the cell, Cdc45 was directly sequestered to the nucleolus with a nucleolar localisation signal and the fluorescent protein CFP. The fusion protein was called CFP-NoLS-Cdc45. HeLa S3 cells transiently expressing CFP-NoLS-Cdc45 and CFP-NoLS as a control were fixed and subjected to fluorescence microscopy (Figure 17, B and C). CFP-NoLS-Cdc45 and CFP-NoLS fusion proteins are sequestered to the nucleolus in all interphase cells observed (Figure 17, B and C, respectively). No phenotype in cells expressing the Cdc45 fusion protein or the CFP-NoLS control fusion protein was observed. HeLa S3 cells transiently expressing CFP-NoLS-Cdc45 were treated with UVC or Actinomycin D, fixed and subjected to fluorescence microscopy (Figure 18). Here CFP-NoLS-Cdc45 fusion protein remained sequestered to the nucleolus following UVC treatment and Actinomycin D treatment. Transient expression of this fusion protein resulted in a level of expression similar to that of endogenous Cdc45 (Figure 17A).

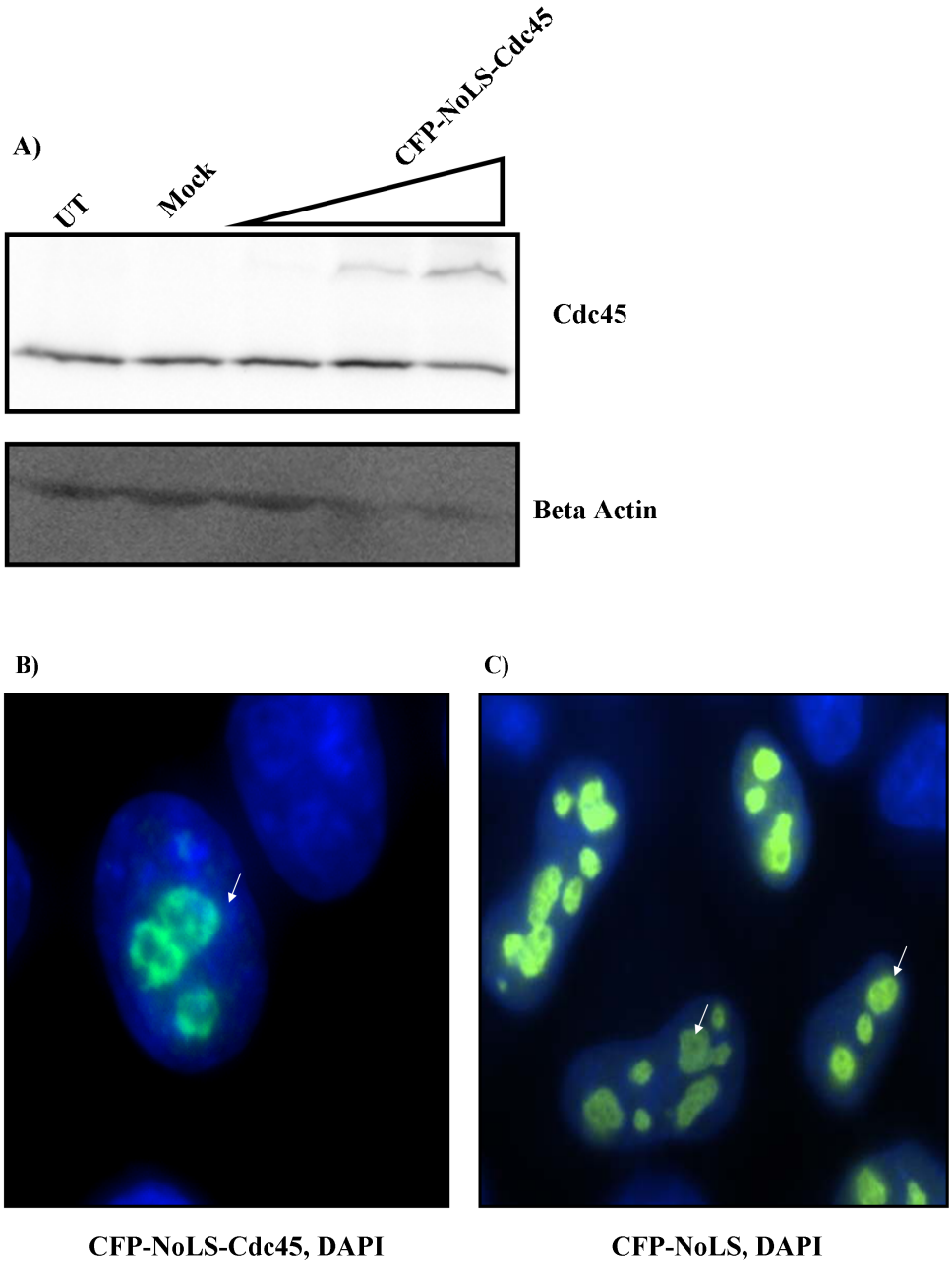

Figure 17: Expression and localisation of CFP-NoLS-Cdc45
A) HeLa S3 cells were untransfected (UT) or mock transfected (Mock) or transfected with plasmid encoding CFP-NoLS-Cdc45 with varying amounts of transfection reagent (indicated by wedge) were harvested 24 hours post-transfection and lysed in RIPA buffer. Lysates were normalised for protein content and subjected to SDS-PAGE and western blotting using antibodies specific to Cdc45, GFP and β-Actin, which acted as a loading control. HeLa S3 cells transiently expressing CFP-NoLS-Cdc45 or CFP-NoLS as a control (panel B and C, respectively), were fixed and analysed by fluorescence microscopy. DAPI stain acts as a marker for the nucleus

3.3.7 Sub-cellular localisation of Cdc45 deletion mutants

In order to determine the regions of Cdc45 responsible for its sub-cellular localisation to the nucleus and nucleolus, full length and deletion mutants of Cdc45, all with a single C-terminal FLAG tag, were transiently expressed in HeLa S3 cells (Figures 19 and 20). Expression of each deletion mutant was confirmed by FLAG-immunoprecipitation with SDS PAGE and western blotting (Chapter 2 and data not shown). Cells were fixed and subjected to immunofluorescence microscopy using antibody raised against FLAG (Figure 19B**).** Full length C-terminally FLAG-tagged Cdc45 showed nuclear and nucleolar localisation similar to localisation observed using the C45-3G10 antibody. The FLAG-tagged ΔNT Cdc45 deletion mutant, localised to the nucleus and had some nucleolar and cytosolic localisation (Figure 19B). The Δ(aa101-190) deletion mutant was found in the cytosol (Figure 19B)**.** In contrast, the Δ(aa101-190) deletion mutant with an NLS (PKKKRKVG) added to the N-terminus, was directed to the nucleus but no discernable nucleolar enrichment could be detected. The Cdc45 mutants Δ(aa191-290), Δ(aa291-390), Δ(aa391-488) and ΔCT were all found into the nucleus and showed localisation to the nucleolus**.**

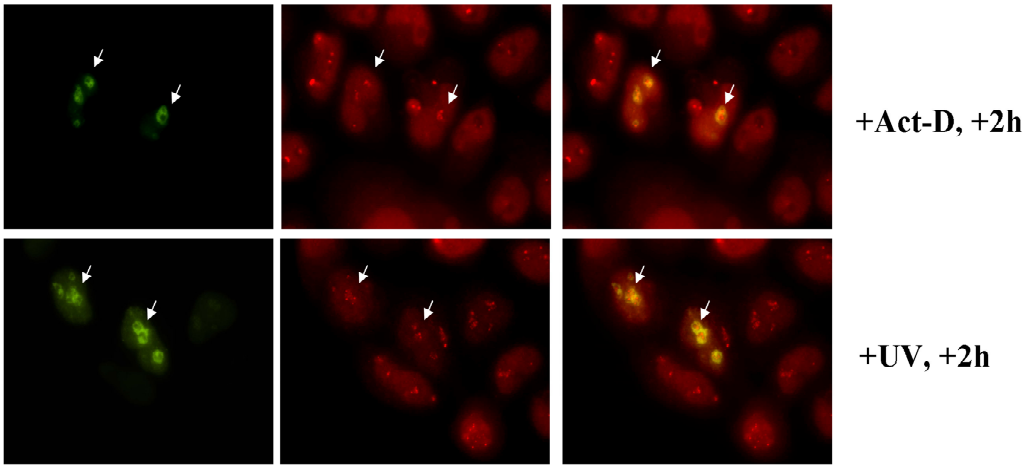

Figure 18: CFP-NoLS-Cdc45 remains in the nucleolus following UVC and Actinomycin D treatment
HeLa S3 cells transiently expressing CFP-NoLS-Cdc45 were treated with 30 J/m^2 of UVC (+UVC) or with 0.1 µg/ml of Actinomycin D (Act-D) and harvested 2 hours post-treatment. Cells were fixed and analysed by immunofluorescence microscopy using antibody specifc to UBF1/2, which acts as a marker for the nucleolus. DyLight 594-labelled secondary antibody was employed for red staining.

The first 190 amino acids of Cdc45 fused to a C-terminal FLAG were transported into the nucleus and nucleolus. (Figure 20B). The Cdc45 deletion mutant Δ(aa101-155) remained in the cytosol, and the addition of an NLS (PKKKRKVG) to the N-terminus of this construct rescues nuclear localisation and this fusion protein shows nucleolar localisation (Figure 20B). When the Δ(aa156-173) was ectopically expressed, a nuclear localisation with no enrichment in the nucleolus was observed (Figure 20B). Localisation in the nucleus with some globular nucleolar localisation was observed when expressing the Cdc45 deletion mutant Δ(aa169-182) (Figure 20B) and expression of the Cdc45 deletion mutant Δ(aa174-190) resulted in nuclear localisation with clear nucleolar enrichment of this fusion protein (Figure 20 B).

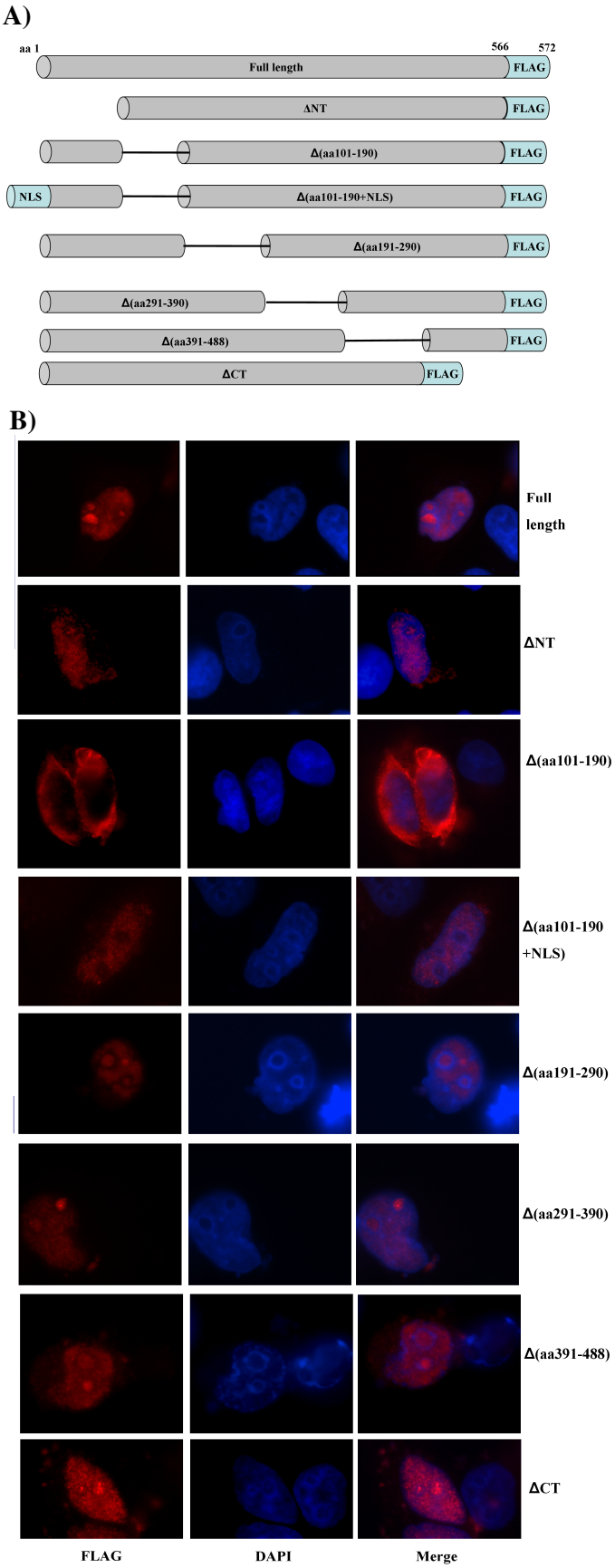

Figure 19: Sub-cellular localisation of Cdc45 deletion mutants

A) Schematic representation of C-terminally FLAG-tagged Cdc45 fusion protein and C-terminally FLAG-tagged deletion mutants. Amino acids removed are indicated, and in the case of Δ(aa101-190+NLS), the NLS from SV40 lagre T-antigen (PKKKRKVG) has been added to the N-terminus. **B)** HeLa S3 cells were transfected with plasmid encoding C-terminally FLAG-tagged Cdc45 (Full Length) or with plasmids encoding C-terminally FLAG-tagged deletion mutants (ΔNT, Δ(aa101-190), Δ(aa101-190+NLS), Δ(aa191-290), Δ(aa291-390), Δ(aa 391-488) and ΔCT). Cells were harvested, fixed and subjected to immunofluorescence microscopy using an antibody specific for FLAG. DAPI staining acts as a marker for the nucleus and nucleolus. DyLight 594 secondary antibody was used for red staining.

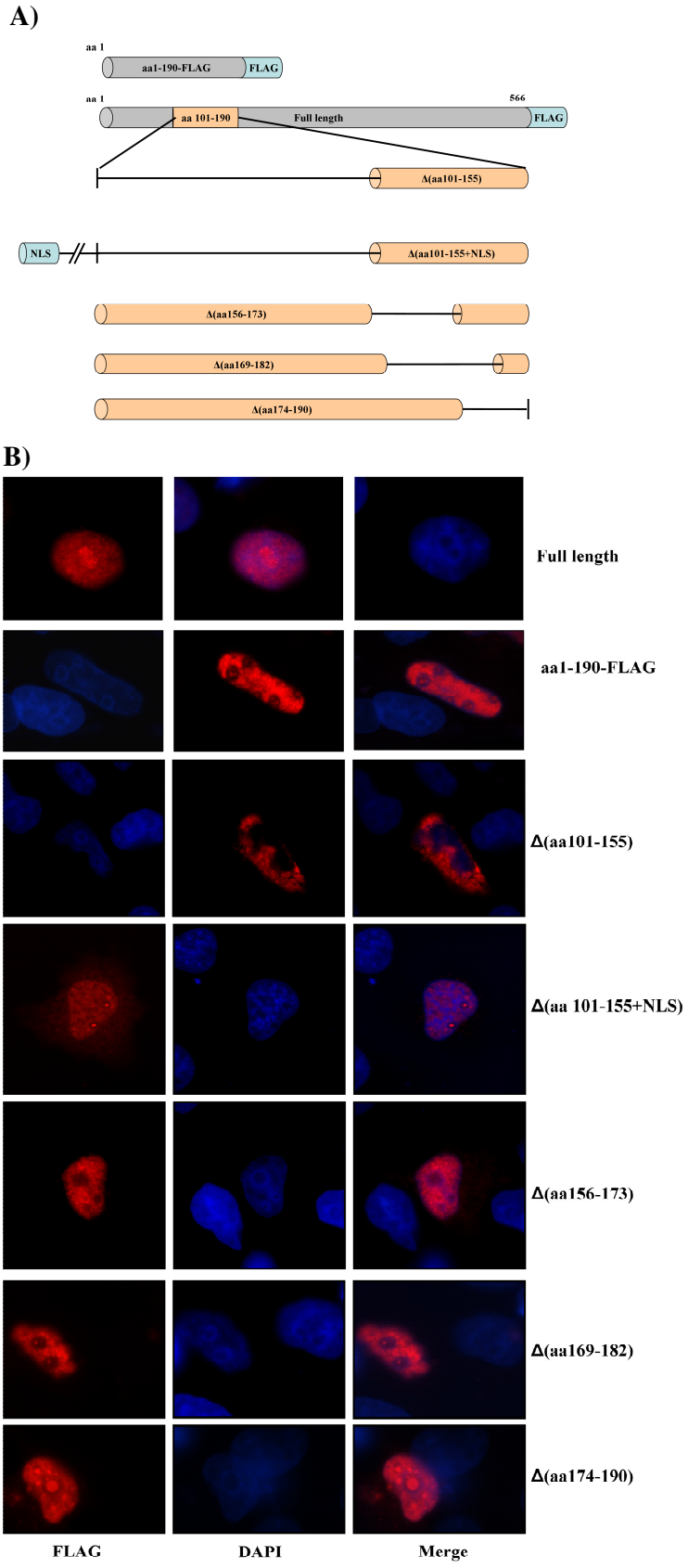

Figure 20: Sub-cellular localisation of Cdc45 deletion mutants

A) Schematic representation of C-terminally FLAG-tagged Cdc45 fusion protein and C-terminally FLAG tagged deletion mutants. Amino acids removed are indicated, and in the case of Δ(aa101-155+NLS), the NLS from SV40 large T-antigen (PKKKRKVG) has been added to the N-terminus. **B)** HeLa S3 cells were transfected with plasmid encoding C-terminally FLAG-tagged Cdc45 (Full length) or C-terminally FLAG-tagged Cdc45 deletion mutants (ΔNT, Δ(aa101-190), Δ(aa101-190+NLS), Δ(aa191-290), Δ(aa291-390), Δ(aa 391-488) and ΔCT). Cells were harvested, fixed and subjected to immuno-fluorescence microscopy using an antibody specific for FLAG. DAPI staining acts as a marker for the nucleus and nucleolus. DyLight 594-labelled secondary antibody was used for red staining.

3.3.8 Gel filtration chromatography analyses of isolated nucleoli

In order to determine if Cdc45 found in isolated nucleoli was in any distinct complex which would suggest a function for Cdc45 within the nucleolus, HeLa S3 cells, or isolated nucleoli from HeLa S3 cells were lysed in a low stringency lysis buffer with chromatin or nucleic acid-associated proteins solubilised by benzonase digestion (Broderick et al, 2012). Lysates were normalised for protein content and subjected to gel filtration chromatography, SDS-PAGE and western blotting (Figure 21). In HeLa S3 cell extract for Cdc45, we find a mixture of complex sizes, the most prevalent an apparently monomeric population and a complex of the same size as the thyroglobulin standard (669 kDa). For comparison, Mcm7 protein was

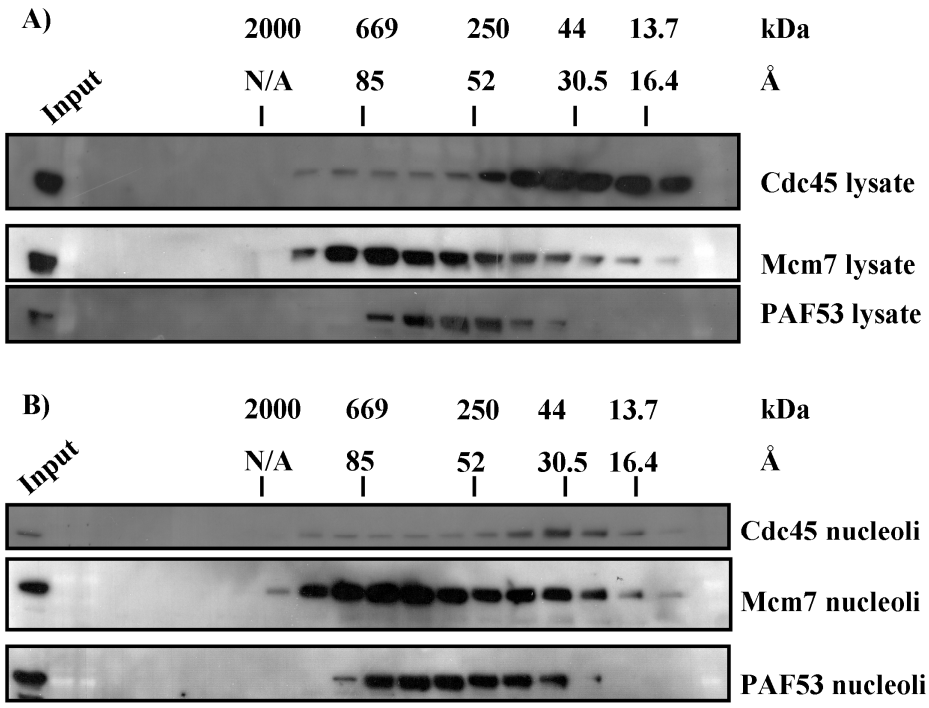

Figure 21: Gel filtration chromatography analyses of Cdc45 from HeLa lysate and from isolated nucleoli
Asynchronous HeLa S3 cells (panel A), or isolated nucleoli from asynchronous HeLa S3 cells (panel B) were lysed and subjected to gel filtration chromatography. Fractions were collected, lyophilised and subjected to SDS-PAGE and western blotting using antibodies specific to Cdc45, Mcm7 and PAF53. Mcm7 acts as a known interaction partner for Cdc45 as part of the CMG, preRC and RPC complexes. PAF53 acts as a control for a protein which is highly enriched in the nucleolus. Size markers for protein standarts in kDa and angstrom are overlayed. Input fractions from each lysate serve as a positive control.

analysed as a protein known to interact with Cdc45 in the process of DNA replication. The nucleolar protein, PAF53, was also analysed as a control for a protein which is highly enriched in nucleoli. In extract prepared from isolated nucleoli for Cdc45 we find again a mixture of complex sizes, with the most prevalent being an apparently monomeric population and a complex of the same size as the thyroglobulin standard (669 kDa). Mcm7 and PAF53 proteins were also examined for comparison. The complex sizes observed in both of these lysates are similar to those obtained from gel filtration chromatography experiments in a HeLa S3 cell line stably expressing eGFP-Cdc45 (Broderick et al, 2012).

3.4 Discussion

In interphase HeLa S3 and U20S cells, subcellular localisation of Cdc45 was investigated using immunofluorescence microscopy. A nucleoplasmic localisation, with little cytosolic localisation and an apparent enrichment in the nucleolus of these cells was observed. This demonstrates that this localisation pattern is cell line-independent. Nucleolar localisation of Cdc45 was confirmed in HeLa S3 cells by immunofluorescence by co-staining with antibodies specific for Fibrillarin (a marker for the fibrillar centres) and UBF1/2 (a marker for the dense fibrillar component). In both cases Cdc45 was found as enriched in nucleoli but did not precisely co-localise with Fibrillarin or UBF1/2. This suggests that any Cdc45 present in nucleoli is localised to the granular component of the nucleoli of human cells.

Cdc45 has a well characterised role in DNA replication. Therefore, we investigated if the nucleolar localisation of Cdc45 plays a role in the regulation of cellular DNA replication including the regulation of replication of nucleolar DNA. Here, the association of Cdc45 with nucleoli was investigated. HeLa S3 cells pre-extracted with Triton before fixation and immunofluorescence microscopy to remove Cdc45 from the cell, which was not tightly associated to chromatin or DNA as previously described (Bauerschmidt et al, 2007; Liu et al, 2006). This pre-extraction abrogated nucleolar enrichment of Cdc45 leaving only sparse, dot-like nucleoplasmic localisation present. This result indicates that the majority of Cdc45 present in the nucleolus is not tightly associated to DNA or chromatin.

Treatment of HeLa S3 cells with UVC or with Actinomycin D resulted in an apparent reduction of enrichment of Cdc45 in the nucleolus**.** Treatment with UVC showed a dose and time-dependent reduction in nucleolar enrichment, with cells treated with 5 J/m^2 UVC showing a loss of enrichment 2h post-treatment with some recovery by 8h. For cells treated with 30 J/m^2 UVC loss of enrichment was also observed 2h post treatment with no recovery in enrichment following damage. This suggests that replication stress induced by UVC may modulate the localisation of Cdc45. Actinomycin D inhibits Pol I transcription (Dellaire & Bazett-Jones, 2007) and can itself cause replication stress (Woodward et al, 2006), either of which may account for the loss of Cdc45 localisation to nucleoli following treatment with this drug. Conversely, changes which occur to the nucleolar proteome and nucleolar

structure following Actinomycin D or UVC treatment (Dellaire & Bazett-Jones, 2007) may cause exclusion of Cdc45 from the nucleolus.

In order to confirm the presence of any Cdc45 in the nucleolus biochemically, nucleoli from HeLa S3 cells were isolated, lysed and analysed by SDS-PAGE and western blotting. Isolated nucleoli without paraformaldehyde cross-linking showed small amounts of Cdc45 present, which were above background contaminant (β-Actin) and above levels of another protein involved in DNA replication (RPA32) which is not seen to be enriched in the nucleolus of cells when examined by immunofluorescence microscopy (Stephan et al, 2009). Upon cross-linking, more Cdc45 is retained in isolated nucleoli**.** Levels of contaminant (β-Actin) remain as low as non-crosslinked nucleoli, however low amounts of RPA32 are seen upon crosslinking. This may be due to RPA32 involved in replication of rDNA which is better retained by crosslinking, or that contaminant RPA32 present at or around the heterochromatic shell which surrounds the nucleolus is pulled down.

Crosslinked nucleoli which had been treated with UVC or with Actinomycin D were isolated, lysed and subjected to SDS-PAGE and quantitative western blotting. The signal for Cdc45 in UVC treated cells was 50% that of untreated control cells as assayed by quantitative western blotting. The levels of Cdc45 in Actinomycin D treated cells were 10% of the control cells as assayed by the same assay. These results fit well with the immunofluorescence microscopy assays carried out and provide evidence that less Cdc45 is present in nucleoli following UVC and Actinomycin D treatment.

To examine the sub-cellular localisation of Cdc45 in interphase cells without the use of thymidine or other drugs, asynchronous HeLa S3 cells were labelled with EdU (a marker for S-phase cells) or phospho-Histone H3 (a marker for late G2 or mitotic cells) and Cdc45 and were assayed by immunofluorescence microscopy. Here, enrichment in the nucleolus is observed in cells labelled for EdU, for phospho-Histone H3 and in cells not labelled with either marker. This suggests that nucleolar localisation of Cdc45 does not occur in a cell cycle-dependent manner and may occur in all interphase cells.

Various plasmid constructs encoding Cdc45 fusion proteins were generated and their transient expression in HeLa S3 cells was assayed. In all cases where an epitope tag was added to the N-terminus of Cdc45, nucleoplasmic localisation was observed, with a globular localisation pattern observed in some cells in the nucleolus. This localisation pattern is consistent with the idea that addition of a tag to the N-terminus of Cdc45 may still allow localisation to the nucleolus, but may cause aggregation of Cdc45 fusion proteins within the nucleolus itself. It is of note that at least one of these constructs, N-terminally tagged GFP-Cdc45 appears to be functional in DNA replication as assayed by co-IP and gel filtration chromatography experiments (as seen in chapter 4 of this thesis). In the case of Cdc45 tagged with a single FLAG-tag to its C-terminus, a localisation more akin to the antibody staining obtained with C45-3G10 antibody suggests that addition of this tag does not interfere with nucleolar localisation of Cdc45 in any way. Localisation of these constructs to the nucleolus also confirms the localisation pattern observed with antibody staining.

In order to determine if sequestering of Cdc45 to the nucleolus caused any aberrant phenotype, plasmid constructs coding for Cdc45 fusion proteins were generated with CFP-NoLS-tagged Cdc45 and a control CFP-NoLS. Addition of the NoLS resulted in transport of these fusion proteins to the nucleolus. No apparent phenotype, change in morphology of the cell or morphology of the nucleolus was observed after CFP-NoLS-Cdc45 or CFP-NoLS expression. This suggests that retention of Cdc45 to the nucleolus does not have any detrimental effect on the cell.

Analyses of subcellular localisation of Cdc45 deletion mutants revealed the regions in Cdc45 containing NLS and NoLS. Initial deletion mutants showed that deletion of aa 101-190 resulted in loss of nuclear localisation. Transient expression of aa 1-190 of Cdc45 showed a nuclear localisaiton with some enrichment in the nucleolus. Addition of an NLS to the N-Terminus of the aa 101-190 deletion mutant resulted in a construct which localised to the nucleus, but lacked nucleolar enrichment. Therefore, it was reasonable to assume that the NLS and NoLS sequences of Cdc45 reside within this 90 amino acid stretch. Further deletion mutants were analysed for their sub-cellular localisation using immunofluorescence microscopy. Deletion of aa 101-155 resulted in cytosolic localisation and addition of an N-terminal NLS to this construct resulted in nuclear localisation with some nucleolar enrichment. This

finding suggested that the NLS of Cdc45 is located within aa 101-155 and is distinct from the NoLS. Deletion of residues 156-173, 169-182 or 174-190 revealed that only deletion of aa 156-173 resulted in a complete loss of nucleolar localisation of Cdc45. Therefore, the NoLS of Cdc45 is most likely mediated by aa 156-169.

In order to determine if Cdc45 in the nucleolus is part of large protein complex, in a distinct form from the DNA replication machinery or forms other than previously characterised protein complexes, the isolated nucleoli were solubilised in whole cell extraction buffer, (which contained detergents and benzonase) and subjected to gel filtration chromatography analyses. For comparison, a whole cell lysate from intact HeLa S3 cells was generated in parallel using the same buffer and analysed by gel filtration chromatography. Although no difference in the size pattern of Cdc45-containing complexes of in isolated nucleoli compared to a lysate generated from intact cells was observed, in nucleoli, less monomeric Cdc45 was retained when compared to extracts from in-tact cells. On analyses of the chromatograms generated, Cdc45 from isolated nucleoli was found in the same fractions on as Cdc45 from intact cells. The ratio of Cdc45 in each fraction was similar in both protein extracts (whole cell and nucleoli) with apparently monomeric Cdc45 being the most prevalent species in each case, and a secondary multisubunit form of Cdc45-containing complexes migrating at the same size as the thyroglobulin standard (669 kDa) was also observed. Mcm7, a known interactor of Cdc45 and a subunit of the DNA helicase machinery (Liu et al, 2006) also appeared in the same fractions and ratios in both the whole cellular and nucleolar extract, and was present in the same fractions as Cdc45 complexes (669 kDa). In nucleoli, slightly less monomeric Cdc45 was retained, however the possibility of loss of monomeric Cdc45 during nucleolar isolation cannot be ruled out, as for technical reasons PFA crosslinking of cells could not be carried out before gel filtration chromatography analyses of these samples. These results suggest that any Cdc45 present in nucleoli is either in a multisubunit complex as part of the DNA replication machinery or is monomeric Cdc45. No evidence of Cdc45 enriched in a large complex in nucleoli that is distinct from the complexes in lysate from whole cells is detected. This suggests no alternative function for Cdc45 within the nucleolus, besides the already elucidated function of DNA replication. Harsh detergent extraction can ablate nucleolar enrichment of Cdc45, and only Cdc45 complexes associated to chromatin

during DNA replication remain. Also gel filtration chromatograms reveal the majority of nucleolar Cdc45 is monomeric. Therefore, it is reasonable to assume that the majority of Cdc45 observed in nucleoli by immunofluorescence staining is monomeric free Cdc45 or loosely associated with other proteins whose interaction is lost during biochemically handling of the samples, with only a small amount of the Cdc45 within nucleoli involved in DNA replication. The addition of replication stress to the cell may result in either modification of Cdc45 or changes in nucleolar proteomics and or structure which do not allow monomeric Cdc45 to reside within the nucleolus. This model is supported by the observation of reduction, but not complete ablation of Cdc45 signal from quantitative western blots of isolated nucleoli following replication stress.

Taken together, these results suggest that Cdc45 is not excluded from nucleoli of interphase cells. The amounts of Cdc45 resident in nucleoli is negatively affected by replication stress which may be due to modification of Cdc45 or changes in the nucleolar structure and/or proteome. Enrichment of Cdc45 to the nucleolus is dependent upon amino acids 156-169 and Cdc45 resident in nucleoli is present in the same size of complexes as in the whole cell. These results indicate that Cdc45 present in nucleoli has no novel function and is required only for DNA replication of the rDNA repeats. These data suggest a model of non-exclusion of Cdc45 from the nucleolus, mediated by aa 156-169, which allows Cdc45 to be present in order to initiate replication at the rDNA repeats.

3.5 Materials and methods

3.5.1 Cell culture

All cell lines were obtained from the American type culture collection (ATCC). HeLa S3 and U20S cells were cultured in Dulbecco's modified Eagle's medium (Sigma) supplemented with 10% foetal calf serum (Sigma), 100 units/ml penicillin (Lonza) and streptomycin (Lonza). Cells stably expressing eGFP-Cdc45 and FLAG-Cdc45 were selected and cultured in DMEM supplemented with 500 µg/ml G418 sulphate (Lonza) 10% foetal calf serum (Sigma), 100 units/ml penicillin (Lonza) and streptomycin (Lonza).

3.5.2 Cell storage

For long term storage in liquid nitrogen or -80 °C cells were grown to near confluency. 24h before freezing down of the cells medium was changed. On the next day adherent cells were removed from dishes by Trypsin-EDTA treatment (Sigma) according to the manufacturer's recommendations. Cells were centrifuged at 250 x g for 5 min and resuspended in FCS (Sigma) supplemented with 10% DMSO (Sigma) and transferred to vials for freezing. Vials of cells were frozen to -80 °C using a "cryo 1 °C" container (NalGENE) filled with isopropanol (Sigma) overnight in a -80 °C freezer before transfer to liquid nitrogen storage. Cells were resuscitated by warming to 37 °C in a waterbath, resuspension in 5 ml of media at 37 °C followed by centrifugation at 250 x g for 5 min. Cell pellets were then resuspended in an appropriate volume of growth medium and placed back in tissue culture.

3.5.3 Competent E. coli cells

For all routine cloning procedures Top 10 or One Shot® CcdB Survival™ 2 T1R competent cells (Invitrogen) were used. For preparation of chemically competent E. coli 125 ml cultures of E. coli in luria broth (LB) were prepared with a typical A_{600} of 0.6. This culture was incubated for 10 min at 4 °C, collected by centrifugation at 250 x g for 10 mins and washed in ice cold TB buffer (10 mM PIPES pH 6.7, 15 mM $CaCl_2$, 250 mM KCL, 55 mM $MnCl_2$). Cells were again pelleted and

resuspended in LB supplemented with 7% DMSO and were aliquoted, snap frozen and stored at -80 °C.

3.5.4 E. coli transformations

An aliquot of competent cells was thawed on ice and an appropriate amount of DNA was added and cells were incubated on ice for 30 mins. Cells were then heat-shocked by incubation at 42 °C for 90 seconds and placed on ice for a further 3 mins. 1 ml LB was then added to the aliquot and cells were incubated at 37 °C for 30 mins before plating an appropriate amount of cells onto an LB agar plate with the correct antibiotic resistance followed by incubation overnight at 37 °C.

3.5.5 Plasmid mini and midi prep

Single colonies of transformed E. coli were selected and overnight cultures of LB supplemented with the appropriate antibiotics were inoculated and grown at 37 °C on a shaker. Appropriate volumes of overnight culture were centrifuged at 4000 x g for 10 min before purification of plasmid DNA by mini or midi prep. For plasmid mini preps and plasmid midi preps Sigma GenElute plasmid mini prep and Sigma GenElute plasmid midi prep kits were used according to the manufacturer's recommendations.

3.5.6 Agarose gel electrophoresis

Agarose gel electrophoresis was carried out as previously described (Sambrook & Russell, 2001). Briefly, agarose gels were prepared by dissolving appropriate amounts of agarose (Sigma) in 1 x TAE buffer. Gels were run in 1 x TAE buffer in gel electrophoresis rigs (BioRad) and incubated in ddH_2O supplemented with 0.5 µg/ml ethidium bromide (Sigma) to stain DNA. 1 kb ladder and 6 x loading buffer (Fermentas) for agarose gel electrophoresis were used according to the manufacturer's recommendations. Gels were visualised and images acquired using a UV transilluminator and specialised software (Apha Innotech ChemiImager 5500).

3.5.7 Restriction digests

For all restriction digests performed, restriction enzymes, buffers and additives were obtained from NEB and used according to the manufacturer's recommendations. Up to 1 μg of DNA was digested for between 1h to overnight at 37 °C.

3.5.8 Ligation procedures

Ligations were carried out using T4 DNA ligase kit from NEB according to the manufacturer's recommendations for either 2h at 25 °C or overnight at 4 °C. Ligations into pGEM-T Easy vector were carried out using pGEM-T Easy kit (Promega) according to the manufacturer's recommendations either for 2h at 25 °C or overnight at 16 °C.

3.5.9 LR Clonase II reactions

DNA fragments were cloned into the pENTR3C entry vector and then recombined into any of a number of destination vectors using the Gateway® LR Clonase® II enzyme mix kit (Invitrogen) according to the manufacturer's recommendations.

3.5.10 Polymerase chain reaction (PCR)

For PCR using Taq Polymerase, Sigma Taq polymerase kit was used according to the manufacturer's recommendations using the following programme for the PCR cycle:

Table 1: Taq PCR programme

Number of Cycles	Temperature	Time
	94 °C	3 mins
30 x	94 °C	45 secs
	60 °C	1 min
	72 °C	1 min
	72 °C	7 mins
	4 °C	∞

For PCR reactions employing KOD DNA Polymerase to reduce mutations in gene of interest, KOD PCR kit (Novagen) was used according to the manufacturer's recommendations and using the following programme for the PCR cycle:

Table 2: KOD PCR programme

Number of Cycles	Temperature	Time
	95°C	2 mins
30 x	95°C	30 secs
	58/63/68 °C	30 secs
	72 °C	3 min
	72 °C	5 mins
	4°C	∞

3.5.11 Oligonucleotides and DNA sequencing services

Oligonucleotides for cloning were obtained from Integrated DNA Technologies (IDT).

DNA sequencing services were provided by LGC Genomics. Oligonucleotide design and analysis of sequencing data was carried out using CLC Sequence Viewer 6 and DNA Baser software.

Table 3: Oligonucleotides

	Sequence (5'-3')
Fwd FLAG-Cdc45	CGAGGATCCATGGACTACAAGGACGACGATGACAAGATG TTCGTGTCCGATTTCCG
Fwd Cdc45	CGAGGATCCATGTTCGTGTCCGATTTCCG
Rev FLAG-Cdc45	CCGGAATTCTACTTGTCATCGTCGTCCTTGTAGTCGGACAG GAGGGAAATAAGTGCG
Rev Cdc45	CCGGAATTCTAGGACAGGAGGGAAATAAGTGCG
CFP-NoLS Fwd	ACGCGTCGACCAGCAAGAGGCCCAGGCGACTGC
CFP-NoLS Rev	CGCGGATCCGTGGCCTTGGAGTCCAGTCACTAGAGC
GFP-NoLS Fwd	ATCGCCACCATGGTGAGCAAGGGCGAGGAGC
GFP-NoLS Rev	GCGCTCGAGGATATTCCGTGGCCTTGGAGTCCAGTCACTA GAGC
NoLS Fwd	ATCGCCACCATGAGCAAGAGGCCCAGGCGACTGC
NoLS Rev	GCGCTCGAGGATATTCCGTGGCCTTGGAGTCCAGTCACTA GAGC
aa1-190 FLAG Rev	CGCCGGAATTCTACTTGTCATCGTCGTCCTTGTAGTCCTGC TCGTAGTCAAAGAGGATGTC
Δ(aa101-155) Fwd	GTGTGTGACACCAAGCGCACACGGTTAGAAGAGG
Δ(aa101-155) Rev	CCGTGTGCGCTTGGTGTCACACACAAAGAATATAG
Δ(aa156-173) Fwd	GAGCCTTCTGAGCGGCGAGAGTGGGAGGCC
Δ(aa156-173) Rev	CCG TGT GCG CTT GGT GTC ACA CAC AAA GAA TAT AG
Δ(aa169-182) Fwd	GAGCAAACCATGGACATC CTC TTT GAC TAC GAG CAG
Δ(aa169-182) Rev	CAAAGAGGATGTCCATGGTTTGCTCCACTATCTCC
Δ(aa174-190) Fwd	CGGAGGAGGCAGTATGAATATCATGGGACATCGTC
Δ(aa174-190) Rev	CATGATATTCATACTGCCTCCTCCGCATGGTTTGC
NLS Fwd	TCGACTATGCCAAAAAAGAAGAGAAAGGTAG
NLS Rev	GATCCTACCTTTCTCTTCTTTTTTGGCATAG
ΔNT Fwd	CGAGGATCCATGCATAGGCCAGTCAATGTCGTC
Δ(aa101-190)	GTGTGTGACACCTATGAATATCATGGGACATCGTC

Fwd	
Δ(aa101-190) Rev	CATGATATTCATAGGTGTCACACACAAAGAATATAGTG
Δ(aa191-290) Fwd	GACTACGAGCAGTGCAACACCAGCTATACCG
Δ(aa191-290) Rev	GCTGGTGTTGCACTGCTCGTAGTCAAAGAGG
Δ(aa291-390) Fwd	CATGACAGCCTGGGCTCAGGGACAGATCACTTC
Δ(aa291-390) Rev	GTCCCTGAGCCCAGGCTGTCATGGAGGGACCAG
Δ(aa391-488) Fwd	CCCGAGAAGGATCTGCCCCTGGTGATGGCTGC
Δ(aa391-488) Rev	CACCAGGGGCAGATCCTTCTCGGGGCTCTCCATC
ΔCT Rev	CCGGAATTCTACTTGTCATCGTCGTCCTTGTAGTCCAGTT TGCAGCGCCGGTTCTTTGTC

3,5.12 Generation of plasmid constructs for FLAG-Cdc45 and FLAG-Cdc45 deletion mutants.

CDC45L ORF and deletion mutants with a C-terminal FLAG tag were amplified by PCR or fusion PCR using KOD PCR kit according to the manufacturer's recommendations. PCR products were cloned into the Gateway entry vector pENTR3C (Invitrogen) in frame between the BamHI and EcoRI restriction sites and recombined into the Gateway destination vector pT-Rex-DEST30 (Invitrogen) using the LR-Clonase II enzyme mix (Invitrogen) according to the manufacturers recommendations.

3.5.13 Generation of eGFP-Cdc45 and CFP-Cdc45 plasmid constructs

The CDC45L ORF was amplified by PCR using KOD PCR kit according to the manufacturer's recommendations and cloned into the gateway entry vector pENTR3C (Invitrogen) between the BamHI and EcoRI restriction sites. The ORF was then recombined into a gateway-adapted eGFP vector based on the pIC113 backbone (pIC113gw, a generous gift from Prof. K. Sullivan) and a gateway adapted CFP vector (pdECFP, a generous gift from Prof. B. McStay) using the LR Clonase II enzyme kit (Invitrogen), as described by the manufacturer. The CDC45L ORF was also directly ligated into the backbone of the pEGFPC1 backbone between the Bgl II and EcoR I restriction sites in the MCS of this vector.

3.5.14 Generation of CFP- NoLS-Cdc45 and CFP-NoLS vectors

The nucleolar localisation sequence (NoLS sequence), described by LeChertier and colleagues (Lechertier et al, 2007) was amplified by PCR from a plasmid encoding GFP-NoLS (obtained as a generous gift from Dr. T. Lechertier) encoding GFP-NoLS in the peGFPC1 vector backbone and directly ligated in frame at the 5' end of the Cdc45 ORF in the CFP-Cdc45 vector. To generate the control vector, the Cdc45 ORF was subsequently excised and the vector backbone re-ligated.

3.5.15 Cell treatment

Cells were treated with UVC by removing media from cells, washing once in PBS at 37℃, removing excess PBS and exposing cells to UVC for precise amounts of time to control dose using a UVC lamp (Benda, Germany) at room temperature. Actinomycin D was dissolved as a stock in DMSO. Cells were treated with 0.1 ng/ml Actinomycin D for 2h before harvest in all experiments shown.

3.5.16 Cell synchronisation

HeLa S3 cells and eGFP-Cdc45-expressing HeLa S3 cells were enriched in late G1 to early S phase by performing two consecutive thymidine blocks as previously described (Bauerschmidt et al, 2007). In short, cells were cultured for 24h in media without thymidine before addition of 5 mM thymidine for 16h. Subsequently, cells were washed 2 times with PBS and allowed to grow in DMEM without thymidine for 12h before a second treatment with 5 mM thymidine for 16h with harvest of the cells at various timepoints post-release from the second thymidine block.

3.5.17 Antibodies

Antibodies recognizing Cdc45 (C45-3G10) and RPA32 (RBF-4E4) and P-RPA32 S4/S8 (Pestryakov et al, 2003; Stephan et al, 2009) were obtained from Dr. E. Kremmer's group at Helmholtz Zentrum München. Anti-Mcm7 antibody was obtained from Neomarkers (47DC141). Antibodies raised against β-Actin(A5441) and FLAG (F1804) were obtained from Sigma. Antibody Antibodies specific for UBF1/2, Fibrillarin and PAF53 were a generous gift from Prof. B. McStay.

Antibody raised against GFP was obtained from Roche (11814460001). Antibody raised against pS10-Histone H3 (06-570) was obtained from Upstate.

3.5.18 Cell Lysis

Total cell lysates were prepared in RIPA buffer (1% Triton X-100, 0.5% deoxycholate, 1% Sodium Dodecyl Sulphate (SDS) in PBS, pH 7.4) supplemented with phosphatase inhibitor cocktail II (Sigma) and ETDA free protease inhibitor cocktail (Roche Applied Sciences). Briefly, cells were lysed for 20 mins at room temperature and centrifuged at 18,000 x g for 10 mins at 4°C. Supernatants were collected and used for subsequent experiments.

Lysates for gel filtration chromatography experiments were prepared in 50 mM Tris-HCL pH 7.4, 250 mM NaCl, 5 mM EGTA, 3 mM MgCl2 0.1% NP-40 supplemented with phosphatase inhibitor cocktail II (Sigma) and ETDA free protease inhibitor cocktail (Roche Applied Sciences). Briefly, cells were lysed for 20 min on ice before addition of Benzonase (Sigma, adjusted to 250 U/10^7 cells) and incubation at 25°C for 30 min to solubilise chromatin associated proteins. Lysates were then clarified by centrifuging for 30 min at 100,000 x g at 4 ºC. Supernatants were collected and used as input for gel filtration chromatography.

3.5.19 SDS-PAGE and immunoblotting

Lysates were normalised for protein content using Bradford assay and subjected to SDS-PAGE and western blotting. Bradford reagent was obtained from Sigma. Bradford assay, SDS-PAGE and western blotting was carried out as described (Sambrook & Russell, 2001).

Cell extracts were resolved by SDS-PAGE using Hoeffer gel electrophoresis chambers (Hoeffer, Germany) and transferred to PVDF membrane using BioRad transfer set up (BioRad) and analysed by western blotting using antibodies raised against various proteins. Western blots were then probed with horseradish peroxidase-conjugated secondary antibodies (HRP, Jackson Immuno Research) and visualized using the ECL or ECL Plus chemiluminescent solution (GE Healthcare).

3.5.20 Quantitative western blotting

For quantitative western blotting, images of western blots were acquired using a LAS3000 imaging system and software (Fuji). Images were analysed quantitatively using densitometry analysis software (Multi Gauge V2.2 (Fuji)) to determine the relative signal intensities of distinct bands.

3.5.21 Lipid-mediated transfection of human cells

Transfection of human cells with lipid-based transfection reagents was carried out using either Rotifect Plus transfection reagent (Roth) or Fugene X-tremeGENE HP DNA transfection reagent (Fugene) according to the manufacturer's recommendations**.**

3.5.22 Gel filtration chromatography

Gel filtration of clarified lysates was carried out using a Superdex 200 PC 3.2/30 column and an Äkta Ettan HPLC machine (Amersham Biosciences) with a 50 µl injection loop. The column was calibrated using a high molecular weight (HMW) gel filtration calibration kit (28-4038-42 GE Healthcare) and 300 µg of clarified cell lysate was then loaded onto the column. Fractions of 100 µl volume were collected, snap frozen and lyophilised using a freeze dryer (Labconco). Freeze-dried fractions were then resuspended in 20 µl 1x Laemmli buffer (Laemmli, 1970), boiled for 5 mins and analysed by SDS-PAGE and western blotting.

3.5.23 Immunofluorescence microscopy.

Cells were grown on glass coverslips (Alpha-Hartenstein, Germany) in culture, were washed twice in PBS and fixed using 4% paraformaldehyde (PFA) for 10 mins at 37℃ and rinsed 3 times in PBS. In some cases cells were pre-permiabilised before fixation using 0.1% Triton X-100 in CSK buffer for 5 mins at 4℃,

Cells were rinsed 3 times in PBS before subsequent fixation. Cells were permeabilised with 0.2% Triton-X100 in PBS for 10 mins at 37℃ and rinsed 3 times in PBS and transferred to a humidified chamber. Fixed cells were blocked using blocking solution (5% BSA, 10% Goat Serum in PBS-T (0.025% Tween)) or in cases where an anti-sheep antibody was employed, cells were blocked in 5% BSA, 10% Donkey Serum in PBS-T (0.025% Tween). Primary antibodies were

diluted in blocking solution and blocked cells were incubated for 1h at 37℃ with primary antibody.

Coverslips were then washed 3 times for 5 min in PBS-T (0.025% Tween) before incubation with secondary antibodies. Secondary antibodies were appropriately diluted in blocking solution and coverslips were incubated with secondary antibody for 1h at 37℃. Coverslips were washed 3 times for 5 min with PBS-T (0.025% Tween) before mounting on glass slides (Alpha-Hartenstein, Germany) using Vectashield mounting medium with DAPI (Vector Laboratories). For analysis of expression of fluorescent proteins, cells were fixed as described and directly mounted on coverslips using Vectashield mounting medium with DAPI. Images were acquired using an Olympus IX51 Brightfield microscope and Cell R software.

3.5.24 EdU labelling

For immunofluorescence microscopy experiments analysing cells incorporating EdU, the Click-iT™ EdU alexafluor 488 kit (Invitrogen) was employed in accordance with the manufacturer's recommendations. Briefly, cells in culture were pulse labelled with 10 μM EdU for 15 min before fixation with 4% PFA and permeabilisation as described above. Following permeabilisation and before the blocking step, EdU labelling with alexafluor 488 dye was carried out according to the manufacturer's protocol. Coverslips were then blocked and stained as normal for immunofluorescence microscopy.

3.5.25 Nucleolar isolation protocol

Nucleoli were isolated from Hela S3 cells using a procedure adapted from (Busch et al, 1963). Briefly, Hela S3 cells were grown to 80-90% confluency on 10 × 150 mm dishes. In some instances Hela S3 cells were fixed with 1% PFA for 10 mins at room temperature. Cells were then scraped into 40 ml ice cold PBS, transferred to a 50 ml falcon tube and washed 3 times with ice cold PBS, centrifuging at 220 × g for 5 mins at 4°C between washes. The cells were then resuspended in 10 ml Buffer A (10 mM HEPES, pH 7.9, 10 mM KCl, 1.5 mM MgCl2, 0.5 mM DTT supplemented with 1x protease inhibitor cocktail (Roche)) on ice until the cell membranes swelled sufficiently.

Afterwards, the swollen cells were transferred to a 15 ml dounce homogeniser (Wheaton, USA) on ice and given 20 dounces with a tight pestle to yield intact nuclei with various cytoplasmic materials attached. Homogenised nuclei were then centrifuged at 220 × g for 5 min at 4 °C and resuspended in 3ml S1 solution (0.25 M Sucrose, 10 mM $MgCl_2$ supplemented with 1x protease inhibitor (Roche)). Resuspended nuclei were then layered over 3 ml S2 solution (0.35 M Sucrose, 0.5 mM $MgCl_2$ supplemented with 1x protease inhibitor (Roche)) and centrifuged at 1430 × g for 5 min at 4 °C to yield highly purified nuclei. Purified nuclei were then resuspended in 3 ml S2 buffer and sonicated with 3 × 5 second pulses @ 50% of maximum amplitude on ice using a Branson digital sonicator to disrupt the nuclear membrane, releasing nucleoli into solution. Sonicated nuclei were then layered over 3 ml S3 buffer (0.88 M Sucrose, 0.5 mM $MgCl_2$ supplemented with 1x protease inhibitor (Roche)) and centrifuged at 3000 x g for 10 min at 4 °C to yield highly purified nucleoli. These nucleoli were then directly snap frozen or in some cases resuspended in 0.5 ml S2 buffer and snap frozen. Nucleoli were prepared for SDS-PAGE analysis by resuspending in 1x Laemmli buffer and boiling for 5 mins, followed by sonication using Bioruptor sonicating water bath at full power with 30 second interval pulses for 5 mins.

Chapter 4

Cell cycle-dependent mobility of Cdc45 determined *in vivo* by fluorescence correlation spectroscopy

4.1 Abstract

Eukaryotic DNA replication is a dynamic process requiring the co-operation of specific replication proteins. We measured the mobility of eGFP-Cdc45 by Fluorescence Correlation Spectroscopy (FCS) *in vivo* in asynchronous cells and in cells synchronized at the G1/S transition and during S phase. Our data show that eGFP-Cdc45 mobility is faster in the G1/S transition compared to S phase suggesting that Cdc45 is part of larger protein complex formed in S phase. Furthermore, the size of complexes containing Cdc45 was estimated in asynchronous, G1/S and S phase-synchronized cells using gel filtration chromatography; these findings complemented the *in vivo* FCS data. Analysis of the mobility of eGFP-Cdc45 and the size of complexes containing Cdc45 and eGFP-Cdc45 after UVC-mediated DNA damage revealed no significant changes in diffusion rates and complex sizes using FCS and gel filtration chromatography analyses. This suggests that after UV-damage, Cdc45 is still present in a large multi-protein complex and that its mobility within living cells is consistently similar following UVC-mediated DNA damage.

4.2 Introduction

Duplication of chromosomal DNA is an essential process for both normal cell division and to maintain stability of the genome (Hoeijmakers, 2001). Replication of damaged DNA or errors in DNA replication can lead to genetic mutation, with accumulated mutations leading to diseases such as cancer (Hoeijmakers, 2001). In human cells, accurate duplication of the genome is carried out by the "replisome progression complex" (RPC), a large multi-subunit complex consisting of replication proteins. These proteins work in concert at different stages of the cell cycle to facilitate DNA replication (Bauerschmidt et al, 2007; Broderick & Nasheuer, 2009; Gambus et al, 2009; Machida et al, 2005; Takeda & Dutta, 2005; Zhu et al, 2007). Eukaryotic DNA replication begins with the binding of the multi-subunit origin recognition complex (ORC) to the origins of replication at the early G1 phase of the cell cycle (Blow & Dutta, 2005; Nasheuer et al, 2006). This allows the binding of additional proteins such as Cdc6 (cell division cycle protein 6) and Cdt1 (Cdc10-dependent target) to ORC mediating the loading of the Mcm2–7 (mini-chromosome maintenance) complex to chromatin, forming the pre-replicative

complex (preRC) (Blow & Dutta, 2005; Nasheuer et al, 2006). Activation of the preRC is mediated by CDKs (cyclin-dependent kinases) and DDK (Dbf4-dependent kinase) to allow the binding of Cdc45 and the GINS (go-ichi-ni-san (five-one-two-three)) complex to the Mcm2-7 (Blow & Dutta, 2005; Moyer et al, 2006; Nasheuer et al, 2006). This activation of the helicase function of Mcm2-7 allows the formation of a larger multi-subunit protein machinery required for the elongation phase of DNA replication (Im et al, 2009; Moyer et al, 2006) and the production of single-stranded DNA, which is coated by RPA (replication protein A). DNA polymerase α-primase (Pol-prim) synthesizes the first RNA primer for DNA replication in the origin of replication, which is elongated by its DNA polymerase activity. The RNA–DNA is recognized by RFC (replication factor C), which loads PCNA (proliferating-cell nuclear antigen) (Blow & Dutta, 2005; Nasheuer et al, 2006). RFC and PCNA, together with RPA, allow a polymerase switch from Pol-prim to Pol (DNA polymerase) ε or *δ*, synthesizing the bulk DNA synthesis on the leading strand and lagging strand, respectively (Blow & Dutta, 2005; Nasheuer et al, 2006).

Cdc45 protein has a key function in the initiation and elongation phases of DNA replication (Masuda et al, 2003) and recent data indicate that Cdc45 is part of the CMG (Cdc45 Mcm2-7 GINS) complex formed at the onset of S phase, progressing to a larger RPC complex present at the elongation phase of DNA replication (Gambus et al, 2006). Protein-protein interaction studies showed that human Cdc45 interacts with Mcm5, Mcm7 and members of the GINS complex as well as with Pols δ and ε in S phase cells (Bauerschmidt et al, 2007). The current model suggests that in the RPC, Cdc45 forms a molecular bridge between the helicase and DNA polymerase components of the complex (Broderick & Nasheuer, 2009). Cdc45 is also the target of a Chk1-mediated intra-S-phase checkpoint (Liu et al, 2006).

Changes in the overall size of protein complexes containing Cdc45 after activation of the intra-S-phase checkpoint have not been examined and the question remains whether Cdc45 remains as part of the RPC after activation of this checkpoint. Biochemical data demonstrate the role of Cdc45 in initiation and elongation phases of DNA replication, but no *in vivo* data exists to elucidate how Cdc45 is regulated inside cells as part of a multi-protein complex (Broderick & Nasheuer, 2009). To shed light on this function, here we used Fluorescence

Correlation Spectroscopy (FCS) to examine the dynamics of Cdc45 in living cells. FCS is a proven technique to measure mobility of fluorescent molecules *in vivo* by analyzing the temporal fluorescence fluctuations arising from molecules diffusing through a femto-liter detection volume (Brazda et al, 2011; Dross et al, 2009; Mahen et al, 2011; Renz & Langowski, 2008; Schwille et al, 1999; Wachsmuth et al, 2000; Wang et al, 2006; Weidtkamp-Peters et al, 2009). The small detection volume may be obtained by the use of confocal optics (Qian & Elson, 1991). Typical concentrations of fluorescently tagged molecules in FCS are in the nanomolar range, corresponding to one or a few molecules simultaneously present in the observation volume. These low intracellular protein concentrations pose a limit for *in vivo* FCS measurements, as does the heterogeneity of the cellular environment, e.g., movement of organelles and of the entire cell (Mahen et al. (2011)). Furthermore, the autofluorescent protein tag must exhibit a high photostability (such as eGFP), to avoid photobleaching on the time scale of the measurement. Recently, we used FCS to study dynamics of RPA in living cells (Braet et al, 2007). Here, we measured the mobility of eGFP-Cdc45 by FCS *in vivo* in asynchronous cells and in cells synchronized at the G1/S transition and during S phase. Our data show that eGFP-Cdc45 moves faster at the G1/S transition than during S phase. Furthermore, the size of protein complexes containing endogenous Cdc45 and eGFP-Cdc45 was estimated for the same cell cycle stages *in vitro* by lysis in a low stringency buffer and gel-filtration chromatography. These data show that eGFP-Cdc45 is part of a multi-protein complex at the G1/S transition and of a very large complex in S phase, which complements the FCS studies obtained *in vivo*. Furthermore, the mobility of eGFP-Cdc45 and the size of complexes containing Cdc45 and eGFP-Cdc45 were studied, following UVC-mediated DNA damage using FCS and gel-filtration chromatography. Surprisingly, both techniques did not reveal significant changes in the mobility and complex sizes. This suggests that after UV-damage Cdc45 is still present in large multi-protein complexes.

4.3 Results

4.3.1 Generation of HeLa S3 cells stably expressing eGFP-Cdc45

HeLa S3 cells stably expressing N-terminally tagged eGFP-Cdc45 were generated to analyse Cdc45 in living cells (Figure 1a). This cell line was generated by transfection of a plasmid coding for eGFP-Cdc45 fusion protein under the control of the CMV promoter followed by selection of G418-resistant cells. G418-resistant cells were seeded in culture at a low density to isolate single clones. Clones were selected, expanded and screened for expression of eGFP-Cdc45 by western blotting. Quantitative western blotting showed that eGFP-Cdc45 is expressed at 25% of endogenous untagged Cdc45 in these cells (Figure 1b). In this analysis the signal for eGFP-Cdc45 was compared to the endogenous Cdc45 signal from the same blot. The latter was arbitrarily set to 100%. Since this low level of expression caused problems to detect eGFP-Cdc45 by fluorescence microscopy, eGFP-Cdc45 was also transiently expressed to the same level as the endogenous protein. In this case we observed nucleoplasmic localisation, consistent with earlier immunofluorescence studies using an antibody specific for Cdc45 (Bauerschmidt et al, 2007).

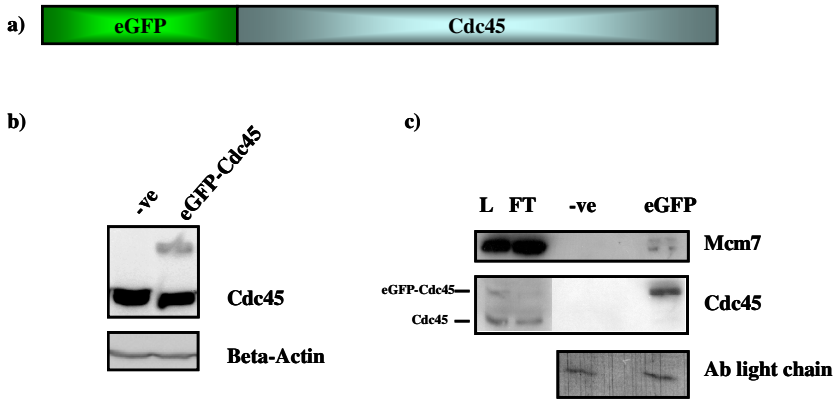

Figure 1: HeLa S3 cells stably expressing eGFP-Cdc45
Panel a, schematic diagram of eGFP-Cdc45 protein encoded by Cdc45L ORF cloned into pIC113gw vector. Panel b, total cell extract HeLaS3 cells (-ve) and Hela S3 cells stably expressing eGFP-Cdc45 (eGFP-Cdc45) normalized for protein content and analysed by western blotting using antibodies raised against Cdc45 and β-Actin, which serves as a loading control. Panel c, western blot analysis of immunoprecipitation of eGFP-Cdc45 using GFP-Trap IP from HeLa S3 cells transiently expressing eGFP-Cdc45. Verification of purification of eGFP-Cdc45 and co-immunoprecipitation of Mcm7 was carried out using antibodies raised against Mcm7 and Cdc45. Input (L), unbound (FT), mock IP (-ve) and IP from cells expressing eGFP-Cdc45 (eGFP) indicate yield of the IP and co-

immunoprecipiation. Antibody light chain acts as a loading control. Note Cdc45 panel is a composite of a long and short exposure of the same blot.

In addition, the co-immunoprecipitation of eGFP-Cdc45 with a known interacting protein, in this case Mcm7 (Bauerschmidt et al, 2007; Liu et al, 2006) was carried out and verified by western blotting (Figure 1c). This indicates that the eGFP-Cdc45 fusion protein interacts with essential components of the DNA replication machinery.

4.3.2 Chromatin association of Cdc45 in the cell cycle and following UVC-mediated DNA damage

To verify our method, we tested whether chromatin association of Cdc45 correlated with published data. Chromatin association of Cdc45 as well as Mcm5, Mcm7, p125 and p261 of Pol δ and ε, respectively, were analysed through the cell cycle (Figure 2a). Low levels of Cdc45 associated with chromatin at the G1/S transition whereas Cdc45 maximally bound to chromatin 6h after the release from the thymidine arrest (Figure 2a left panel) when nearly all cells were in S phase of the cell cycle as determined by FACS analysis (Figure 2a, right panel). The levels of Cdc45 association with chromatin were minimal 12h after release from thymidine block when most cells were in G2 or M phase. Chromatin association of the Mcm2-7 proteins was already very high at the G1/S transition and remained persistently high throughout S phase, whereas association of replicative DNA polymerases was maximal during S phase.

In addition, chromatin association of Cdc45 was analysed following a sub-lethal dose of UVC (Figure 2b). Two hours after UV treatment, chromatin association of Cdc45 was reduced to about 35% of the level of untreated cells, with recovery to normal levels by 5h post-treatment, as determined by quantitative western blotting. The level for asynchronously growing cells was arbritrarly set to 100%. Here, Cdc45 has similar chromatin dissociation kinetics when compared to previous data obtained using a low dose of the carcinogen BPDE, which induced a Chk1-dependent dissociation of Cdc45 from the chromatin (Liu et al, 2006).

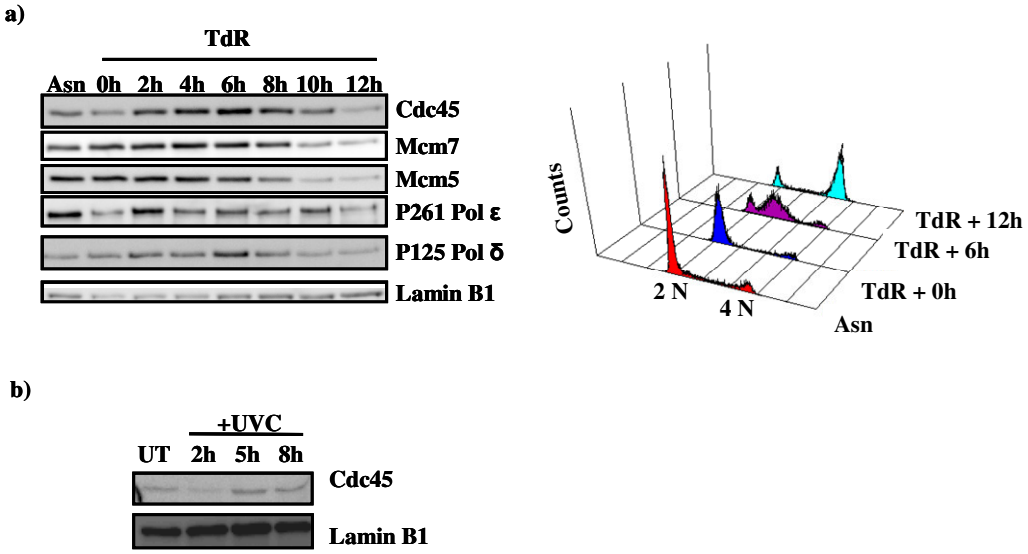

Figure 2 Association of Cdc45 with chromatin synchronized HeLa S3 cells and after DNA damage
Panel a, chromatin-associated lysate from 1 x 10^6 Hela S3 cells synchronized at various cell cycle stages by two consecutive thymidine block analysed by western blotting using antibodies raised against Cdc45, Mcm7, Mcm5, Lamin B1, P261 and P125 of Pol ε and δ, respectively. The latter serves as a loading control. Asynchronous control cells (Asn) or cells analysed at times ranging from 0 to 12h following release from the second thymidine block (TdR 0 to TdR 12) were analysed in parallel by FACS. Corresponding FACS profiles for relevant timepoints are also shown. Panel b, western blot of chromatin-associated Cdc45 following UVC treatment. HeLa S3 cells treated with 5J/m^2 UVC harvested at indicated timepoints post treatment with untreated cells (UT) acting as a control. Chromatin-associated lysates normalized for protein content were analysed by western blotting using antibodies raised against Cdc45 and Lamin B1, which serves as a loading control.

4.3.3 Changes of the diffusion coefficient of eGFP-Cdc45 in HeLa cells during the cell cycle and after UV-mediated DNA damage

The mobility and complex formation of eGFP-Cdc45 during the cell cycle and after UV damage was also studied by FCS in HeLa S3 cells stably expressing eGFP-Cdc45. Fluorescence autocorrelation functions (ACFs) were fitted with a free or anomalous diffusion model with a one- or two-component fit. For the single-component free diffusion model, residuals (quality of 3-dimensional diffusion model fit to experimental data) show a systematic deviation from the fit

(Supplementary Figure S1). The single-component anomalous diffusion model provides a good residual fit with an anomaly parameter $\alpha \sim 0.7 \pm 0.1$ (standard deviation), however the diffusion time and calculated diffusion coefficient obtained with this model show a large standard deviation (Supplementary Figure S2 and Table S1), which is difficult to interpret in our model system. Similarly, a two-component anomalous diffusion model gave a good residual fit, but the anomaly parameter α showed large standard deviations with α being around 1, which corresponds to free diffusion (Wachsmuth et al, 2000) (Supplementary Figure S3 and Table S2). The large deviations in the anomaly parameter α are due to the noise on the ACF and led us to use a two component free diffusion model which gave a very good fit with residuals close to zero (Figure 3, lower panel).

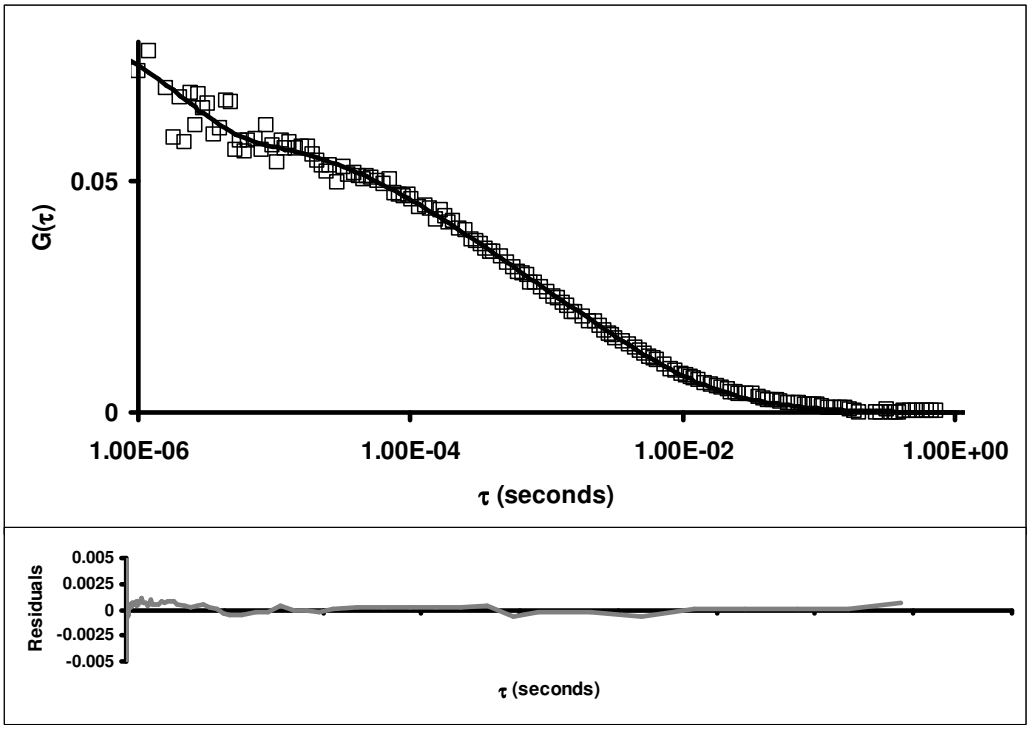

Figure 3: Auto-correlation curves of eGFP-Cdc45
The figure shows typical auto-correlation curves of eGFP-Cdc45 (□) in asynchronous HeLa S3 cells stably expressing eGFP-Cdc45. In the upper panel the solid black line corresponds to a two-component free diffusion model and in the lower panel the gray line is the residual of the fit.

The intercellular diffusion coefficient of eGFP and eGFP-Cdc45 analysed with the two-component free diffusion model are summarized in Table 1. The fractions r1 and r2 of the slow and the fast component, were about 40% and 60%, respectively,

Table 1: Diffusion coefficient of eGFP-Cdc45 at G1 to S phase transition and in S phase and after UV damage

	D1 ± SD ($\mu m^2 s^{-1}$)	r1	D2 ± SD ($\mu m^2 s^{-1}$)	r2
eGFP	34 ± 4.0	0.59 ± 0.17	500 ± 200	0.41 ± 0.17
eGFP-Cdc45	8.2 ± 3.0	0.41 ± 0.17	159 ± 97	0.59 ± 0.17
eGFP-Cdc45 G1/S	9.7 ± 2.0	0.43 ± 0.2	175 ± 340	0.57 ± 0.2
eGFP-Cdc45 S phase	3.6 ± 1.2	0.3 ± 0.1	60 ± 37	0.7 ± 0.1
eGFP-Cdc45 UVC	7.7 ± 3.0	0.49 ± 0.2	116 ± 73	0.51 ± 0.19

Mean and standard deviations obtained from at least 15 cells.

and remained similar throughout the cell cycle and after UVC treatment. The fast component (*D*2) was observed in eGFP transfected and eGFP-Cdc45 stably expressing HeLa S3 cells, but not in untransfected HeLa S3 cells. The diffusion times of the fast component were in the range of 30 – 120 µs, which is in the range of the known non-diffusive component of the ACF due to protonation/ deprotonation kinetics of eGFP (Haupts et al, 1998). The diffusion coefficients *D2* of the fast component were at least a magnitude larger than the *D1* values of the slow component and did not interfere with our measurements. The ratio of the diffusion coefficients of the slow to those of fast component were constant throughout the cell cycle, therefore, we will focus on the slow component for further discussion and interpretation. Hereafter the diffusion coefficient of the slow component will be called as *D*. We determined the *in vivo* diffusion coefficient *D* of eGFP to be 34 ± 4 $\mu m^2 s^{-1}$, similar to values found by other labs (Baudendistel et al, 2005; Chen et al, 2002; Dross et al, 2009; Mahen et al, 2011). The rather large variations among reported values, including our own, is most probably due to variations in cell lines, growth conditions, and other biological variation.

The FCS measurements yielded a number of 20 to 40 (average: 31 ± 10) eGFP-Cdc45 molecules per femtolitre in these stably eGFP-Cdc45-expressing HeLa S3 cells. With a nuclear volume of about 500 to 600 fl for the HeLa S3 cells (Braet et

al, 2007) this would yield 10,000 to 20,000 molecules of eGFP-Cdc45 per cell. Our quantitative western blot experiments shown in Figure 1b revealed that the ratio of eGFP-Cdc45 to endogenous Cdc45 is 1 to 4 resulting in an estimate endogenous Cdc45 number of 40,000 to 80,000 per cell, which is in agreement with previous estimated numbers of Cdc45 molecules per cell being 45,000 (Pollok et al, 2007).

The diffusion coefficient *D* of eGFP-Cdc45 in asynchronous cells shows a broad range, suggesting large variation in the sizes of the protein complexes containing eGFP-Cdc45 and may be act in cell cycle dependent manner (Table 1). In cells arrested at the G1/S transition, the diffusion coefficient *D* of eGFP-Cdc45 is comparable to asynchronous cells, but with a smaller standard deviation (Table 1) suggesting less variability in the sizes of eGFP-Cdc45-containing complexes. In S phase, we determined *D* of eGFP-Cdc45 as 3.6 $\mu m^2 s^{-1}$ with standard deviations of 1.2 $\mu m^2 s^{-1}$ in comparison to *D* of 9.7 ± 2 $\mu m^2 s^{-1}$ in G1/S transition phase. The molecular brightness (CPSM) of eGFP-Cdc45 in S phase did not change significantly compared to G1/S transition or to eGFP, excluding higher oligomeric states (Table S4) (Slaughter & Li, 2010). Estimating sizes of protein complexes in living cells by FCS remains very difficult due to variability in the intracellular environment (Dross et al, 2009). Nevertheless, we attempted to estimate the relative molecular masses of the diffusing complexes from the diffusion times as suggested by Brazda and colleagues (Brazda et al, 2011), assuming that the molecule has a spherical shape. To achieve this, we compared the diffusion times of eGFP-Cdc45 and eGFP. The molecular mass of the eGFP-Cdc45-complexes varied from 1 MDa during G1/S transition to 30 MDa during S phase of the cell cycle, while the monomeric form weighed approximately 95 kDa. After UVC-mediated DNA damage, we observed no significant change in the diffusion coefficient of eGFP-Cdc45. To complement the FCS data generated, we examined the sizes of complexes containing eGFP-Cdc45 and endogenous Cdc45 at different cell cycle stages and after UVC mediated DNA damage by gel filtration chromatography.

4.3.4 Analysis of Cdc45 containing complexes by gel filtration chromatography

Figure 4 shows examples of western blots of gel filtration profiles. We find a mixture of complex sizes, the most prevalent an apparently monomeric population and a complex of the same size as the thyroglobulin standard (669 kDa). In

asynchronous cells the monomeric Cdc45 is the prominent component, whereas in G1/S synchronized cells we observed a shift of the Cdc45-containing complexes towards the 700 kDa-sized complex (Figure 4, compare panel a with b). In S phase-synchronized cells the size of the Cdc45-containing protein complexes further increased, with the largest complexes approaching 2 MDa (Figure 4a). In these gel filtration experiments endogenous Cdc45 and eGFP-Cdc45 behave identically, taking into account that the monomeric eGFP-Cdc45 is 27 kDa larger than monomeric endogenous Cdc45. Interestingly, as observed in the FCS experiments (Table 1), the complex formation of Cdc45 did not change after treating asynchronous cells with UVC (Figure 4, compare panel a with panel d).

For comparison, Mcm5 protein was analysed in the same fractions of the gel filtration chromatogram as eGFP-Cdc45 in asynchronous, G1/S transition- and S phase-synchronized cells. In contrast to Cdc45 and Mcm5, the heterotrimeric RPA complex shows approximately the same size in asynchronous and synchronized cells in the gel filtration experiments as marked by the second largest subunit of RPA, RPA32 (Figure 4 a to c, lowest panels). Moreover, we found no changes in the overall size of complexes containing Cdc45, Mcm5 and RPA32 after UVC treatment, with phosphorylation of RPA32 observed in UVC treated cells (Figure 4). These findings fit well with gel filtration chromatography analyses of isolated CMG complexes from *Drosophila*, with a size of the CMG complex roughly equal to thyroglobulin (669kDa) (Moyer et al, 2006). A separate study in budding yeast estimated the size of RPC, with the CMG complex at its core, to about 2 MDa in S phase synchronized extracts (Gambus et al, 2006).

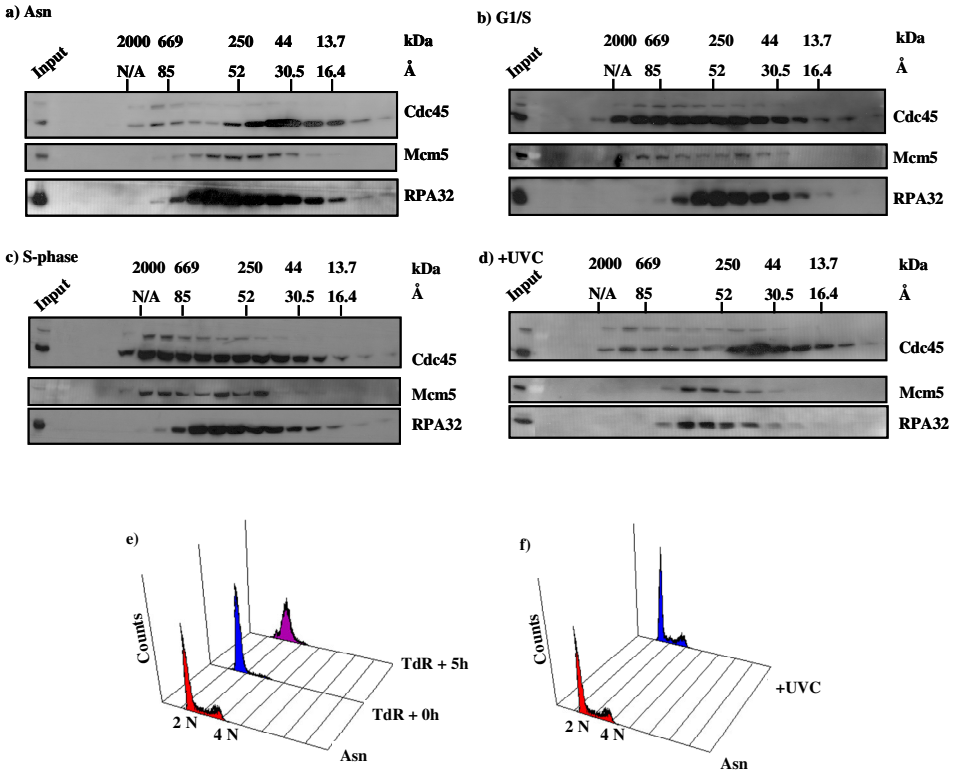

Figure 4 Analysis of the size distribution of Cdc45-containing protein complexes during the cell cycle and after UV damage

Asynchronous (Asn) UVC-treated (+UVC, 5 J/m^2, 1h post-treatment), G1/S transition or S phase synchronized HeLa S3 cells stably expressing eGFP-Cdc45 were lysed and normalized for protein content and separated by gel filtration chromatography analysed by western blotting using antibodies raised against Cdc45, Mcm5 and RPA 32. (panels a, b, c, and d, respectively). Theoretical molecular weight (kDa) and Stoke's radius (Å) of protein standards are overlayed. RPA32 acts as a marker for DNA damage response following UVC treatment. FACS analysis is provided for asynchronous (Asn), G1/S transition and S phase synchronized cells (e) and asynchronous cells treated with 5 J/m^2, 1h post-treatment (f).

4.5 Discussion

To study the replication protein Cdc45 *in vivo*, we generated HeLa S3 cells that stably expressed eGFP-Cdc45. The expression levels of eGFP-Cdc45 in these cells were approximately 25% of that of the endogenous Cdc45. These low levels were particularly suitable for FCS studies. Functionally, we could show that the eGFP-Cdc45 fusion protein behaved identically to endogenous Cdc45 in all biochemical assays (Bauerschmidt et al, 2007). Co-immunoprecipitation of Mcm7 with eGFP-Cdc45 also validated its functionality. Interestingly, little endogenous Cdc45 co-immunoprecipitated with eGFP-Cdc45, suggesting that the eGFP-Cdc45-containing CMG and RPC complexes contain only one molecule of Cdc45 per complex. Transiently expressed eGFP-Cdc45 localized in the nucleoplasm of HeLa S3 cells, similar to previously published localisation data for Cdc45 (Bauerschmidt et al, 2007). Moreover, gel filtration chromatography showed eGFP-Cdc45 in the same fractions as the endogenous protein, suggesting that eGFP-Cdc45 can form the same complexes as endogenous Cdc45.

The mobility of eGFP-Cdc45 was measured by FCS in asynchronous HeLa S3 cells, G1/S transition-, S phase-synchronized cells and in asynchronous cells following UVC-induced DNA damage. The mobility of eGFP-Cdc45 was broadly distributed in asynchronous HeLa S3 cells (Table 1) whereas its mobility in S phase was reduced approx. 3 times compared to G1/S transition (Table 1). Recent reports show that fluorescently tagged Cdc20 protein (~85 kDa) (Wang et al, 2006) and PLK1 protein (~93 kDa) (Mahen et al, 2011), which are similar in molecular weight to eGFP-Cdc45, diffuse slowly in living cells. Unbound, monomeric Cdc20 protein in living cells moved six times faster than the bound/complexed form (Wang et al, 2006). Upon mutation, the catalytic activity of PLK1 protein decreased and its mobility increased, reflecting a reduction in complex size (Mahen et al, 2011). The difference in diffusion rates between unbound and the bound complexes indicates that eGFP-Cdc45 is in part of multi-protein complex. We estimated the sizes of Cdc45-containing complexes to be about 1 MDa at the G1/S transition and 30 MDa in S phase using FCS mobility data. To corroborate these results, we investigated the sizes of complexes containing both endogenous and eGFP-tagged Cdc45 by gel filtration chromatography. A low stringency lysis buffer was used to solubilise proteins whilst keeping protein complexes intact (Behlke-Steinert et al, 2009). Size

analysis of eGFP-Cdc45-containing complexes by gel filtration chromatography gave results consistent with similar analyses of isolated CMG complexes from *Drosophila* of an estimated size of about 0.7 MDa (Moyer et al, 2006). The observation of a larger complex during S phase, approaching 2 MDa, is consistent with gel filtration analyses of proteins from budding yeast, where isolated RPCs incorporating the CMG complex had an estimated molecular mass of about 2 MDa (Gambus et al, 2006). The hypothesis that these complexes observed in gel filtration chromatography assays are indeed the CMG and RPC is supported by the observation that Mcm5 protein is present in the same fractions as Cdc45 in the G1/S transition and S phase-synchronized cells. The estimated sizes of Cdc45-containing complexes at the G1/S transition were slightly larger in living cells, as determined by FCS, than in the cell extracts determined by gel filtration. A possible explanation is that either proteins other than the Mcm2-7 and the GINS complexes may associate with Cdc45 *in vivo*, that the complexes bind transiently to immobile structures, or that the assumption needs to be reconsidered that the Cdc45 protein complex has a spherical shape. In the latter case, a different model for the molecular shape might yield a molecular mass closer to the CMG core complex.

Even so, the gel filtration data correlate well with the FCS-observed diffusion rates for eGFP-Cdc45, which confirms that the *in vitro* biochemical assay reflects the dynamics of the actual *in vivo* eGFP-Cdc45-containing complexes. As the cell progresses to S phase, Cdc45 as part of the CMG complex forms an active RPC complex (Gambus et al, 2006). Although both methods showed an increased size of the S phase Cdc45 complexes compared to the G1/S complex, the complex sizes determined by gel filtration and FCS, 2 MDa versus 30 MDa, clearly differ. This finding could be explained in different ways. First, proteins including RPA might have been lost during gel filtration and therefore the size of S phase Cdc45 complex in living cells was underestimated *in vitro*. This is consistent with the findings that the gel filtration carried out did not contain some proteins which are part of RPC, such as RPA. The protein diffusion in living cells is governed not only by the size of a complex but also by interactions with stable scaffolds such as chromatin (Fritsch & Langowski, 2011; Hemmerich et al, 2011). Therefore, the slower mobility of Cdc45-containing complex might be caused by the Cdc45-containing transiently binding to DNA or other cellular structures as previously discussed

for RPA (Braet et al, 2007).

Analyses of chromatin association of replication proteins presented here support the model that these proteins form the functional RPC on chromatin (Im et al, 2009). Our chromatin association data are consistent with reports showing the formation of the CMG complex after the G1/S transition as chromatin association of Mcm2-7 proteins is seen here as well as some chromatin association of Cdc45 (Im et al, 2009). Association of Cdc45 to chromatin at the G1/S transition with maximal association at S phase is consistent with data demonstrating binding of Cdc45-GINS to Mcm2-7 to form the CMG complex in a CDK- and DDK-dependent manner. This would activate the helicase function of the complex at the onset of S phase (Moyer et al, 2006), coinciding with the formation of the fully functional RPC. Maximal association of the elongating DNA polymerases during S phase is consistent with binding of these proteins to the active CMG as well as other factors including Mcm10, Pol-prim, RFC, RPA, Claspin/Timeless/Tipin, and Ctf4/And1 to create the RPC (Bauerschmidt et al, 2007; Gambus et al, 2006; Kaufmann, 2009; Nasheuer et al, 2006; Unsal-Kacmaz et al, 2007). Following UVC treatment the affinity of Cdc45 for chromatin is reduced between 0 and 2h post treatment, with a recovery between 2h and 5h post-treatment. In addition, phosphorylation of RPA32 is observed in UV-treated samples, indicating the activation of damage response. These data display similar kinetics when compared with previously observed Chk1-dependent reductions in chromatin-association of Cdc45 following treatment of H1299 cells with BPDE (Liu et al, 2006). However, FCS and gel filtration chromatography showed no discernable effect on the overall complex size of replisomes containing Cdc45 and on the distribution of eGFP-Cdc45, Mcm5 or RPA32 after UV treatment when compared to the asynchronous control. This lack of change in size of eGFP-Cdc45-containing complexes following UV-mediated DNA damage suggests that intact RPCs containing Cdc45 are present following damage and might be reloaded as such to start DNA replication again. These findings are consistent with a model where RPCs containing Cdc45 undergo a conformational change following UV-mediated damage, but still contain Cdc45. Recent studies demonstrate that the CMG complex can exist in a “locked” form and a more open “notched” form (Costa et al, 2011), where the gap observed between Cdc45 and the most proximal Mcm2-7 proteins is larger in the “notched”

conformation than in the "locked" form. A change in the overall structure or conformation of the RPC complex containing Cdc45 following fork stalling could explain the observed reduction in Cdc45's affinity for chromatin, its affinity for Mcm proteins, and the lack of a significant change in complex size or diffusion rate for eGFP-Cdc45 in living cells after UVC treatment (Table 1). Alternatively, it may well be that the fraction of Cdc45 associated to chromatin in asynchronous cells is too small to be detected by the FCS and gel filtration chromatography assays.

We show that FCS can be used to characterize the mobility and the dynamics of eGFP-Cdc45 *in vivo* in real time. The mobility change of eGFP-Cdc45 and the size of eGFP-Cdc45 and Cdc45-containing complexes as analysed by FCS and gel-filtration suggests that the association state of the protein is different at the G1/S transition and during S phase. In contrast, we did not observe a significant change in eGFP-Cdc45 mobility or complex size after UVC-induced DNA damage, but did see a reduction in Cdc45-chromatin association after damage; this suggests that large Cdc45 complexes remain stable after removal from chromatin. These observations merit further investigation by biochemical methods and FCS.

4.5 Materials and Methods

4.5.1 Cell Culture

HeLa S3 cells (ATCC CCL2.2) (Bauerschmidt et al, 2007) were cultured in Dulbecco's modified Eagle's medium (Sigma) supplemented with 10% foetal calf serum (Sigma), 100 units/ml penicillin (Lonza) and streptomycin (Lonza). Cells stably expressing eGFP-Cdc45 were selected and cultured in media supplemented with 500 μg/ml G418 sulphate (Lonza). For FCS, HeLa S3 cells that which stably express eGFP-Cdc45 were grown in eight-well chambered cover glass slides (Nunc, Denmark), Dulbecco's modified Eagle's medium (DMEM, GIBCO) without phenol red, with 10% Foetal calf serum (Sigma), 1% L-glutamine (Sigma) at 37°C in a humidified incubator containing 5% CO_2.

4.5.2 Antibodies

Antibodies recognizing Cdc45 (C45-3G10-111) (Bauerschmidt et al, 2007), p125 of Pol δ (PGD-5E1) (Pollok et al, 2007) and RPA 32 (RBF-4E4) (Pestryakov et al, 2003; Stephan et al, 2009). Anti-Mcm5 antibody was obtained from Prof R. Knippers (Ritzi et al, 1998). Mcm7 antibody was obtained from Neomarkers (47DC141). Antibody raised against β-Actin was obtained from Sigma (A5441). Antibody raised against Lamin β1 was obtained from Abcam (ab16048). P261 Pol ε antibody was obtained from BD Biosciences (#611238).

4.5.3 Generation of eGFP-Cdc45 plasmid constructs

The ORF of Cdc45 was cloned into the gateway entry vector pENTR3C (Invitrogen) between the BamH1 and EcoRI restriction sites. The ORF was then recombined into a gateway-adapted eGFP vector based on the pIC113 backbone (pIC113gw, a generous gift from Prof. K. Sullivan) using the LR Clonase II enzyme kit (Invitrogen), as described by the manufacturer.

4.5.4 Fluorescence correlation spectroscopy

FCS measurements were carried out in laboratory-built set up as described in (Dross et al, 2009). In short, confocal laser scanning microscopy (CLSM) was performed with a built in FCS module attached via an X-Y galvanometer scanner to

an inverted microscope (Olympus IX70, Hamburg, Germany) with an UplanApo / IR 60 X water immersion objective lens (Numerical aperture: 1.2). For *in vivo* imaging and FCS, HeLa S3 cells stably expressing eGFP-Cdc45 were plated into eight-well chambered coverslips (Nunc, Denmark) and measured at 37 °C in a 5% CO_2 humidified atmosphere, in an incubator chamber surrounding the entire microscope. An argon-krypton laser with a 488 nm laser created the fluorescence excitation, and emissions were detected between 515 to 545 nm with avalanche photodiodes (APDs) (SPCM-AQR-13, Perkin-Elmer, Wellesley, USA) after passage through appropriate dichroic mirrors and filters for spectral separation. Home-made control software allowed us to choose points from confocal fluorescence images of nuclei for FCS measurements. The signals coming from the APDs were fed into an ALV-5000/E correlator card (ALV Laser GmbH, Langen, Germany), which accumulated the autocorrelation function in parallel for all time delays and in real time.

Nuclei were imaged using CLSM and 5 random positions were selected. Autocorrelation measurements of 5 runs of 10 seconds each were performed on each measurement point. The laser power was 6 µW; no significant change in count rate due to photo-bleaching was observed. For each dataset, we measured at least 15 cells on different days. Data sets that showed unusual variation or oscillation in the count rates were excluded from our analysis. The setup was calibrated using 20 nM AlexaFluor 488 dye (Molecular Probes) in water as described (Dross et al, 2009).

4.5.5 Data analysis

The autocorrelation curves of multiple runs at each individual measured point were fitted by a non-linear fitting using the QuickFit software employing the Marquardt-Levenberg algorithm (http://www.dkfz.de/Macromol/quickfit/). The autocorrelation curves of were fitted with a two diffusional component, triplet correction and a term for eGFP blinking (Brazda et al, 2011; Wachsmuth et al, 2000).

$$G(\tau) = \frac{1 - T - \Theta_c + Te^{-\tau/\tau_{tr}} + \Theta_c e^{-\tau/\tau_c}}{1 - T - \Theta_c} Gdiff \qquad (1)$$

where

$$G_{diff}^{free}(\tau) = \frac{1}{N}\left[r_1 \left(1 + \frac{\tau}{\tau_1}\right)^{-1} \left(1 + \frac{\tau}{S^2\tau_1}\right)^{-1/2} + r_2 \left(1 + \frac{\tau}{\tau_2}\right)^{-1} \left(1 + \frac{\tau}{S^2\tau_2}\right)^{-1/2} \right] \qquad (2)$$

$$G_{diff}^{anomal}(\tau) = \frac{1}{N}\left[r_1 \left(1 + \left(\frac{\tau}{\tau_1}\right)^{\alpha 1}\right)^{-1} \left(1 + \frac{1}{S^2}\left(\frac{\tau}{\tau_1}\right)^{\alpha 1}\right)^{-1/2} + r_2 \left(1 + \left(\frac{\tau}{\tau_2}\right)^{\alpha 2}\right)^{-1} \left(1 + \frac{1}{S^2}\left(\frac{\tau}{\tau_2}\right)^{\alpha 2}\right)^{-1/2} \right]$$

(3)

The autocorrelation function with the term accounting for triplet state formation and dark state formation due to protonation (i.e. blinking) and the term accounting for diffusion are (G_{diff}) were considered when analysing the data (Haupts et al, 1998). N is the average number of fluorescently or tagged molecules in the confocal volume, τ is the lag time. In the triplet term T denotes the equilibrium molar fraction of flurophores in the triplet state and τ_{tr} is the triplet life time (Widengren & Rigler, 1998). The protonation mechanism (Haupts et al, 1998) is characterized by the molecular fraction Θ_c and the correlation time τ_c.

Two diffusion terms were assumed: a slow species with mole fraction r_1 and diffusion time τ_1, and fast species with mole fraction r_2= 1- r_1 and diffusion time τ_2. S denotes the structure factor, which depends on the focal volume and is given by $S = \mathbf{Z}_0/w_0$, where $\mathbf{Z}_0$ is the axial and w_0 the lateral dimension of the confocal volume. The anomaly parameter α corresponds to the mechanism of diffusion; α = 1 corresponds to free diffusion while α < 1 corresponds to obstructed diffusion (Wachsmuth et al, 2000). Anomalous diffusion can result from transient binding or molecular crowding (Guigas & Weiss, 2008).

The diffusion time τ_i (i=1,2) is related to the diffusion coefficient D by:

$$\tau_i = (w_0)^2 / 4D \qquad (4).$$

The lateral radius (w_0) at 488nm excitation was estimated from the diffusion coefficient of Alexa Fluor 488 (20 nM in deionized water). The calculated lateral

radius was w_0 = (250 ± 5) nm, taking D as 435 $\mu m^2 s^{-1}$ at 22.5 °C (Petrasek et al, 2010).

The change in apparent molecular mass of proteins was calculated based on the Stokes-Einstein equation (Brazda et al, 2011). Assuming the diffusing species as spheres,

$$M_{eGFP-Cdc45}^{apparent} / M_{eGFP} = \left(D_{eGFP} / D_{eGFP-Cdc45}\right)^3 = \left(\tau_{eGFP-Cdc45} / \tau_{eGFP}\right)^3 \quad (5)$$

where M_{eGFP} = 27 kDa is the molecular mass of eGFP, D and τ correspond to the diffusion coefficient and diffusion time of eGFP-Cdc45 and eGFP as indexed.

4.5.6 Cell synchronisation

HeLa S3 cells and eGFP-Cdc45-expressing HeLa S3 cells were enriched in late G1 to early S phase by performing two consecutive thymidine blocks as previously described (Bauerschmidt et al, 2007). In short, cells were cultured for 24h in media without thymidine before addition of 5 mM thymidine for 16h. Subsequently, cells were washed 2 times with PBS and allowed to grow in DMEM without thymidine for 12h before a second treatment with 5 mM thymidine for 16h. After this incubation time, cells synchronized at the G1/S transition were analysed using FCS. Cells were washed with PBS, fresh media was added and 5h later, FCS measurements were carried out for S phase-synchronized cells.

4.5.7 Cell lysis and immunoblotting

Total cell lysates were prepared in RIPA buffer (1% Triton X-100, 0.5% deoxycholate, 1% Sodium Dodecyl Sulphate (SDS) in PBS, pH 7.4) supplemented with phosphatase inhibitor cocktail II (Sigma) and ETDA-free protease inhibitor cocktail (Roche Applied Sciences). Lysates for immunoprecipitation were prepared in TGN buffer (50 mM Tris-HCl pH 7.5, 200 mM NaCl, 50 mM sodium β-glycerophosphate, 50 mM Sodium Fluoride, 1% Tween-20, 0.2% NP-40) supplemented with phosphatase inhibitor cocktail II (Sigma) and ETDA free protease inhibitor cocktail (Roche Applied Sciences). Briefly, cells were lysed for 20 min on ice and centrifuged for 10 min at 13,000 x g at 4°C. Supernatant fractions were collected and used as input for immunoprecipitation experiments.

Lysates for gel filtration chromatography experiments were prepared in 50 mM Tris-HCL pH 7.4, 250 mM NaCl, 5 mM EGTA, 3 mM MgCl2 0.1% NP-40 supplemented with phosphatase inhibitor cocktail II (Sigma) and ETDA free protease inhibitor cocktail (Roche Applied Sciences). Cells were lysed for 20 min on ice before addition of Benzonase (Sigma, adjusted to 250 U/10^7 cells) and incubation at 25°C for 30 min to solubilise chromatin associated proteins. Lysates were then clarified by centrifuging for 30 min at 100,000 x g at 4 ºC. Supernatants were collected and used as input for gel filtration chromatography.

Lysates to analyse chromatin association of various proteins, were prepared in a procedure adapted from Liu and colleagues (Liu et al, 2006). In brief, 1 x 10^7 HeLa S3 cells were rinsed once in PBS and scraped into a minimal volume of ice cold PBS. Cells were then centrifuged at 1000 x g for 2 min and resuspended in 250 µl CSK buffer (10 mM PIPES, pH 6.8, 100 mM NaCl, 300 mM sucrose, 3 mM $MgCl_2$, 1 mM EGTA, 1 mM dithiothreitol, 0.1 mM ATP, 1 mM Na_3VO_4, 10 mM NaF, and 0.1% Triton X-100) supplemented with EDTA free protease inhibitor cocktail (Roche Applied Sciences) and incubated on ice for 4 min. Lysates were then centrifuged at 1000 x g for 2 min, and the supernatant was collected as the triton-soluble fraction. Triton-insoluble pellet was washed once in 1 ml CSK buffer and resuspended in 100 µl CSK buffer. RNase-free DNaseI (Applichem), adjusted to 250 U/10^7 cells was then added and lysates were incubated for 30 min at 25 °C to release chromatin-associated proteins. Lysates were then centrifuged at 4 ºC and 10,000 x g for 10 min and the supernatant fractions collected as chromatin-associated fractions.

Cell extracts were resolved by SDS-PAGE, transferred to PVDF membrane and analysed by western blotting using antibodies raised against specific proteins. Western blots were then probed with horseradish peroxidase-conjugated secondary antibodies (HRP, Jackson Immuno Research) and visualized using the ECL or ECL Plus chemiluminescent solution (GE Healthcare).

4.5.8 Quantitative western blotting

For quantitative western blotting, images of western blots were acquired using a LAS3000 imaging system and software (Fuji). Images were analysed quantitatively

using Multi Guage V2.2 software (Fuji) to determine the relative signal intensities of distinct bands.

4.5.9 Immunoprecipitation

eGFP-Cdc45 was immunoprecipitated from cells using GFP-Trap® (ChromoTek) and low adhesion tubes (Bioquote Limited). Briefly, 2 x 10^7 HeLa S3 cells were transfected with 20 µg plasmid coding for eGFP-Cdc45 protein using Fugene/ X-tremeGENE HP transfection reagent (Roche Applied Sciences), harvested 24h post-transfection and lysed in TGN buffer. Protein A/G agarose resin (Calbiochem) was washed three times in TGN buffer and 5 mg lysate was incubated with this resin for 30 min at 4°C to pre-clear. 20 µl packed GFP-Trap®-A resin was washed three times in TGN buffer and incubated with 5 mg pre-cleared lysate from cells transfected with eGFP-Cdc45 plasmid or from mock-transfected control cells. Lysates were incubated with the resin for 2h at 4°C and washed four times with 1 ml of TGN buffer. Bound proteins were solubilised by boiling beads in 40 µl of 2x Laemmli buffer and centrifugation at 5,000 x g for 5 min. Supernatant fractions were collected and analysed by SDS-PAGE and western blotting.

4.5.10 Flow cytometry and FACS analysis

1x 10^6 HeLa S3 cells were trypsinized, washed in ice cold PBS and resuspended in 1 ml PBS. Ice cold ethanol was added to a final concentration of 75% to fix samples for flow cytometry. Before FACS analysis samples were centrifuged at 1500 x g, the supernatant was removed, and the cell pellet was resuspended in 1 ml propidium iodide with RNAse solution (BD Biosciences) and incubated overnight at 4°C. Flow cytometry was carried out using a FACS CANTO flow cytometer (BD Biosciences) and flow cytometry data was analysed using WinMDI software.

4.5.11 Gel filtration chromatography

Gel filtration of lysates was carried out using a Superdex 200 PC 3.2/30 column and an Äkta Ettan HPLC machine (Amersham Biosciences) with a 50 µl injection loop. The column was calibrated using a high molecular weight (HMW) gel filtration calibration kit (28-4038-42 GE Healthcare) and 300 µg of lysate prepared for gel filtration chromatography as described above was then loaded onto the column.

Fractions of 100 µl volume were collected, snap frozen and lyophilised using a freeze dryer (Labconco). Freeze-dried fractions were then resuspended in 20 µl 1x Laemmli buffer, boiled for 5 min and analysed by SDS-PAGE and western blotting.

4.6 Supplementary information

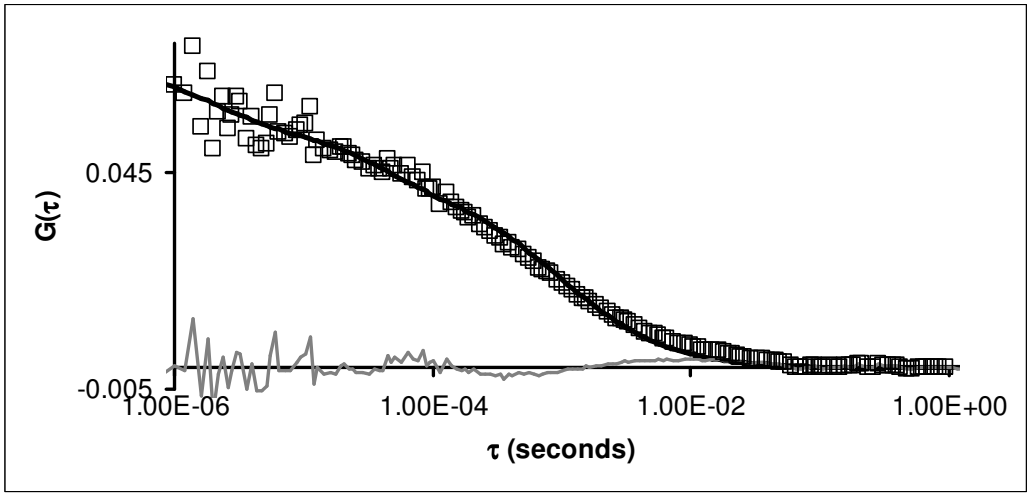

Figure S1: Autocorrelation function of eGFP-Cdc45 in asynchronous HeLa S3 cells stably expressing eGFP-Cdc45 fitted to one-component free diffusion model. (□) corresponds to experimentally determined autocorrelation function the solid black line is the diffusion model fit and the gray line corresponds to the residual of the fit.

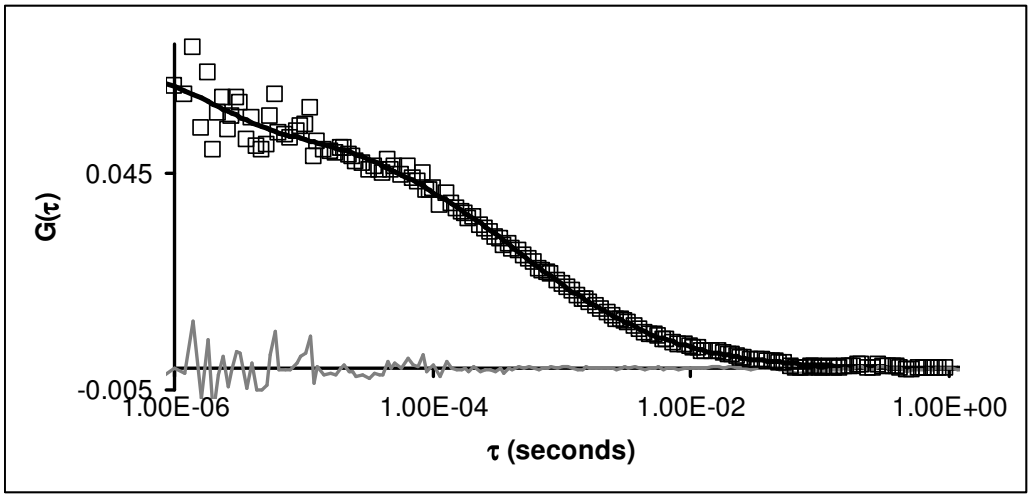

Figure S2: Autocorrelation function of eGFP-Cdc45 in asynchronous HeLa S3 cells stably expressing eGFP-Cdc45 fitted to one-component anomalous diffusion model. (□) corresponds to experimentally determined autocorrelation function. The solid black line corresponds to the diffusion model fit and the gray line corresponds to the residual of the fit.

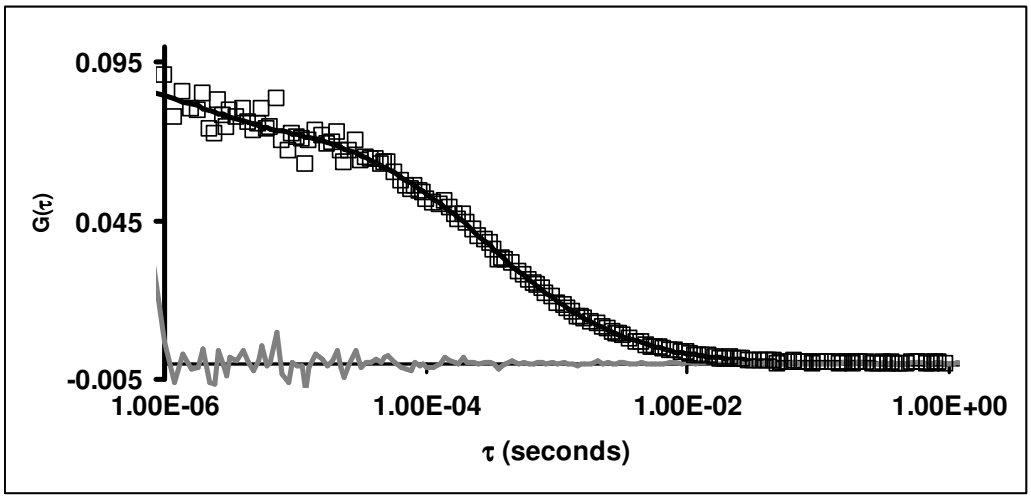

Figure S3: Autocorrelation function of eGFP-Cdc45 in asynchronous HeLa S3 cells stably expressing eGFP-Cdc45 fitted to a two-component anomalous diffusion model. (□) corresponds to experimentally determined autocorrelation function. The solid black line corresponds to the diffusion model fit and gray line corresponds to the residual of the fit.

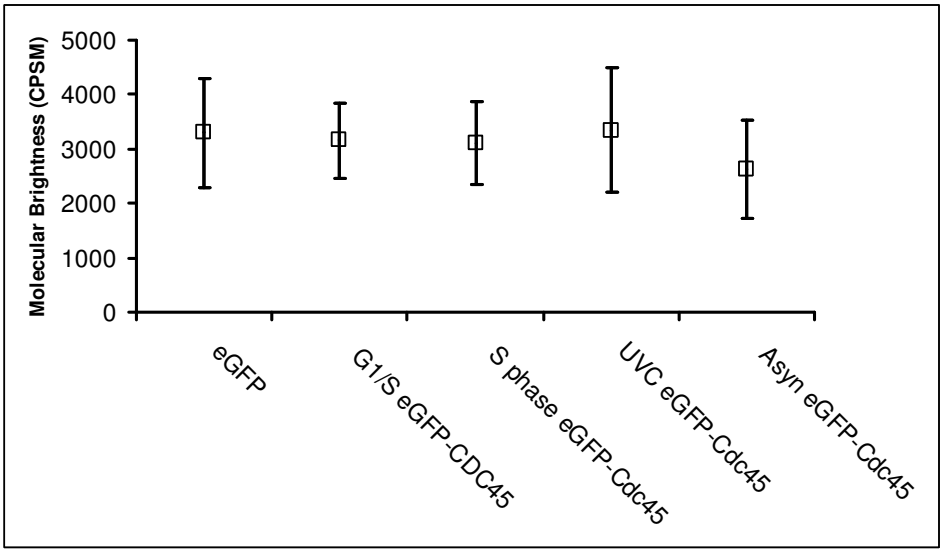

Figure S4: Molecular brightness (CPSM) of eGFP and HeLa S3 cells stably expressing eGFP-Cdc45 in different cell cycle stages, in UV treated and Asynchronous cells. Error bars correspond to standard deviation from at least 15 cells.

Table S1: Single-component anomalous diffusion model fit to eGFP, eGFP-Cdc45 in different cell cycle stages and UVC treatment.

	$D \pm$ SD ($\mu m^2 s^{-1}$)	Anomality (α) ± SD
eGFP	71.6 ± 16.1	0.79 ± 0.12
eGFP-Cdc45	36.2 ± 10.2	0.72 ± 0.1
eGFP-Cdc45 G1/S	38.6 ± 9.4	0.7 ± 0.1
eGFP-Cdc45 S phase	31 ± 13.0	0.7 ± 0.1
eGFP-Cdc45 UVC	30.3 ± 13.0	0.69 ± 0.08

SD: standard deviations from at least 15 cells.

Table S2: Two-component anomalous diffusion model fit to eGFP, eGFP-Cdc45 in different cell cycle stages and following UVC treatment.

	*D*1 ± SD ($\mu m^2 s^{-1}$)	r1 ± SD	α1 ± SD	*D*2 ± SD ($\mu m^2 s^{-1}$)	r2 ± SD	α2 ± SD
eGFP	51.5 ± 19.0	0.52 ± 0.16	1.17 ± 0.3	265 ± 135	0.48 ± 0.26	0.56 ± 0.5
eGFP-Cdc45	10.0 ± 3.0	0.42 ± 0.13	0.88 ± 0.3	127 ± 64	0.58 ± 0.14	0.93 ± 0.4
eGFP-Cdc45 G1/S	11.0 ± 3.0	0.48 ± 0.2	0.6 ± 0.3	68.7 ± 27.6	0.52 ± 0.26	1.04 ± 0.26
eGFP-Cdc45 S phase	5.1 ± 2.1	0.35 ± 0.16	0.89 ± 0.25	66 ± 16	0.65 ± 0.16	1.03 ± 0.35
eGFP-Cdc45 UVC	10.4 ± 4.0	0.44 ± 0.23	0.86 ± 0.3	80.6 ± 60	0.55 ± 0.23	0.78 ± 0.66

SD: standard deviations from at least 15 cells.

Chapter 5

Conclusions and Future Outlook

5.1 Conclusions

The Cdc45 protein has been shown to be crucial for the initiation and elongation of DNA replication, and plays a role in the intra-S-phase checkpoint following DNA damage (Broderick et al, 2009). The protein-protein interactions of the essential protein Cdc45 have been analysed in variety of model organisms such as yeast, xenopus and human (Aparicio et al, 2009; Bauerschmidt et al, 2007) and some contradictions have emerged from these studies awaiting clarification. In human cells the interactions of Cdc45 with Mcm5, Mcm7, members of the GINS complex and the replicative Pols δ and ε have been shown (Aparicio et al, 2009; Bauerschmidt et al, 2007). Recent studies in yeast and xenopus, and in some *in vitro* experiments, revealed new interacting partners of Cdc45, including Claspin and RPA (Uno & Masai, 2011, Nakaya et al, 2010), which raised the question as to whether human Cdc45 interacts with any of these proteins in human cells.

The expression pattern of Cdc45, and several other replication factors throughout the cell cycle have not been determined using methods which avoid inducing cellular stress, asking the question whether the expression and protein-protein interaction patterns observed for these proteins are likely to occur as such *in vivo*. Although several Cdc45-protein interactions have characterised throughout the cell cycle such as Cdc45 with Pol δ (Bauerschmidt et al, 2007), the timing of interactions between Cdc45 and other members of the RPC in the cell cycle in human cells had not yet been analysed in detail. To enhance the structural basis for the protein-protein interactions of Cdc45 an analysis of the regions of Cdc45, which mediates its interactions with the other proteins of the RPC, is required. Furthermore, the current model for Cdc45 as a factor, which is part of the CMG complex at the onset of S-phase and a core componet of RPC during DNA replication, is based on biochemical analyses, and a confirmation of this model via biophysical techniques in living cells had not been carried out but would provide important information in our understanding of Cdc45 function.

Reciprocal co-immunoprecipitations of Cdc45 with Claspin and RPA were performed, showing for the first time that Cdc45 and RPA bind to each other *in vivo* in human cells independently of the affinity purification method. Previous studies analysing the interactions of Cdc45 employed a Cdc45-specific monoclonal antibody, however, the use of C-terminally FLAG-tagged Cdc45 in

our hands was highly successful and provided immunoprecipitations of Cdc45 with very little unspecific binding proteins and minimal interference of protein binding assays. The expression patterns of several replication factors and the interaction of Cdc45 with Pol δ, Claspin and RPA throughout the cell cycle was analysed by elutriation of human cells followed by co-immunoprecipitation experiments. Claspin and RPA were shown to maximally interact with FLAG-Cdc45 in S phase of the cell cycle, both novel findings, with Pol δ acting as a positive control in these experiments verifying te reproducibility of these results and the functionality of the recombinant, FLAG-tagged Cdc45 protein.

Via the use of Cdc45 deletion mutants and co-immunoprecipitation experiments it was also determined that the C-terminus of Cdc45 is the main part of the protein to interact with Claspin, which is a novel finding. Other Cdc45-interacting proteins were analysed by these experiments, namely RPA32 p125 of Pol δ, p261 of Pol ε and Mcm7 however no deletion mutant was seen to be deficient in binding, suggesting that these interactions are probably also mediated by other proteins whose binding to Cdc45 is not disturbed by these mutations. In these experiments we also showed that aa 101-190 is the epitope recognised by the monoclonal C45-3G10 antibody, which is valuable new information for other groups working with this antibody.

Although the sub-cellular localisation of Cdc45 throughout the cell cycle has been previously assayed, following release from consecutive thymidine blocks (Bauerschmidt et al, 2007), the localisation of Cdc45 following activation of the intra-S-phase checkpoint had yet not been determined. Analysis of the subcellular localisation of Cdc45 in asynchronous cells and in cells at various stages of the cell cycle showed a nuclear and nucleolar localisation for Cdc45 in interphase cells, with Cdc45 distinct from chromatin in mitotic cells, a result which agrees with a previous localisation study (Bauerschmidt et al, 2007). Analysis of the sub-cellular localisation of Cdc45 deletion mutants also formally determined the location of the NLS of Cdc45, which was previously unknown, and characterised the region of Cdc45 responsible for its nucleolar localisation. The loss of nuclear localisation of Cdc45 was also shown to be critical for its function, as both the expression and interaction of this deletion mutant with various members of the RPC was enhanced by addition of the SV40 NLS to the N-terminus of this fusion protein.

Furthermore, the analysis of the mobility of eGFP-Cdc45 *in vivo* in human cells by fluorescence correlation spectroscopy and a comparison of these data with gel filtration chromatography analyses provided a validation of the existing model for the function of Cdc45 in DNA. Moreover, this also showed for the first time the dynamics of the replication machinery in real time in living cells. The findings suggest that the CMG complex exists as a freely difussable complex at the G1/S transition which contradicts the current assumptions that single proteins are loaded into chromatin and form there functional units. Following the cells entrance into S phase and the start of chromosomal DNA replication the Cdc45-containing complex is transformed into a new complex with a significantly larger apparent molecular mass as determined by FCS and gel filtration.

Cdc45 has been shown to play a role in the intra-S-phase checkpoint following replication stress. The chromatin association of Cdc45 and the interaction between Cdc45 and Mcm7 on chromatin were diminished upon treatment of Cdc45 with a UVC-mimetic drug (Liu et al, 2006). These effects were ablated by inhibition or knocking down Chk1 protein (Liu et al, 2006). As in the studies presented here neither UCN-01, Caffeine nor Wortmannin treatment rescued the loss of interaction between Cdc45 and Claspin, this finding suggests that the regulation of Cdc45-claspin interactions may operate via a distinct pathway to the Chk-1 dependent pathway describe by Liu and colleagues (Liu et al, 2006). However, the mechanism of regulation of Cdc45 in this pathway, whether Cdc45 itself is post-translationally modified in this process, or whether Cdc45 remains as part of the RPC or dissociated into a smaller sub-complex or is actively removed from the RPC after activation of this checkpoint must be elucidated in the future.

In order to address the issues relating to the role of Cdc45 in the intra-S-phase checkpoint, the interactions of human Cdc45 with Claspin and RPA, as well as the sub-cellular localisation and intracellular mobility of Cdc45 following activation of the intra-S-phase checkpoint were investigated. The interaction between Cdc45 and Claspin, but not RPA was shown to decrease following UVC and HU treatment, in a UCN-01-, Caffeine- and Wortmannin-independent manner. These novel results indicate that the regulation of Cdc45-Claspin interactions may operate via a distinct pathway to the Chk1-dependent regulation of Cdc45 described by Liu and colleagues (Liu et al, 2006).

The subcellular localisation of Cdc45 was also assayed following activation of the intra-S-phase checkpoint, with nucleolar localisation of Cdc45 diminished in a dose- and time-dependent manner following UVC treatment and, interestingly, the inhibition of nucleolar transcription. In contrast, FCS studies in human cells following UVC treatment did not observe a significant change in eGFP-Cdc45 mobility or complex size after UVC-induced DNA damage, but a reduction in Cdc45-chromatin association after damage was determined, suggesting that large Cdc45 complexes remain stable after activation of this checkpoint.

5.2 Future outlook

The regulation of the initiation of eukaryotic DNA replication is still not fully understood. The replication factor Cdc45 is an essential factor in the replication machinery. To understand its role and that of its key interacting proteins in the cell cycle and after DNA damage, large scale purification of Cdc45-containing complexes from human cells should be carried out. They would be followed by mass-spectrometry to identify novel interacting proteins that function with Cdc45 as part of the RPC. In addition, these analyses could be used to elucidate if Cdc45 itself whether Cdc45 is post-translationally modified in the cell cycle or after activation of the intra-S-phase checkpoint. Further biochemical purification and proteomic analyses of Cdc45-containing complexes after UVC treatment will also shed light on the composition of the RPC following DNA damage. These experiments were tested for feasibility during the course of this study, employing a cell line stably expressing N-terminally FLAG-tagged Cdc45. However, during the studies here it was observed that C-terminally FLAG-tagged Cdc45 reproducibly co-immunoprecipitated more of the known RPC components and it was decided to characterise the C-terminally FLAG-tagged Cdc45 in more detailed before carrying out the large scale purifications needed for mass spectrometry analyses.

Additional Cdc45 deletion mutants could also be constructed to screen for Cdc45 mutants deficient in their interaction with other replication factors. These deletion mutants could also be used for *in vitro* experiments, in either in pull down assays or binding assays with other purified replication factors to determine if these mutants are deficient in direct physical interaction with the various proteins tested. Following on from this, mutation of highly conserved residues identified within the

regions mediating direct physical interactions could be identified. Using the elutriation method described here on replication factors not analysed by this study could also provide new insights into the regulation of their expression in the cell cycle and hence the regulation of DNA replication. Also, the timing of the interaction between Cdc45 and other replication factors not assayed in this work presented here could be carried out by this method, allowing a more complete picture of the cell cycle-dependent regulation of Cdc45's protein-protein interactions.

For future studies fluorescence cross correlation spectroscopy (FCCS) using eGFP-Cdc45 and mCherry-tagged subunits of the Mcm2-7 complex, and other members of the CMG and RPC complexes should be produced to measure in living cells the formation of the CMG and RPC complexes and to study the re-arrangements of the RPC following DNA damage *in vivo.* Further biochemical purification and proteomic analyses of Cdc45-containing complexes after UVC treatment will also shed light on the composition of the RPC following DNA damage in human cells.

Bibliography

Alabert C, Groth A (2012) Chromatin replication and epigenome maintenance. *Nat Rev Mol Cell Biol* **13**(3)**:** 153-167

Alberts B, Johnson A, Lewis J, Raff M, Roberts K, Walter P (2008) *Molecular biology of the cell*, N. Y., London: Garland Science.

Aparicio T, Guillou E, Coloma J, Montoya G, Mendez J (2009) The human GINS complex associates with Cdc45 and MCM and is essential for DNA replication. *Nucleic acids research* **37**(7)**:** 2087-2095

Araki Y, Kawasaki Y, Sasanuma H, Tye BK, Sugino A (2003) Budding yeast mcm10/dna43 mutant requires a novel repair pathway for viability. *Genes Cells* **8**(5)**:** 465-480

Atanasiu C, Deng Z, Wiedmer A, Norseen J, Lieberman PM (2006) ORC binding to TRF2 stimulates OriP replication. *EMBO Rep* **7**(7)**:** 716-721

Bartkova J, Rezaei N, Liontos M, Karakaidos P, Kletsas D, Issaeva N, Vassiliou LV, Kolettas E, Niforou K, Zoumpourlis VC, Takaoka M, Nakagawa H, Tort F, Fugger K, Johansson F, Sehested M, Andersen CL, Dyrskjot L, Orntoft T, Lukas J, Kittas C, Helleday T, Halazonetis TD, Bartek J, Gorgoulis VG (2006) Oncogene-induced senescence is part of the tumorigenesis barrier imposed by DNA damage checkpoints. *Nature* **444**(7119)**:** 633-637

Baudendistel N, Muller G, Waldeck W, Angel P, Langowski J (2005) Two-hybrid fluorescence cross-correlation spectroscopy detects protein-protein interactions in vivo. *Chemphyschem* **6**(5)**:** 984-990

Bauerschmidt C, Pollok S, Kremmer E, Nasheuer HP, Grosse F (2007) Interactions of human Cdc45 with the Mcm2-7 complex, the GINS complex, and DNA polymerases delta and epsilon during S phase. *Genes Cells* **12**(6)**:** 745-758

Behlke-Steinert S, Touat-Todeschini L, Skoufias DA, Margolis RL (2009) SMC5 and MMS21 are required for chromosome cohesion and mitotic progression. *Cell cycle (Georgetown, Tex* **8**(14)**:** 2211-2218

Bell O, Schwaiger M, Oakeley EJ, Lienert F, Beisel C, Stadler MB, Schubeler D (2010) Accessibility of the Drosophila genome discriminates PcG repression, H4K16 acetylation and replication timing. *Nat Struct Mol Biol* **17**(7)**:** 894-900

Bi X, Slater DM, Ohmori H, Vaziri C (2005) DNA polymerase kappa is specifically required for recovery from the benzo[a]pyrene-dihydrodiol epoxide (BPDE)-induced S-phase checkpoint. *The Journal of biological chemistry* **280**(23)**:** 22343-22355

Blow JJ, Dutta A (2005) Preventing re-replication of chromosomal DNA. *Nat Rev Mol Cell Biol* **6**(6)**:** 476-486

Boisvert FM, van Koningsbruggen S, Navascues J, Lamond AI (2007) The multifunctional nucleolus. *Nat Rev Mol Cell Biol* **8**(7)**:** 574-585

Bomgarden RD, Lupardus PJ, Soni DV, Yee MC, Ford JM, Cimprich KA (2006) Opposing effects of the UV lesion repair protein XPA and UV bypass polymerase eta on ATR checkpoint signaling. *EMBO J* **25**(11)**:** 2605-2614

Boyer JC, Kaufmann WK, Brylawski BP, Cordeiro-Stone M (1990) Defective postreplication repair in xeroderma pigmentosum variant fibroblasts. *Cancer Res* **50**(9)**:** 2593-2598

Braet C, Stephan H, Dobbie IM, Togashi DM, Ryder AG, Foldes-Papp Z, Lowndes N, Nasheuer HP (2007) Mobility and distribution of replication protein A in living cells using fluorescence correlation spectroscopy. *Exp Mol Pathol* **82:** 156–162

Brazda P, Szekeres T, Bravics B, Toth K, Vamosi G, Nagy L (2011) Live-cell fluorescence correlation spectroscopy dissects the role of coregulator exchange and chromatin binding in retinoic acid receptor mobility. *J Cell Sci* **124**(Pt 21)**:** 3631-3642

Broderick R, Nasheuer HP (2009) Regulation of Cdc45 in the cell cycle and after DNA damage. *Biochem Soc Trans* **37**(4)**:** 926-930

Broderick R, Ramadurai S, Toth K, Togashi DM, Ryder AG, Langowski J, Nasheuer HP (2012) Cell cycle-dependent mobility of Cdc45 determined in vivo by fluorescence correlation spectroscopy. *PLoS One* **7**(4)**:** e35537

Broderick S, Rehmet K, Concannon C, Nasheuer HP (2010) Eukaryotic single-stranded DNA binding proteins: central factors in genome stability. *Subcell Biochem* **50:** 143-163

Bronze-da-Rocha E, Lin CM, Shimura T, Aladjem MI (2011) Interactions of MCP1 with components of the replication machinery in mammalian cells. *Int J Biol Sci* **7**(2)**:** 193-208

Buongiorno-Nardelli M, Micheli G, Carri MT, Marilley M (1982) A relationship between replicon size and supercoiled loop domains in the eukaryotic genome. *Nature* **298**(5869)**:** 100-102

Busch H, Muramatsu M, Adams H, Steele WJ, Liau MC, Smetana K (1963) Isolation of Nucleoli. *Experimental cell research* **24:** SUPPL9:150-163

Cadet J, Sage E, Douki T (2005) Ultraviolet radiation-mediated damage to cellular DNA. *Mutat Res* **571**(1-2)**:** 3-17

Chen B, Simpson DA, Zhou Y, Mitra A, Mitchell DL, Cordeiro-Stone M, Kaufmann WK (2009) Human papilloma virus type16 E6 deregulates CHK1 and sensitizes human fibroblasts to environmental carcinogens independently of its effect on p53. *Cell cycle (Georgetown, Tex* **8**(11)**:** 1775-1787

Chen Y, Muller JD, Ruan Q, Gratton E (2002) Molecular brightness characterization of EGFP in vivo by fluorescence fluctuation spectroscopy. *Biophys J* **82**(1 Pt 1)**:** 133-144

Chini CC, Chen J (2003) Human claspin is required for replication checkpoint control. *The Journal of biological chemistry* **278**(32)**:** 30057-30062

Chini CC, Chen J (2006) Repeated phosphopeptide motifs in human Claspin are phosphorylated by Chk1 and mediate Claspin function. *The Journal of biological chemistry* **281**(44)**:** 33276-33282

Chini CC, Wood J, Chen J (2006) Chk1 is required to maintain claspin stability. *Oncogene* **25**(30)**:** 4165-4171

Chou DM, Petersen P, Walter JC, Walter G (2002) Protein phosphatase 2A regulates binding of Cdc45 to the prereplication complex. *The Journal of biological chemistry* **277**(43)**:** 40520-40527

Chowdhury A, Liu G, Kemp M, Chen X, Katrangi N, Myers S, Ghosh M, Yao J, Gao Y, Bubulya P, Leffak M (2010) The DNA unwinding element binding protein DUE-B interacts with Cdc45 in preinitiation complex formation. *Mol Cell Biol* **30**(6)**:** 1495-1507

Cleaver JE, Lam ET, Revet I (2009) Disorders of nucleotide excision repair: the genetic and molecular basis of heterogeneity. *Nat Rev Genet* **10**(11)**:** 756-768

Costa A, Ilves I, Tamberg N, Petojevic T, Nogales E, Botchan MR, Berger JM (2011) The structural basis for MCM2-7 helicase activation by GINS and Cdc45. *Nat Struct Mol Biol* **18**(4)**:** 471-477

Costanzo V, Robertson K, Ying CY, Kim E, Avvedimento E, Gottesman M, Grieco D, Gautier J (2000) Reconstitution of an ATM-dependent checkpoint that inhibits chromosomal DNA replication following DNA damage. *Mol Cell* **6**(3)**:** 649-659.

Courbet S, Gay S, Arnoult N, Wronka G, Anglana M, Brison O, Debatisse M (2008) Replication fork movement sets chromatin loop size and origin choice in mammalian cells. *Nature* **455**(7212)**:** 557-560

Coverley D, Laman H, Laskey RA (2002) Distinct roles for cyclins E and A during DNA replication complex assembly and activation. *Nature Cell Biology* **4**(7)**:** 523-528

Dalton S, Hopwood B (1997) Characterization of Cdc47p-minichromosome maintenance complexes in Saccharomyces cerevisiae: identification of Cdc45p as a subunit. *Mol Cell Biol* **17**(10)**:** 5867-5875

Dang HQ, Li Z (2011) The Cdc45.Mcm2-7.GINS protein complex in trypanosomes regulates DNA replication and interacts with two Orc1-like proteins in the origin recognition complex. *The Journal of biological chemistry* **286**(37)**:** 32424-32435

Darzynkiewicz Z, Halicka HD, Zhao H, Podhorecka M (2011) Cell synchronization by inhibitors of DNA replication induces replication stress and DNA damage response: analysis by flow cytometry. *Methods Mol Biol* **761:** 85-96

Dehde S, Rohaly G, Schub O, Nasheuer HP, Bohn W, Chemnitz J, Deppert W, Dornreiter I (2001) Two immunologically distinct human DNA polymerase alpha-primase subpopulations are involved in cellular DNA replication. *Mol Cell Biol* **21**(7)**:** 2581-2593

Delgado-Canedo A, Santos DG, Chies JA, Kvitko K, Nardi NB (2006) Optimization of an electroporation protocol using the K562 cell line as a model: role of cell cycle phase and cytoplasmic DNAses. *Cytotechnology* **51**(3)**:** 141-148

Dellaire G, Bazett-Jones DP (2007) Beyond repair foci: subnuclear domains and the cellular response to DNA damage. *Cell cycle (Georgetown, Tex* **6**(15)**:** 1864-1872

Di Micco R, Fumagalli M, Cicalese A, Piccinin S, Gasparini P, Luise C, Schurra C, Garre M, Nuciforo PG, Bensimon A, Maestro R, Pelicci PG, d'Adda di Fagagna F (2006) Oncogene-induced senescence is a DNA damage response triggered by DNA hyper-replication. *Nature* **444**(7119)**:** 638-642

Dimitrova DS (2011) DNA replication initiation patterns and spatial dynamics of the human ribosomal RNA gene loci. *J Cell Sci* **124**(Pt 16)**:** 2743-2752

Din S, Brill SJ, Fairman MP, Stillman B (1990) Cell-cycle-regulated phosphorylation of DNA replication factor A from human and yeast cells. *Genes Dev* **4**(6)**:** 968-977

Dross N, Spriet C, Zwerger M, Muller G, Waldeck W, Langowski J (2009) Mapping eGFP oligomer mobility in living cell nuclei. *PLoS One* **4**(4)**:** e5041

Errico A, Cosentino C, Rivera T, Losada A, Schwob E, Hunt T, Costanzo V (2009) Tipin/Tim1/And1 protein complex promotes Pol alpha chromatin binding and sister chromatid cohesion. *EMBO J* **28**(23)**:** 3681-3692

Falck J, Mailand N, Syljuasen RG, Bartek J, Lukas J (2001) The ATM-Chk2-Cdc25A checkpoint pathway guards against radioresistant DNA synthesis. *Nature* **410**(6830)**:** 842-847

Falck J, Petrini JH, Williams BR, Lukas J, Bartek J (2002) The DNA damage-dependent intra-S phase checkpoint is regulated by parallel pathways. *Nat Genet* **30**(3)**:** 290-294

Friedberg EC, Aguilera A, Gellert M, Hanawalt PC, Hays JB, Lehmann AR, Lindahl T, Lowndes N, Sarasin A, Wood RD (2006) DNA repair: from molecular mechanism to human disease. *DNA Repair (Amst)* **5**(8)**:** 986-996

Fritsch CC, Langowski J (2011) Chromosome dynamics, molecular crowding, and diffusion in the interphase cell nucleus: a Monte Carlo lattice simulation study. *Chromosome Res* **19**(1)**:** 63-81

Fung TK, Poon RYC (2005) A roller coaster ride with the mitotic cyclins. *Seminars in Cell and Developmental Biology* **16**(3)**:** 335-342

Gaballah M, Slisz M, Hutter-Lobo D (2012) Role of JNK-1 regulation in the protection of contact-inhibited fibroblasts from oxidative stress. *Mol Cell Biochem* **359**(1-2)**:** 105-113

Gambus A, Jones RC, Sanchez-Diaz A, Kanemaki M, van Deursen F, Edmondson RD, Labib K (2006) GINS maintains association of Cdc45 with MCM in replisome progression complexes at eukaryotic DNA replication forks. *Nat Cell Biol* **8**(4)**:** 358-366

Gambus A, van Deursen F, Polychronopoulos D, Foltman M, Jones RC, Edmondson RD, Calzada A, Labib K (2009) A key role for Ctf4 in coupling the

MCM2-7 helicase to DNA polymerase alpha within the eukaryotic replisome. *EMBO J* **28**(19)**:** 2992-3004

Ge XQ, Jackson DA, Blow JJ (2007) Dormant origins licensed by excess Mcm2-7 are required for human cells to survive replicative stress. *Genes Dev* **21**(24)**:** 3331-3341

Gerber JK, Gogel E, Berger C, Wallisch M, Muller F, Grummt I, Grummt F (1997) Termination of mammalian rDNA replication: polar arrest of replication fork movement by transcription termination factor TTF-I. *Cell* **90**(3)**:** 559-567

Guigas G, Weiss M (2008) Influence of hydrophobic mismatching on membrane protein diffusion. *Biophys J* **95**(3)**:** L25-27

Guillou E, Ibarra A, Coulon V, Casado-Vela J, Rico D, Casal I, Schwob E, Losada A, Mendez J (2010) Cohesin organizes chromatin loops at DNA replication factories. *Genes Dev* **24**(24)**:** 2812-2822

H Funabiki IH, S Uzawa, and M Yanagida (1993) Cell cycle-dependent specific positioning and clustering of centromeres and telomeres in fission yeast *J Cell Biol* (121)**:** 961 - 976

Hansen RS, Thomas S, Sandstrom R, Canfield TK, Thurman RE, Weaver M, Dorschner MO, Gartler SM, Stamatoyannopoulos JA (2010) Sequencing newly replicated DNA reveals widespread plasticity in human replication timing. *Proc Natl Acad Sci U S A* **107**(1)**:** 139-144

Haupts U, Maiti S, Schwille P, Webb WW (1998) Dynamics of fluorescence fluctuations in green fluorescent protein observed by fluorescence correlation spectroscopy. *Proc Natl Acad Sci U S A* **95**(23)**:** 13573-13578.

Heffernan TP, Unsal-Kacmaz K, Heinloth AN, Simpson DA, Paules RS, Sancar A, Cordeiro-Stone M, Kaufmann WK (2007) Cdc7-Dbf4 and the human S checkpoint response to UVC. *The Journal of biological chemistry* **282**(13)**:** 9458-9468

Hemmerich P, Schmiedeberg L, Diekmann S (2011) Dynamic as well as stable protein interactions contribute to genome function and maintenance. *Chromosome Res* **19**(1)**:** 131-151

Hoeijmakers JH (2001) Genome maintenance mechanisms for preventing cancer. *Nature* **411**(6835)**:** 366-374

Hopwood B, Dalton S (1996) Cdc45p assembles into a complex with Cdc46p/Mcm5p, is required for minichromosome maintenance, and is essential for chromosomal DNA replication. *Proc Natl Acad Sci USA* **93**(22)**:** 12309-12314

Ibarra A, Schwob E, Mendez J (2008) Excess MCM proteins protect human cells from replicative stress by licensing backup origins of replication. *Proc Natl Acad Sci U S A* **105**(26)**:** 8956-8961

Ilves I, Petojevic T, Pesavento JJ, Botchan MR (2010) Activation of the MCM2-7 helicase by association with Cdc45 and GINS proteins. *Mol Cell* **37**(2)**:** 247-258

Im JS, Ki SH, Farina A, Jung DS, Hurwitz J, Lee JK (2009) Assembly of the Cdc45-Mcm2-7-GINS complex in human cells requires the Ctf4/And-1, RecQL4, and Mcm10 proteins. *Proc Natl Acad Sci U S A* **106**(37)**:** 15628-15632

Kamimura Y, Tak YS, Sugino A, Araki H (2001) Sld3, which interacts with Cdc45 (Sld4), functions for chromosomal DNA replication in Saccharomyces cerevisiae. *Embo J* **20**(8)**:** 2097-2107.

Kannouche PL, Wing J, Lehmann AR (2004) Interaction of human DNA polymerase eta with monoubiquitinated PCNA: a possible mechanism for the polymerase switch in response to DNA damage. *Mol Cell* **14**(4)**:** 491-500

Kaufmann WK (2007) Initiating the uninitiated: replication of damaged DNA and carcinogenesis. *Cell cycle (Georgetown, Tex* **6**(12)**:** 1460-1467

Kaufmann WK (2009) The human intra-S checkpoint response to UVC-induced DNA damage. *Carcinogenesis* **31**(5)**:** 751-765

Kaufmann WK, Schwartz JL (1981) Inhibition of replicon initiation by 12-O-tetradecanoylphorbol-13-acetate. *Biochem Biophys Res Commun* **103**(1)**:** 82-89

Kim ST, Xu B, Kastan MB (2002) Involvement of the cohesin protein, Smc1, in Atm-dependent and independent responses to DNA damage. *Genes Dev* **16**(5)**:** 560-570

Krastanova I, Sannino V, Amenitsch H, Gileadi O, Pisani FM, Onesti S (2011) Structural and functional insights into the DNA replication factor Cdc45 reveal an evolutionary relationship to the DHH family of phosphoesterases. *The Journal of biological chemistry*

Kunkel TA (2004) DNA replication fidelity. *The Journal of biological chemistry* **279**(17)**:** 16895-16898

Laemmli UK (1970) Cleavage of structural proteins during the assembly of the head of bacteriophage T4. *Nature* **227:** 680-685

Lechertier T, Sirri V, Hernandez-Verdun D, Roussel P (2007) A B23-interacting sequence as a tool to visualize protein interactions in a cellular context. *Journal of Cell Science* **120**(2)**:** 265-275

Lee J, Gold DA, Shevchenko A, Dunphy WG (2005) Roles of replication fork-interacting and Chk1-activating domains from Claspin in a DNA replication checkpoint response. *Mol Biol Cell* **16**(11)**:** 5269-5282

Leone G, DeGregori J, Yan Z, Jakoi L, Ishida S, Williams RS, Nevins JR (1998) E2F3 activity is regulated during the cell cycle and is required for the induction of S phase. *Genes and Development* **12**(14)**:** 2120-2130

Levy N, Oehlmann M, Delalande F, Nasheuer HP, Van Dorsselaer A, Schreiber V, de Murcia G, Menissier-de Murcia J, Maiorano D, Bresson A (2009) XRCC1 interacts with the p58 subunit of DNA Pol alpha-primase and may coordinate DNA repair and replication during S phase. *Nucleic acids research* **37**(10)**:** 3177-3188

Li J, Santoro R, Koberna K, Grummt I (2005) The chromatin remodeling complex NoRC controls replication timing of rRNA genes. *EMBO J* **24**(1)**:** 120-127

Li Z, Zhang H, McManus TP, McCormick JJ, Lawrence CW, Maher VM (2002) hREV3 is essential for error-prone translesion synthesis past UV or benzo[a]pyrene diol epoxide-induced DNA lesions in human fibroblasts. *Mutat Res* **510**(1-2)**:** 71-80

Liu P, Barkley LR, Day T, Bi X, Slater DM, Alexandrow MG, Nasheuer HP, Vaziri C (2006) The Chk1-mediated S-phase checkpoint targets initiation factor Cdc45 via a Cdc25A/Cdk2-independent mechanism. *The Journal of biological chemistry* **281**(41)**:** 30631-30644

Luo H, Li Y, Mu JJ, Zhang J, Tonaka T, Hamamori Y, Jung SY, Wang Y, Qin J (2008) Regulation of intra-S phase checkpoint by ionizing radiation (IR)-dependent and IR-independent phosphorylation of SMC3. *The Journal of biological chemistry* **283**(28)**:** 19176-19183

Machida YJ, Hamlin JL, Dutta A (2005) Right place, right time, and only once: replication initiation in metazoans. *Cell* **123**(1)**:** 13-24

Mahen R, Jeyasekharan AD, Barry NP, Venkitaraman AR (2011) Continuous polo-like kinase 1 activity regulates diffusion to maintain centrosome self-organization during mitosis. *Proc Natl Acad Sci U S A* **108**(22)**:** 9310-9315

Martin RG, Stein S (1976) Resting state in normal and simian virus 40 transformed Chinese hamster lung cells. *Proceedings of the National Academy of Sciences of the United States of America* **73**(5)**:** 1655-1659

Masai H, Matsumoto S, You Z, Yoshizawa-Sugata N, Oda M (2010) Eukaryotic chromosome DNA replication: where, when, and how? *Annu Rev Biochem* **79:** 89-130

Masai H, Taniyama C, Ogino K, Matsui E, Kakusho N, Matsumoto S, Kim JM, Ishii A, Tanaka T, Kobayashi T, Tamai K, Ohtani K, Arai K (2006) Phosphorylation of MCM4 by Cdc7 kinase facilitates its interaction with Cdc45 on the chromatin. *The Journal of biological chemistry* **281**(51)**:** 39249-39261

Masuda T, Mimura S, Takisawa H (2003) CDK- and Cdc45-dependent priming of the MCM complex on chromatin during S-phase in Xenopus egg extracts: possible activation of MCM helicase by association with Cdc45. *Genes Cells* **8**(2)**:** 145-161

McGarry TJ, Kirschner MW (1998) Geminin, an inhibitor of DNA replication, is degraded during mitosis. *Cell* **93**(6)**:** 1043-1053

Mechali M (2010) Eukaryotic DNA replication origins: many choices for appropriate answers. *Nat Rev Mol Cell Biol* **11**(10)**:** 728-738

Mitchell DL, Nairn RS (1989) The biology of the (6-4) photoproduct. *Photochem Photobiol* **49**(6)**:** 805-819

Moyer SE, Lewis PW, Botchan MR (2006) Isolation of the Cdc45/Mcm2-7/GINS (CMG) complex, a candidate for the eukaryotic DNA replication fork helicase. *Proc Natl Acad Sci USA* **103**(27)**:** 10236-10241

Nakaya R, Takaya J, Onuki T, Moritani M, Nozaki N, Ishimi Y (2010) Identification of proteins that may directly interact with human RPA. *J Biochem* **148**(5)**:** 539-547

Nasheuer HP, Moore A, Wahl AF, Wang TS (1991) Cell cycle-dependent phosphorylation of human DNA polymerase α. *J Biol Chem* **266**(12)**:** 7893-7903

Nasheuer HP, Pospiech H, Syväoja J (2006) Progress towards the anatomy of the eukaryotic DNA replication fork. In *Genome Integrity: Facets and Perspectives,*, Lankenau DH (ed), pp 27 - 68. (ed.) [DOI: 10.1007/7050_012] Genome Dynamics & Stability, Vol. 1, Berlin-Heidelberg-NewYork: Springer

Nasheuer HP, Smith R, Bauerschmidt C, Grosse F, Weisshart K (2002) Initiation of eukaryotic DNA replication: regulation and mechanisms. *Prog Nucleic Acid Res Mol Biol* **72:** 41-94

Nishiyama A, Frappier L, Mechali M (2010) MCM-BP regulates unloading of the MCM2-7 helicase in late S phase. *Genes Dev* **25**(2)**:** 165-175

Nurse P, Thuriaux P, Nasmyth K (1976) Genetic control of the cell division cycle in the fission yeast Schizosaccharomyces pombe. *Molecular and General Genetics* **146**(2)**:** 167-178

Onn I, Heidinger-Pauli JM, Guacci V, Unal E, Koshland DE (2008) Sister chromatid cohesion: a simple concept with a complex reality. *Annu Rev Cell Dev Biol* **24:** 105-129

Pan YR, Lee EY (2009) UV-dependent interaction between Cep164 and XPA mediates localization of Cep164 at sites of DNA damage and UV sensitivity. *Cell cycle (Georgetown, Tex* **8**(4)**:** 655-664

Pestryakov PE, Weisshart K, Schlott B, Khodyreva SN, Kremmer E, Grosse F, Lavrik OI, Nasheuer HP (2003) Human replication protein A: The C-terminal RPA70 and the central RPA32 domains are involved in the interactions with the 3'-end of a primer-template DNA. *The Journal of biological chemistry* **278:** 17515-17524

Petermann E, Helleday T, Caldecott KW (2008) Claspin promotes normal replication fork rates in human cells. *Mol Biol Cell* **19**(6)**:** 2373-2378

Petrasek Z, Ries J, Schwille P (2010) Scanning FCS for the characterization of protein dynamics in live cells. *Methods Enzymol* **472:** 317-343

Pollok S, Bauerschmidt C, Sanger J, Nasheuer HP, Grosse F (2007) Human Cdc45 is a proliferation-associated antigen. *Febs J* **274:** 3669-3684

Pollok S, Grosse F (2007) Cdc45 degradation during differentiation and apoptosis. *Biochem Biophys Res Commun* **362**(4)**:** 910-915

Pospiech H, Grosse F, Pisani FM (2010) The initiation step of eukaryotic DNA replication. *Subcell Biochem* **50:** 79-104

Prakash S, Johnson RE, Prakash L (2005) Eukaryotic translesion synthesis DNA polymerases: specificity of structure and function. *Annu Rev Biochem* **74:** 317-353

Qian H, Elson EL (1991) Analysis of confocal laser-microscope optics for 3-D fluorescence correlation spectroscopy. *Appl Opt* **30**(10)**:** 1185-1195

Rainey MD, Charlton ME, Stanton RV, Kastan MB (2008) Transient inhibition of ATM kinase is sufficient to enhance cellular sensitivity to ionizing radiation. *Cancer Res* **68**(18)**:** 7466-7474

Reardon JT, Sancar A (2003) Recognition and repair of the cyclobutane thymine dimer, a major cause of skin cancers, by the human excision nuclease. *Genes Dev* **17**(20)**:** 2539-2551

Reardon JT, Sancar A (2004) Thermodynamic cooperativity and kinetic proofreading in DNA damage recognition and repair. *Cell cycle (Georgetown, Tex* **3**(2)**:** 141-144

Remus D, Beuron F, Tolun G, Griffith JD, Morris EP, Diffley JF (2009) Concerted loading of Mcm2-7 double hexamers around DNA during DNA replication origin licensing. *Cell* **139**(4)**:** 719-730

Renz M, Langowski J (2008) Dynamics of the CapG actin-binding protein in the cell nucleus studied by FRAP and FCS. *Chromosome Res* **16**(3)**:** 427-437

Reynolds RC, Montgomery PO, Hughes B (1964) Nucleolar "Caps" Produced by Actinomycin D. *Cancer Res* **24:** 1269-1277

Ritzi M, Baack M, Musahl C, Romanowski P, Laskey RA, Knippers R (1998) Human minichromosome maintenance proteins and human origin recognition complex 2 protein on chromatin. *The Journal of biological chemistry* **273**(38)**:** 24543-24549

Sambrook J, Russell DW (2001) Molecular Cloning, 3. Ed., Cold Spring Harbor Laboratory Press, Cold Spring Harbor, NY, USA.

Sanchez-Pulido L, Ponting CP (2011) Cdc45: the missing RecJ ortholog in eukaryotes? *Bioinformatics* **27**(14)**:** 1885-1888

Sar F, Lindsey-Boltz LA, Subramanian D, Croteau DL, Hutsell SQ, Griffith JD, Sancar A (2004) Human claspin is a ring-shaped DNA-binding protein with high affinity to branched DNA structures. *The Journal of biological chemistry* **279**(38)**:** 39289-39295

Sarkaria JN, Busby EC, Tibbetts RS, Roos P, Taya Y, Karnitz LM, Abraham RT (1999) Inhibition of ATM and ATR kinase activities by the radiosensitizing agent, caffeine. *Cancer Res* **59**(17)**:** 4375-4382

Sarkaria JN, Tibbetts RS, Busby EC, Kennedy AP, Hill DE, Abraham RT (1998) Inhibition of phosphoinositide 3-kinase related kinases by the radiosensitizing agent wortmannin. *Cancer Res* **58**(19)**:** 4375-4382

Schmidt U, Wollmann Y, Franke C, Grosse F, Saluz HP, Hanel F (2008) Characterization of the interaction between the human DNA topoisomerase IIbeta-binding protein 1 (TopBP1) and the cell division cycle 45 (Cdc45) protein. *Biochem J* **409**(1)**:** 169-177

Schwaiger M, Kohler H, Oakeley EJ, Stadler MB, Schubeler D (2010) Heterochromatin protein 1 (HP1) modulates replication timing of the Drosophila genome. *Genome Res* **20**(6)**:** 771-780

Schwaiger M, Stadler MB, Bell O, Kohler H, Oakeley EJ, Schubeler D (2009) Chromatin state marks cell-type- and gender-specific replication of the Drosophila genome. *Genes Dev* **23**(5)**:** 589-601

Schwille P, Haupts U, Maiti S, Webb WW (1999) Molecular dynamics in living cells observed by fluorescence correlation spectroscopy with one- and two-photon excitation. *Biophys J* **77**(4)**:** 2251-2265

Semple JI, Smits VA, Fernaud JR, Mamely I, Freire R (2007) Cleavage and degradation of Claspin during apoptosis by caspases and the proteasome. *Cell Death Differ* **14**(8)**:** 1433-1442

Sercin O, Kemp MG (2011) Characterization of functional domains in human Claspin. *Cell cycle (Georgetown, Tex* **10**(10)**:** 1599-1606

Sivasubramaniam S, Sun X, Pan YR, Wang S, Lee EY (2008) Cep164 is a mediator protein required for the maintenance of genomic stability through modulation of MDC1, RPA, and CHK1. *Genes Dev* **22**(5)**:** 587-600

Slaughter BD, Li R (2010) Toward quantitative "in vivo biochemistry" with fluorescence fluctuation spectroscopy. *Mol Biol Cell* **21**(24)**:** 4306-4311

Smith JA, Martin L (1973) Do cells cycle? *Proceedings of the National Academy of Sciences of the United States of America* **70**(4)**:** 1263-1267

Smith KD, Fu MA, Brown EJ (2009) Tim-Tipin dysfunction creates an indispensible reliance on the ATR-Chk1 pathway for continued DNA synthesis. *J Cell Biol* **187**(1)**:** 15-23

Stephan H, Concannon C, Kremmer E, Carty MP, Nasheuer HP (2009) Ionizing radiation-dependent and independent phosphorylation of the 32-kDa subunit of replication protein A during mitosis. *Nucleic acids research* **37**(18)**:** 6028-6041

Stillman B (1996) Cell Cycle Control of DNA Replication. *Science* **274**(5293)**:** 1659-1663

Strom L, Karlsson C, Lindroos HB, Wedahl S, Katou Y, Shirahige K, Sjogren C (2007) Postreplicative formation of cohesion is required for repair and induced by a single DNA break. *Science* **317**(5835)**:** 242-245

Szyjka SJ, Viggiani CJ, Aparicio OM (2005) Mrc1 is required for normal progression of replication forks throughout chromatin in S. cerevisiae. *Mol Cell* **19**(5)**:** 691-697

Takeda DY, Dutta A (2005) DNA replication and progression through S phase. *Oncogene* **24**(17)**:** 2827-2843

Thomae AW, Pich D, Brocher J, Spindler MP, Berens C, Hock R, Hammerschmidt W, Schepers A (2008) Interaction between HMGA1a and the origin recognition complex creates site-specific replication origins. *Proc Natl Acad Sci U S A* **105**(5)**:** 1692-1697

Tomita Y, Imai K, Senju S, Irie A, Inoue M, Hayashida Y, Shiraishi K, Mori T, Daigo Y, Tsunoda T, Ito T, Nomori H, Nakamura Y, Kohrogi H, Nishimura Y (2011) A

novel tumor-associated antigen, cell division cycle 45-like can induce cytotoxic T-lymphocytes reactive to tumor cells. *Cancer Sci* **102**(4)**:** 697-705

Tsakraklides V, Bell SP (2010) Dynamics of pre-replicative complex assembly. *J Biol Chem* **285**(13)**:** 9437-9443

Unal E, Heidinger-Pauli JM, Koshland D (2007) DNA double-strand breaks trigger genome-wide sister-chromatid cohesion through Eco1 (Ctf7). *Science* **317**(5835)**:** 245-248

Uno S, Masai H (2011) Efficient expression and purification of human replication fork-stabilizing factor, Claspin, from mammalian cells: DNA-binding activity and novel protein interactions. *Genes Cells* **16**(8)**:** 842-856

Unsal-Kacmaz K, Chastain PD, Qu PP, Minoo P, Cordeiro-Stone M, Sancar A, Kaufmann WK (2007) The human Tim/Tipin complex coordinates an Intra-S checkpoint response to UV that slows replication fork displacement. *Mol Cell Biol* **27**(8)**:** 3131-3142

Van C, Yan S, Michael WM, Waga S, Cimprich KA (2010) Continued primer synthesis at stalled replication forks contributes to checkpoint activation. *J Cell Biol* **189**(2)**:** 233-246

Wachsmuth M, Waldeck W, Langowski J (2000) Anomalous diffusion of fluorescent probes inside living cell nuclei investigated by spatially-resolved fluorescence correlation spectroscopy. *J Mol Biol* **298**(4)**:** 677-689

Wang Q, Fan S, Eastman A, Worland PJ, Sausville EA, O'Connor PM (1996) UCN-01: a potent abrogator of G2 checkpoint function in cancer cells with disrupted p53. *J Natl Cancer Inst* **88**(14)**:** 956-965

Wang Z, Shah JV, Berns MW, Cleveland DW (2006) In vivo quantitative studies of dynamic intracellular processes using fluorescence correlation spectroscopy. *Biophys J* **91**(1)**:** 343-351

Watanabe K, Tateishi S, Kawasuji M, Tsurimoto T, Inoue H, Yamaizumi M (2004) Rad18 guides poleta to replication stalling sites through physical interaction and PCNA monoubiquitination. *EMBO J* **23**(19)**:** 3886-3896

Weidtkamp-Peters S, Weisshart K, Schmiedeberg L, Hemmerich P (2009) Fluorescence correlation spectroscopy to assess the mobility of nuclear proteins. *Methods Mol Biol* **464:** 321-341

Widengren J, Rigler R (1998) Fluorescence correlation spectroscopy as a tool to investigate chemical reactions in solutions and on cell surfaces. *Cell Mol Biol (Noisy-le-grand)* **44**(5)**:** 857-879

Woodward AM, Gohler T, Luciani MG, Oehlmann M, Ge X, Gartner A, Jackson DA, Blow JJ (2006) Excess Mcm2-7 license dormant origins of replication that can be used under conditions of replicative stress. *J Cell Biol* **173**(5)**:** 673-683

Yang XH, Shiotani B, Classon M, Zou L (2008) Chk1 and Claspin potentiate PCNA ubiquitination. *Genes Dev* **22**(9)**:** 1147-1152

Yazdi PT, Wang Y, Zhao S, Patel N, Lee EY, Qin J (2002) SMC1 is a downstream effector in the ATM/NBS1 branch of the human S-phase checkpoint. *Genes Dev* **16**(5)**:** 571-582

Zegerman P, Diffley JF (2009) DNA replication as a target of the DNA damage checkpoint. *DNA Repair (Amst)* **8**(9)**:** 1077-1088

Zeng XR, Hao H, Jiang Y, Lee MY (1994) Regulation of human DNA polymerase delta during the cell cycle. *The Journal of biological chemistry* **269**(39)**:** 24027-24033

Zhang S, Roche K, Nasheuer HP, Lowndes NF (2011) Modification of histones by sugar beta-N-acetylglucosamine (GlcNAc) occurs on multiple residues, including histone H3 serine 10, and is cell cycle-regulated. *The Journal of biological chemistry* **286**(43)**:** 37483-37495

Zhao B, Bower MJ, McDevitt PJ, Zhao H, Davis ST, Johanson KO, Green SM, Concha NO, Zhou BB (2002) Structural basis for Chk1 inhibition by UCN-01. *The Journal of biological chemistry* **277**(48)**:** 46609-46615

Zhao H, Russell P (2004) DNA binding domain in the replication checkpoint protein Mrc1 of Schizosaccharomyces pombe. *The Journal of biological chemistry* **279**(51)**:** 53023-53027

Zhou BB, Elledge SJ (2000) The DNA damage response: putting checkpoints in perspective. *Nature* **408**(6811)**:** 433-439

Zhu W, Ukomadu C, Jha S, Senga T, Dhar SK, Wohlschlegel JA, Nutt LK, Kornbluth S, Dutta A (2007) Mcm10 and And-1/CTF4 recruit DNA polymerase alpha to chromatin for initiation of DNA replication. *Genes Dev* **21**(18)**:** 2288-2299

Zou L, Stillman B (2000) Assembly of a complex containing Cdc45p, replication protein A, and Mcm2p at replication origins controlled by S-phase cyclin-dependent kinases and Cdc7p-Dbf4p kinase. *Mol Cell Biol* **20**(9)**:** 3086-3096

Acknowledgements

I would like to thank Dr. Heinz Peter Nasheuer for the oppertinity to underake my Ph.D. studies in his group and for his support and help in the production of this thesis and the publications which resulted from this work. I would also like to thank the other members of the cell cycle control group and the other work colleagues in the centre for chromosome biology whom I have worked with over the last several years, who are too numerous to mention individually.

Special thanks go to Dr. Siva Ramadurai and Dr. Micheael D. Rainey for their input in the production of manuscripts for publication, as well as Prof. Corrado Santocanale and Prof Bob Lahue for their helpful suggestions in preparing said manuscripts for publication. Thanks also to IRCSET and the Thomas Crawford Hayes trust fund, without whose financial support the work outlined here would not have been possible.

Appendix I

Manuscript accepted for publication entitled "Regulation of Cdc45 in the cell cycle and after DNA damage". Full text is available online via the following link http://www.biochemsoctrans.org/bst/037/0926/bst0370926.htm

Appendix II

Manuscript accepted for publication entitled "Cell Cycle-Dependent Mobility of Cdc45 Determined *in vivo* by Fluorescence Correlation Spectroscopy". Full text is available online via the following link http://www.plosone.org/article/info:doi/10.1371/journal.pone.0035537